T.R.
GEBZE TECHNICAL UNIVERSITY
GRADUATE SCHOOL OF NATURAL AND APPLIED SCIENCES

NanoPMOs BUILDING BLOCKS: PROPARGYL FUNCTIONALIZED PHOTOSENSITIZING Zn PHTHALOCYANINES WITH SPACERS OF DIFFERENT LENGTHS AND POSITIONS

ÖMER GÖLER
A THESIS SUBMITTED FOR THE DEGREE OF
MASTER OF SCIENCE
DEPARTMENT OF CHEMISTRY

GEBZE
2017

T.R.
GEBZE TECHNICAL UNIVERSITY
GRADUATE SCHOOL OF NATURAL AND APPLIED SCIENCES

NanoPMOs BUILDING BLOCKS: PROPARGYL FUNCTIONALIZED PHOTOSENSITIZING Zn PHTHALOCYANINES WITH SPACERS OF DIFFERENT LENGTHS AND POSITIONS

ÖMER GÖLER

A THESIS SUBMITTED FOR THE DEGREE OF
MASTER OF SCIENCE
DEPARTMENT OF CHEMISTRY

THESIS SUPERVISOR
ASSIST. PROF. DR. FABIENNE DUMOULIN
II. THESIS SUPERVISOR
PROF. DR. VEFA AHSEN

GEBZE
2017

T.C.
GEBZE TEKNİK ÜNİVERSİTESİ
FEN BİLİMLERİ ENSTİTÜSÜ

NanoPMO YAPI TAŞLARI: FARKLI POZİSYON VE UZUNLUKLARDA ARABAĞLAYICILI, PROPARJİLLİ IŞIĞA DUYARLI Zn FTALOSİYANİNLER

ÖMER GÖLER
YÜKSEK LİSANS TEZİ
KİMYA ANABİLİMDALI

DANIŞMANI
YRD. DOÇ. DR. FABIENNE DUMOULIN
II. DANIŞMANI
PROF. DR. VEFA AHSEN

GEBZE
2017

GEBZE TEKNİK ÜNİVERSİTESİ	YÜKSEK LİSANS JÜRİ ONAY FORMU

GTÜ Fen Bilimleri Enstitüsü Yönetim Kurulu'nun 29/06/2017 tarih ve 2017/35 sayılı kararıyla oluşturulan jüri tarafından 10/08/2017 tarihinde tez savunma sınavı yapılan Ömer GÖLER'ın tez çalışması Kimya Anabilim Dalında YÜKSEK LİSANS tezi olarak kabul edilmiştir.

JÜRİ

ÜYE
(TEZ DANIŞMANI) : Yrd. Doç. Dr. Fabienne DUMOULIN

ÜYE : Prof. Dr. Ayşe Gül. GÜREK

ÜYE : Yrd. Doç. Dr. Derya TOPKAYA TAŞKIRAN

ONAY

Gebze Teknik Üniversitesi Fen Bilimleri Enstitüsü Yönetim Kurulu'nun

...../...../..... tarih ve ...../..... sayılı kararı.

İMZA/MÜHÜR

Doç. Dr. Arif Çağdaş AYDINOĞLU
Gebze Teknik Üniversitesi
Fen Bilimleri Enstitüsü Müdürü

SUMMARY

Treatment of cancer is one of the hottest topics of research for our time. There are number of different ways to approach the problem, one of which is through nanotechnologies, specifically nanomedicine. Nanoparticles are being used in drug delivery systems thanks to their multiple advantages such as but not limited to: the ease of manipulation of size and surface characteristics which could be used for both passive or active drug targeting, controlled and sustain release during transportation as well as the location of the release, choosing an appropriate matrix and alteration of distribution in order to clear from the body help to increase therapeutic efficacy and to decrease possible side effects. Among nanoparticles, especially Periodic Mesoporous Organosilica ones (nanoPMOs) proved to be of high interest due to their remarkable biocompatibility and versatility.

Photodynamic Therapy (PDT) has proven to be effective against cancer and third generation of photosensitizers are being researched to combine their properties with imaging, targeting, photodynamic action, synergic combinations with other therapeutics or two-photon excitation.

Phthalocyanines (Pcs) have huge advantages compared to the existing photosensitizers. Their adsorptions are at longer wavelengths, they have extraordinary stability, superior aggregation tendency and two-photon excitation allow us better imaging. In addition, and so far, Pc-based nanoPMOs are not reported in literature.

Since the position and length of the spacers between the Pc core are likely to affect the properties of the ultimately prepared Pc-based nanoPMOs, alkynated zinc Pcs with different spacer units in peripheral and non-peripheral positions have been designed and prepared to be used as building blocks of nanoPMOs by further click reactions.

KeyWords: Phthalocyanine; Periodic Mesoporous Organosilica Nanoparticle (nanoPMO); Photodynamic Therapy (PDT); Alkynyl.

ÖZET

Günümüzde kanser tedavisi en çok çalışılan araştırma konulardan biridir. Bu konudaki birçok farklı yaklaşımdan bir tanesi de nanoilaçlar ve özellikle nanoteknolojidir. Nanoparçacıklar ilaç yapımında kullanılmaya başlandığından beri pasif ve aktif ilaç hedeflenmesinin kontrolü, ilaç boyutunun ayarlanması, yüzey karakteristiğinin değiştirilmesinde, ilacın geçişi, uygun bölgede salınması, uygun matrikslerin seçilmesiyle vücut için terapötik etkisinin arttırılmasının yanı sıra yan etkilerinin azaltılması gibi birçok avantaj sağlamıştır. Nanoparçacıklar içerisinde özellikle Periyodik Mezopor Organosilika (nanoPMO) olanları biyo-uyumlulukları ve çok yönlülüğü nedeniyle büyük dikkat çekmiştir.

Fotodinamik terapinin (PDT) kansere karşı etkisi kanıtlanmıştır ve araştırmacılar üçüncü nesil fotoduyarlaştırıcı ajanların, görüntüleme, fotodinamik aksiyonları, diğer terapötikler ile olan sinerjik kombinasyonları ve ikili foton uyarımları gibi özelliklerini birleştirmek için araştırmalara başlamışlardır.

Ftalosiyaninler (Pcs) mevcut fotoduyarlaştırıcı ajanlarla kıyaslandığında önemli avantajlara sahiptir. Daha uzun dalga boylarındaki absorbsiyonları, yüksek kararlılıkları ve üstün agregasyon yetenekleri iyi görüntüleme sağlamakla birlikte, iki foton uyarımına olanak tanırlar. Buna ek olarak literatürde şu ana kadar Pc-temelli nanoPMO'lara rastlanmamıştır.

Pc çekirdek bölgesindeki arabağlayıcıların konumu ve uzunluğu en nihayetinde hazırlanacak olan Pc-temelli nanoPMO'ların özelliklerini değiştirebileceğinden, periferal yada periferal olmayan pozisyonlarda farklı arabağlayıcılar ile alkillenmiş, nanoPMO'ların yapı taşları olarak kullanılmak üzere ileride gerçekleşecek klik reaksiyonları için çinko Pc' ler tasarlanıp, hazırlanmıştır.

Anahtar Kelimeler: Ftalosiyanin; Periyodik Mezopor Organasilika Nanoparçacık (nanoPMO); Fotodinamik Terapi (PDT); Alkinil.

ACKNOWLEDGMENTS

I would like to thank my advisor Asst. Prof. Dr. Fabienne Dumoulin for her teachings and continuous support. I will always be thankful for the role she has played in both my professional and personal developments. I would like to thank Prof. Dr. Vefa Ahsen for being my co-advisor, also having me on his project and being very patient with my questions.

I am deeply grateful to committee members for their continuous support, valuable feedback, and great contributions; Prof. Dr. Ayşe Gül Gürek, Asst. Prof. Dr. Derya Topkaya Taşkıran, Assoc. Prof. Dr. Ümit İşçi, Dr. Mehmet Menaf Ayhan and Assoc. Prof. Dr. Yunus Zorlu. I would also like to express my gratitude to the whole GTU Department of Chemistry for the friendly environment they have provided.

I owe special thanks to Zeynel Şahin for his continuous support during laboratory experiments and helping with MestReNova. I could not forget Tuğba Korkmaz Küçük for she was always dependable. I would also like to thank Dr. Emel Önal for her help during spectral measurements. I must also acknowledge my colleagues Dr. Gülçin Ekineker and Serkan Alpugan for their support during my initial adaptation to laboratory.

I could not thank enough to my dear girlfriend Dr. Ayşe Mine Yılmaz, not only she has provided moral support but also has helped me during this work on many occasions. Of course, I would also to thank my parents and my sister for their never-ending patience and moral support.

The Scientific and Technological Research Council of Turkey (TUBITAK) is gratefully acknowledged for their financial support (France-Turkey Bilateral PIA-Bosphorus 115Z864).

INDEX

ABBREVIATIONS AND ACRONYMS

Abbreviation or Acronym		Explanation
DBU	:	1,8-Diazabicyclo [5,4,0] undec-7-ene (1,5-5)
DBN	:	1,5-Diazabicyclo[4.3.0]non-5-ene
DMAE	:	2-(Dimethylamino)ethanol
DMF	:	Dimethyl formamide
FT-IR	:	Fourier Transform Infrared
DMSO	:	Dimethyl sulfoxide
EtOH	:	Ethanol
eq.	:	Equivalent
HOMO	:	Highest Occupied Molecular Orbital
LUMO	:	Lowest Unoccupied Molecular Orbital
H_2Pc	:	Metal Free Phthalocyanine
MPc	:	Metallated Phthalocyanine
Hz	:	Hertz
J	:	Coupling Constant
LUMO	:	Lowest Unoccupied Molecular Orbital
m	:	Multiplet
MALDI-TOF	:	Matrix-Assisted Laser Desorption/Ionization Time-of-Flight
MHz	:	Megahertz
mL	:	Milliliter
mp	:	Melting Point
MPc	:	Metallated Phthalocyanine
m/z	:	mass-to-charge ratio
PDT	:	Photodynamic Therapy
nanoPMO	:	Periodic Mesoporous Organosilica Nanoparticle
MSN	:	Mesoporous Silica Nanoparticle
EPR	:	Enhanced Permeability and Retention
o-DCB	:	Ortho Dichloro Benzene

LIST OF FIGURES

LIST OF TABLES

1.INTRODUCTION

Clinically approved, minimally invasive Photodynamic therapy (PDT) is a therapeutic procedure that utilizes a selective cytotoxic activity toward malignant cells [1]. It is based on the conversion of oxygen into its singlet radical toxic state upon the irradiation of a photosensitizer at appropriate wavelengths. It is particularly used against cancer and the third generation of photosensitizers are being developed [2] to combine several properties such as imaging, targeting, specific excitation in the therapeutic window or synergic combinations with other therapeutic effects.

Scientists have been showing great interest to phthalocyanines thanks to their unusual chemical and physical properties since their first laboratory synthesis in 1907 [3]. Their distinct functionality comes from the aromatic system composed of 18-π electrons and their ability of coordination with most of the metal atoms if not all. Nowadays, their versatility is being used in many different fields ranging from dyes to cancer therapy or to nanotechnology. PDT is one of the important applications.

Nanotechnology provides diverse design features that inspires exploration for cancer theranostics [4]. Nanoparticle drugs having a sizeable loading capacity, ability to protect the payload from degradation, or controlled / sustained release and also large surface area to conjugate targeting ligands are a few examples of that diversity. Nano-sized medicines also accumulate preferentially in tumor tissue thanks to the particular leaky nature of tumor neovasculature and are retained due to reduced lymphatic drainage. This process is known as enhanced permeability and retention (EPR) effect [5].

Periodic Mesoporous Organosilica Nanoparticles (nanoPMOs) proved to be of high interest in nanomedicine [6]. They can be formed by cross-linking silylated organic fragments and can be further functionalized and/or encapsulate other molecules. They are remarkable by their biocompatibility and versatility.

As of today, there are porphyrin based nanoPMOs for PDT [6-12] but no phthalocyanine based nanoPMOs have been reported in the literature. It has been assumed that phthalocyanine-based nanoPMOs would have advantages compared to the existing porphyrin-based nanoPMOs: their maximum absorptions would be at longer wavelengths, their superior aggregation tendency and two-photon excitation would allow better imaging.

As it is the first time that phthalocyanines will be used for the preparation of nanoPMOs, a number of structural parameters have to be explored such as the position of the connexion on the macrocycle and their distance to the phthalocyanine macrocycle. Each of these structural variations is likely to have an impact on the desired aggregation of the phthalocyanines and on the porosity and size of the nanoPMOs.

2. THEORETICAL BASIS AND LITERATURE

2.1. Phthalocyanines

2.1.1. Introduction to Phthalocyanines

Phthalocyanines, also known as tetrabenzo tetraaza porphyrins are planar macrocycles consisting of four iminoisoindoline units. They have 18 π electrons delocalized over the macrocycle system (Fig. 2.1) [13] that confer them exceptional stability as well as outstanding electronic, spectroscopic and physical properties [14]. Ability to form complexes with most of the metals of the periodic table not only tailors these properties but also allows them to have a wide range of applications [15].

Phthalocyanines are tetrapyrrolic derivatives. The simplest member of tetrapyrrole family is called porphyrin, which contains four pyrrole groups. Phthalocyanines have benzene (isoindole subunits) and nitrogen atoms attached to pyrrole groups hence its name tetraaza tetrabenzo porphyrin (Fig. 2.1).

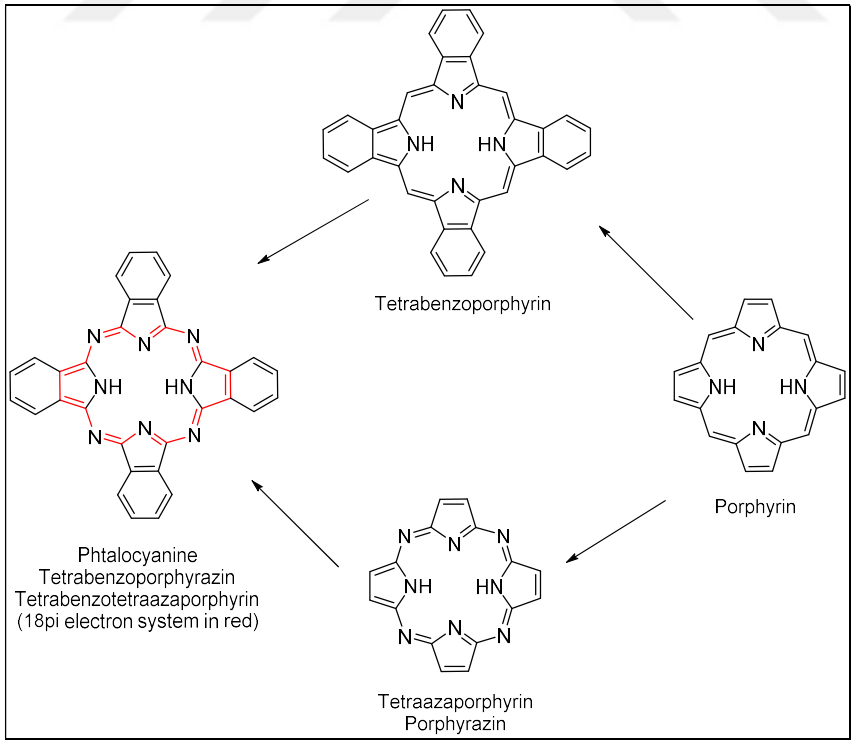

Figure 2.1: Macrocycle of porphyrin and its analogs.

Phthalocyanines are widely used as dyes in industry due to having vibrant, deep colors ranging from blue to green thanks to their specific absorption wavelengths of the visible light and near infra-red region of the spectrum (between 650 nm – 750 nm). It is one of the most striking characteristic property of phthalocyanines at the same time it is the base of their extraordinary optical properties [14] which could be tailored via different designs of the structures.

Solubility in common organic or aqueous solvents was one of the problems in early examples phthalocyanines since they were unsubstituted. Nevertheless, research boosted tremendously after the synthesis of soluble substituted phthalocyanines. Substituents of the macrocycle can be categorized in 3 groups depending upon their positions; peripheral or non-peripheral, and/or axial (Fig. 2.2). 4 and/or 5 substituted phthalonitriles produce peripheral phthalocyanines, whereas 3 and/or 6 substituted phthalonitriles produce non-peripheral ones. Ligands or substituents on the metal center are classified as axial position.

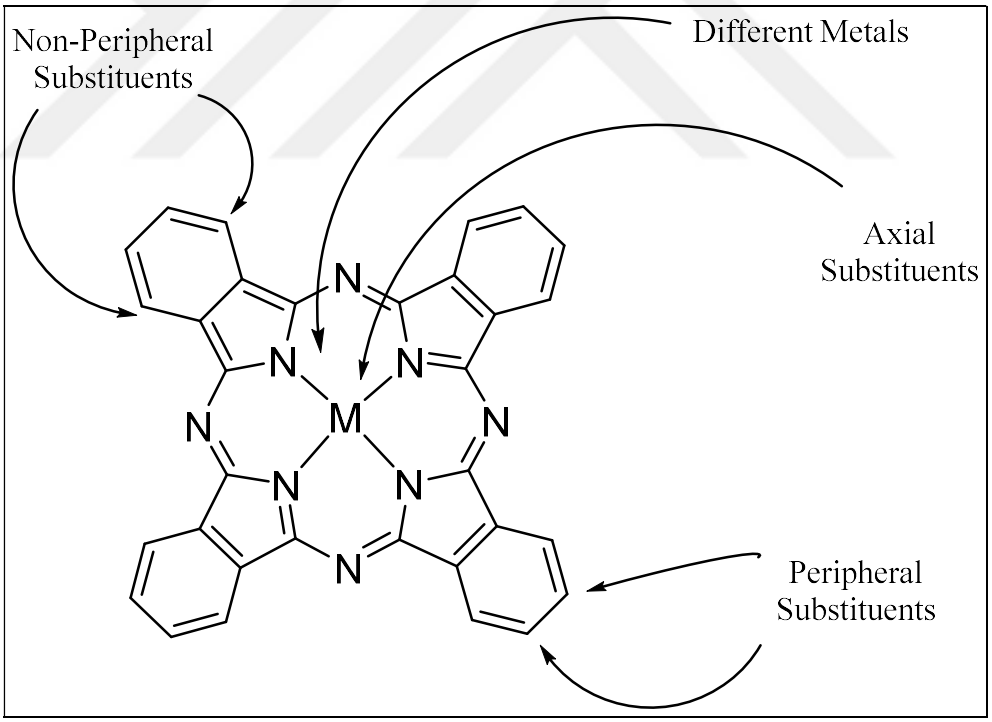

Figure 2.2: Substituent positions for phthalocyanines.

2.1.2. The History of Phthalocyanines

As quite a few of the worthwhile discoveries are found by accident so does the first metal-free phthalocyanine (H_2Pc). It was obtained in yields of less than 1% as a by-product during the preparation of 2-cyanobenzamide in 1907 by A. V. Braun and J. Tcherniac at the South Metropolitan Gas Company, London [16]. Twenty years later in 1927, Diesbach and Weid from Fribourg University identified a blue compound [17] which turned out later to be metal free and copper phthalocyanines. The events leading to the elucidation of the phthalocyanine structure starts in 1928 at Scottish Dyes Ltd. Grangemouth plant during phthalimide production from phthalic anhydride [18]. A blue-green substance was observed on a crack of a steel reactor due to a leakage from the inside. In 1934 Linstead *et al*, prepared series of metallated phthalocyanines and enlighten their structures for the first time [19, 20]. Linstead gave the name phthalocyanine due to its oily nature (phthal) and its blueish color (cyan).

Industrially, first pigment (blue) from copper phthalocyanine was produced in 1935 by an English company accompanied by others in Germany and USA. Today, peripheral or non-peripheral copper phthalocyanine derivatives, and approximately 70 different other metals are being used as central atoms in all kinds of phthalocyanines [21].

2.1.3 Synthesis of Phthalocyanines

Even though phthalocyanines could be synthesized from the plethora of starting compounds (Fig. 2.3), most preferred and common of them are phthalonitriles. In order to synthesize metal free phthalocyanines, suitably substituted phthalonitrile precursors are refluxed in high boiling point solvents such as DMF or pentanol, or heated up without solvent. Synthesis of metallated phthalocyanines requires metal ions, generally in the form of metal salts. Template effect from metal ions yields metallated phthalocyanines.

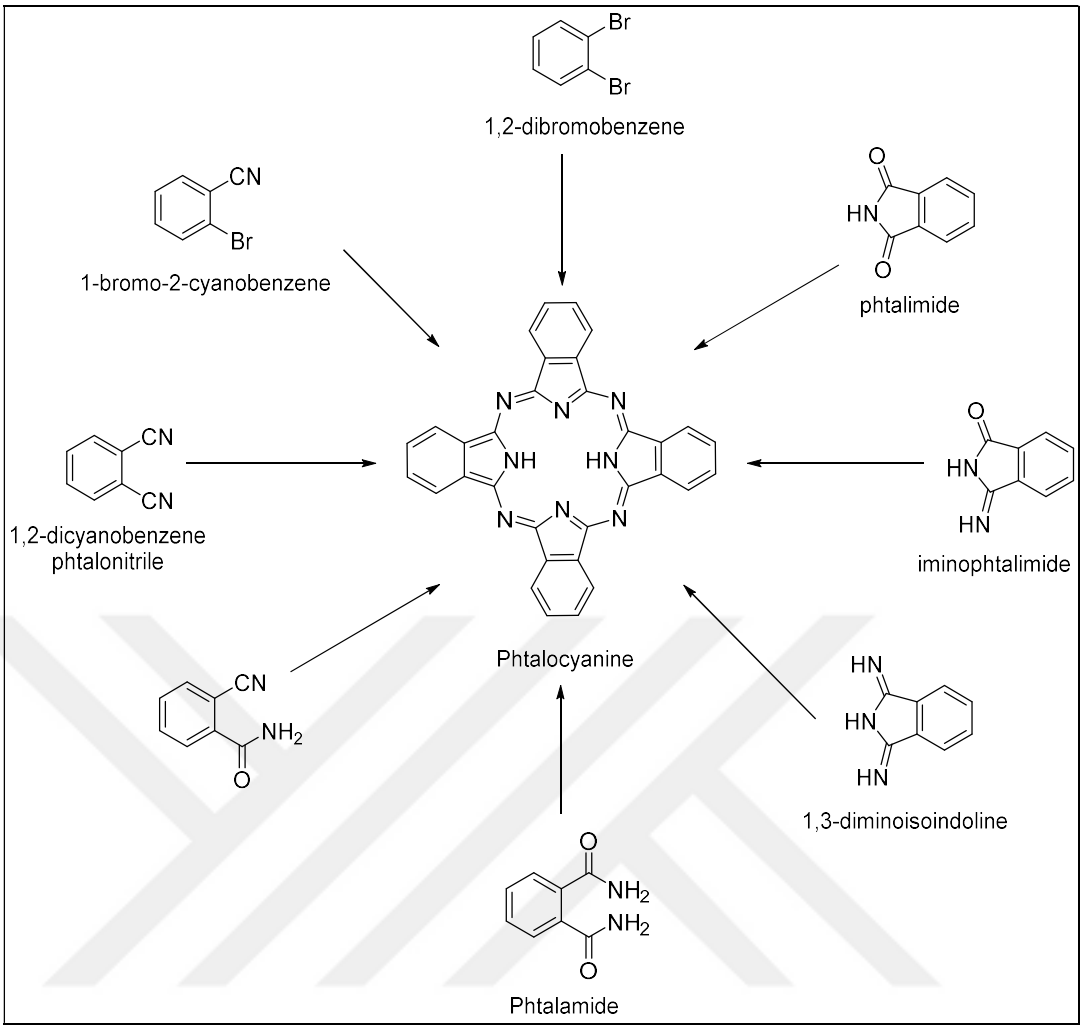

Figure 2.3: Common starting compounds for synthesis of phthalocyanines.

Most common method of synthesis for symmetric phthalocyanines (A_4) is again through cyclotetramerization of suitably substituted phthalonitriles. Phthalonitriles could be heated up directly or could be refluxed in high boiling point solvents with corresponding metal salts. Metal ions in the reaction, acts as a template for cyclotetramerization of the corresponding phthalonitrile and yields the metallated phthalocyanine as product. The most common solvents are *n*-pentanol, DMF, DMAE or *o*-DCB. Also, the presence of bases like DBU or DBN boosts their formation [22]. It should also be noted that, in comparison to conventional techniques, microwave-promoted reactions speed up the process and increase the yield [23].

As it can be seen from Figure 2.4 below, cyclotetramerization of monosubstituted phthalonitriles yields symmetric phthalocyanines as a mixture of four constitutional isomers with different symmetries. It is theoretically possible to isolate

the constitutional isomers of symmetric A_4 phthalocyanines, however, it is unclear at this stage as to how it would affect the nanoPMO structure.

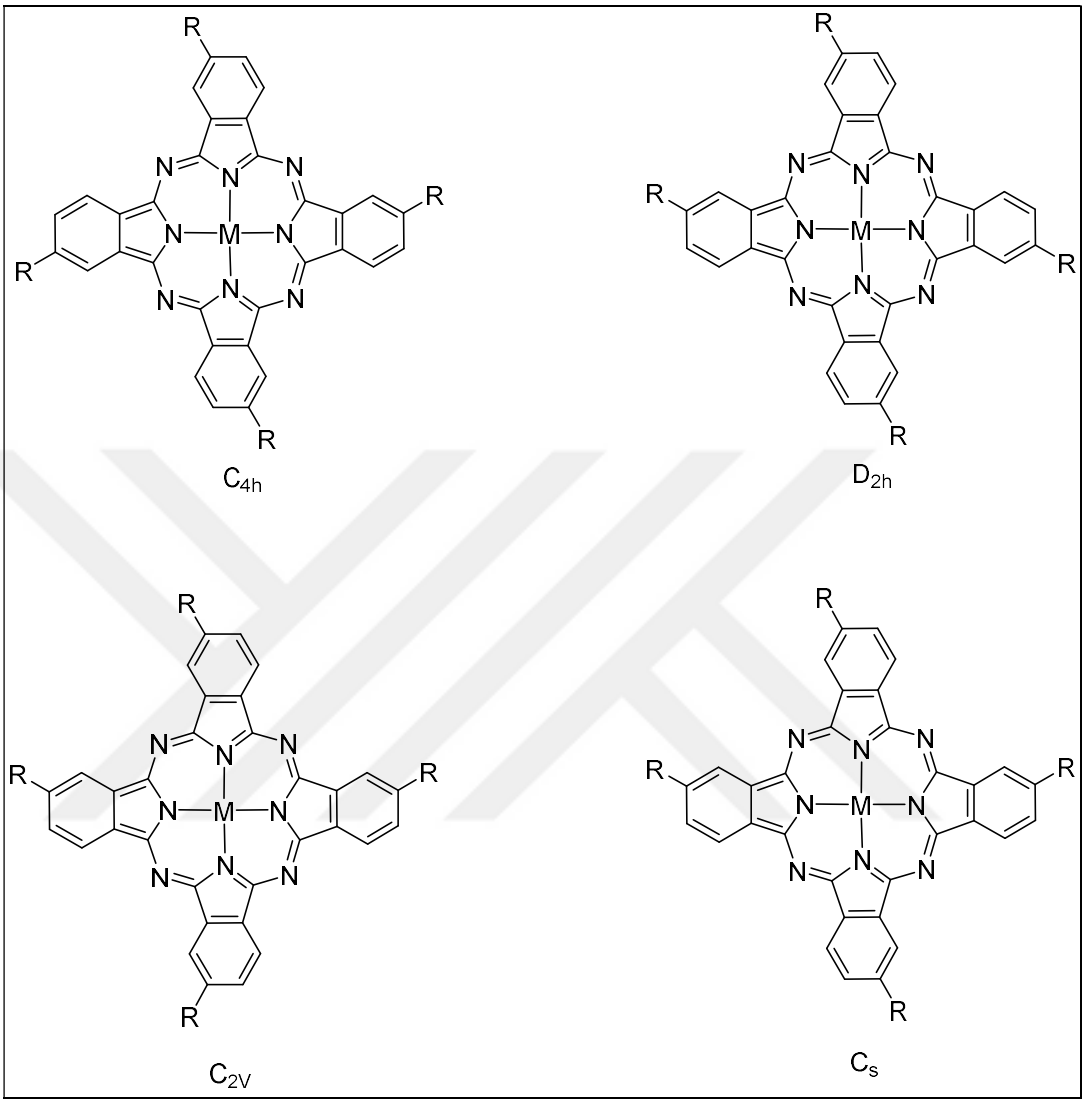

Figure 2.4: Four constitutional isomers of symmetric A4 phthalocyanines.

Synthesis of other types of phthalocyanines such as asymmetric are beyond the scope of this work so they are not mentioned here.

2.1.4. Properties of Phthalocyanines

2.1.4.1. Chemical and Physical Properties of Phthalocyanines

Phthalocyanine cores which are planar macrocycles consisting of four iminoisoindoline units, are quite strained. Their chemical properties vary depending on the central metal and substituents [24]. They are more susceptible to redox reactions compared to porphyrins. Reduction or oxidation could be reversible or irreversible and could take place at the central metal, the macrocycle or at the substituents. Almost all phthalocyanines oxide into phthalimide if exposed to potassium permanganate or nitric acid [25].

The most noteworthy physical features of phthalocyanines are their exceptional stability and color ranging usually from blue to green. Main reason for color differences is in the chemical and crystalline structures [26] namely α-and β-forms (Fig 2.5), which affect their electronic absorption spectra.

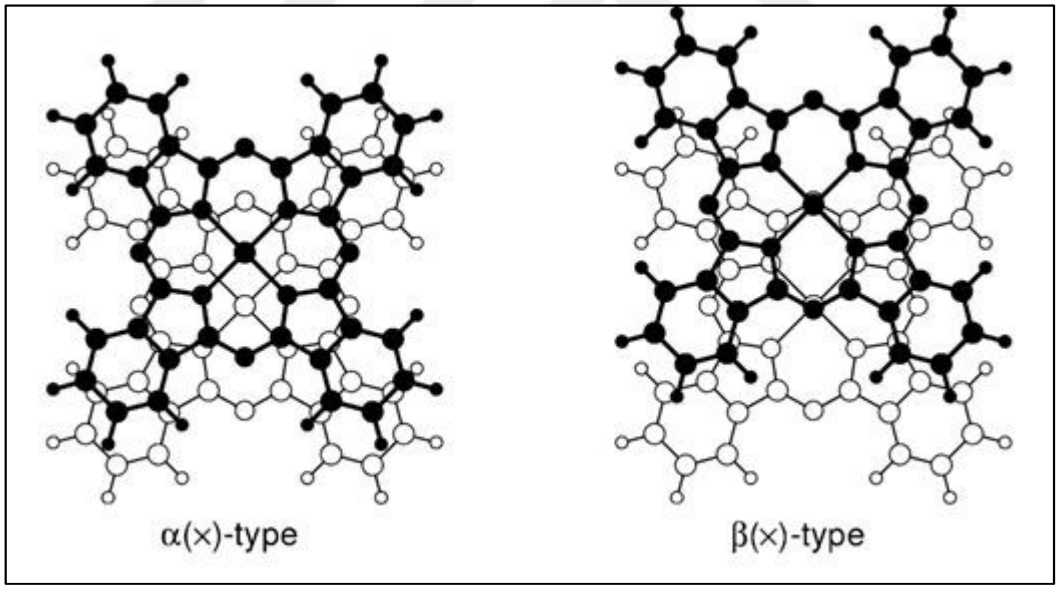

Figure 2.5: Crystalline forms of phthalocyanines.

2.1.4.2. Characterization of Phthalocyanines

Infrared spectroscopy of phthalocyanines is quite important. Metal free phthalocyanines have N-H stretching around 3300 cm^{-1}, N-H bending around 1540 cm^{-1}, C-C and C-N vibrations around 1650-1200 cm^{-1} [27]. Substituent specific vibrations gain importance during characterization of substituted phthalocyanines.

NMR spectroscopy is a very essential tool in characterization of soluble phthalocyanines if the central atom is not paramagnetic like copper. Due to magnetic anisotropy, the resonance of the protons outside the aromatic rings appears downfield whereas the resonance of the protons inside or atop the aromatic ring appears upfield [28]. The ^{1}H NMR spectra of phthalocyanines are known to show large diamagnetic ring current shifts due to the macrocyclic π-system. The signals of aromatic protons of phthalocyanines appear downfield. Protons of axially bonded groups show a large shift to upfield [29].

Mass spectroscopy is one of the most powerful characterization tool of phthalocyanines. It is possible to see the exact molecular weight of the material.

2.1.4.3. Spectroscopic Properties of Phthalocyanines

Gouterman's four orbital model also known as linear combination of atomic orbitals (LCAO) helps us understand the electronic structure of the macrocycles of the phthalocyanines [30]. Absorption spectra displays two specific bands, namely Q band and Soret band (B) (Fig. 2.6). Usually located between 600 nm and 750 nm, the Q band is responsible for the color of phthalocyanines. $\pi \rightarrow \pi^*$ transitions from HOMO to LUMO orbitals are responsible for Q bands [30]. Q bands are also effected to a certain degree by a few parameters such as the nature of the metal center, oxidation state of the metal center, axial ligation, solvents, substituents, aggregations and conjugations [31]. So, analysis of the Q band's position and shape provides a lot of information about the phthalocyanines (Fig. 2.6) such as if its metallated or not [31, 32]. B bands are observed around 350 nm thanks to $\pi \rightarrow \pi^*$ transitions from the lower energy molecular orbitals to LUMO [32].

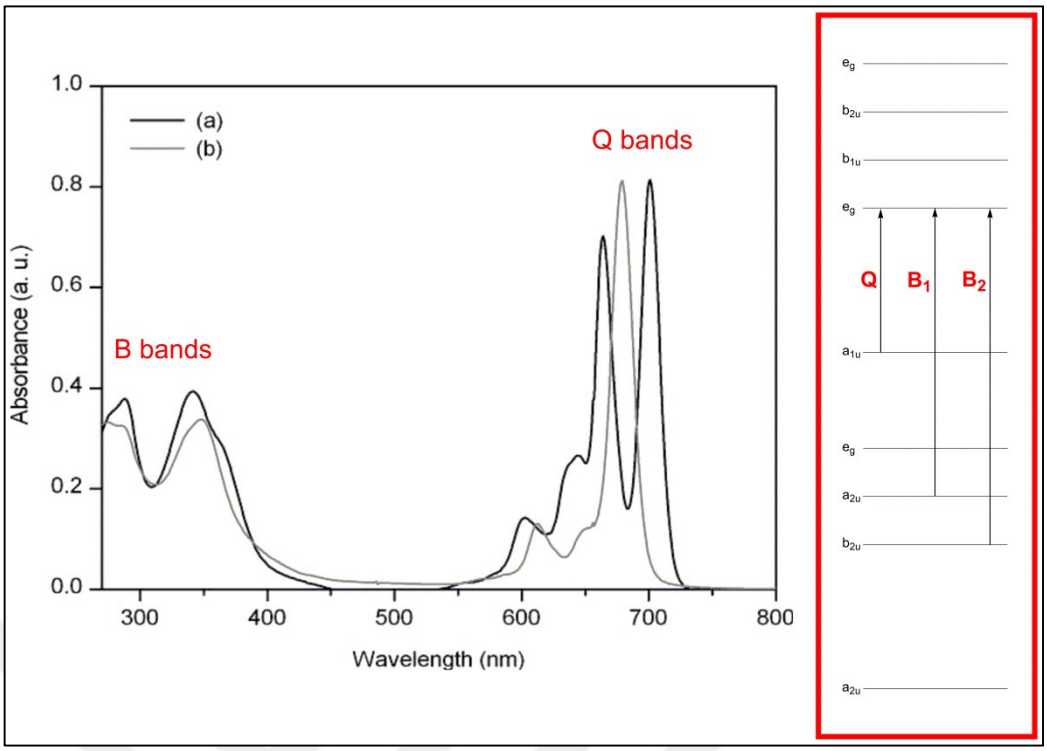

Figure 2.6: Typical UV-vis spectra of metallated (b) and metal free phthalocyanine (a). (Reproduced with the authorization of Royal Society of Chemistry).

The emission of light by a substance from singlet ground state to a singlet excited state is called fluorescence after it has absorbed light or other electromagnetic radiation [33]. Phthalocyanines are well-known fluorophores and their fluorescence property has been studied extensively.

Most of the time the emitted light has higher wavelength, lower frequency meaning lower energy, than the absorbed light. One of the most well-known example of fluorescence in forensics, could be observed on blood spatters. Even after blood is cleaned with water, amino acid residues containing phenylalanine, tyrosine, and/or tryptophan remains behind. These amino acids could be seen if exposed to UV light [34]. This is due to the amino acid residues absorbing radiation in the ultraviolet region of the electromagnetic spectrum thus invisible to the human eye, while the emitted radiation is in the visible part of the spectrum, which gives the fluorescence substance in the residue a distinct color under UV light [33].

Fluorescent substances cease to glow as soon as the radiation source ceases. Once a molecule has absorbed energy in the form of electromagnetic radiation, there are a number of routes by which it can return to ground state. Jablonski diagram (Fig. 2.7) shows a few of these processes. If the photon emission occurs between states of the same spin state fluorescence occurs. If the spin state of the initial and final energy levels is different the emission is called phosphorescence. Nonradiative deactivation processes are also significant here: internal conversion (IC) and intersystem crossing (ISC). Internal conversion is the radiationless transition between energy states of the same spin state and intersystem crossing is a radiationless transition between different spin states.

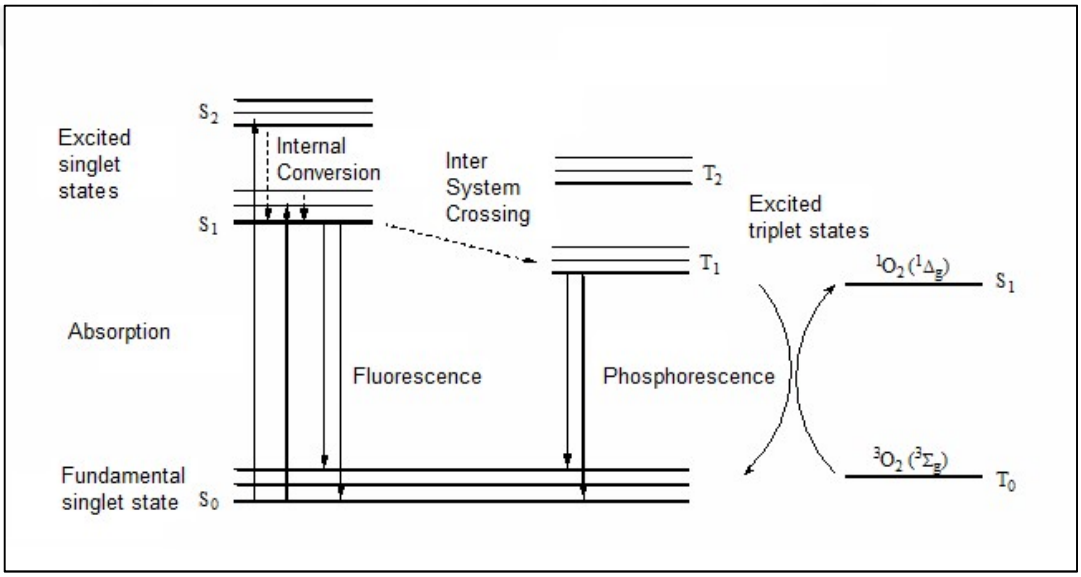

Figure 2.7: Typical Jablonski energy diagram. (Reproduced with the courtesy of Fabienne Dumoulin).

Spectroscopic properties of phthalocyanines can be tuned through structural modifications on the macrocycle or at the metal center. One possible structural modification is on the substitution pattern: the attachment atom, the hydrophilicity or hydrophobicity, the introduction of functional groups and the bulkiness of the substituents. The position, peripheral or non-peripheral, as well as the number of substituents (Tetra or Octa) also have effects on the spectroscopic properties. The second type of possible structural modification is the metal center. Zn gathers several advantages, mainly its diamagnetism suitable for singlet oxygen generation thanks to richly populated triplet excited state and syntheses of Zn phthalocyanines are relatively easy and high yielding. These properties make Zn, one of the most common metals for PDT. Isomerically pure, octasubstituted phthalocyanines **A-D** in Figure 2.8 [35], are very good examples to show these modification effects on the macrocycle.

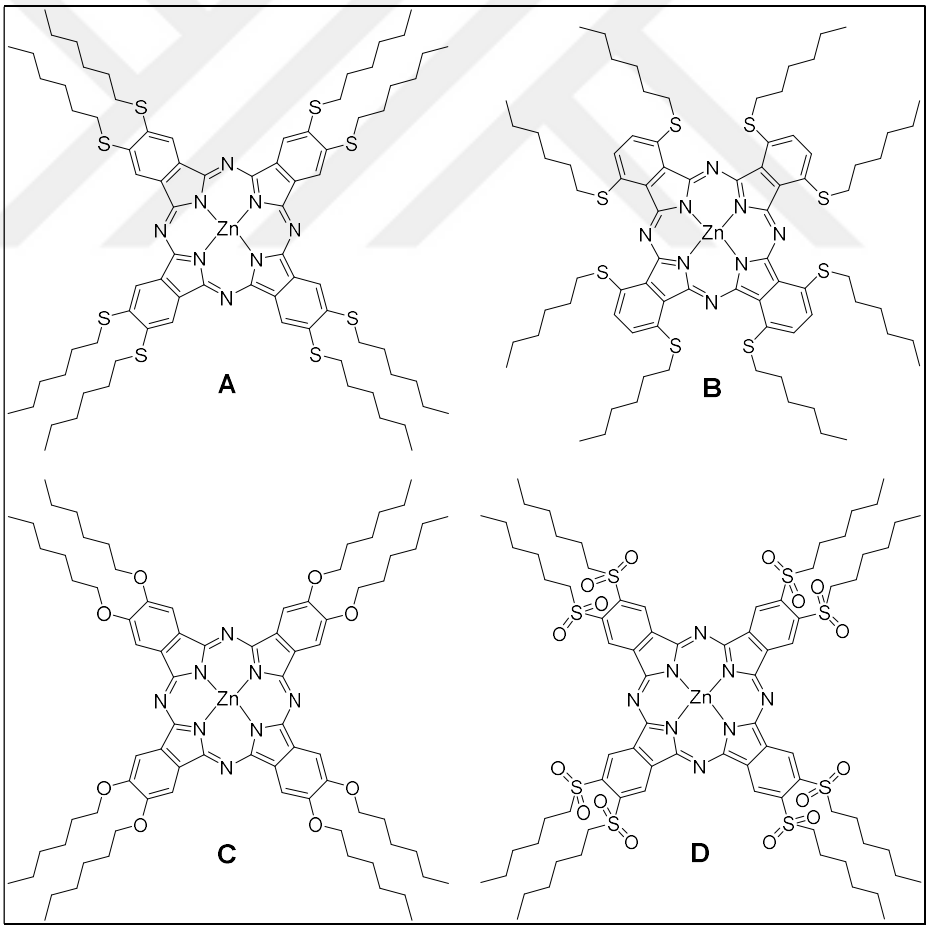

Figure 2.8: Zinc phthalocyanine derivatives **A-D**. (Reproduced with the authorization of Royal Society of Chemistry).

All octasubstituted phthalocyanines in Figure 2.8, were designed to be isomerically pure to avoid regioisomeric effects and to have variations only at the attachment point: a hexyl chain is attached by a sulfur atom via a sulfanyl function in peripheral (**A**) and non-peripheral (**B**) position, or by an oxygen atom via an ether function (**C**) or by a sulfonyl function (**D**) in peripheral positions. Thus, it was possible to investigate the substitution pattern effects such as: the substituent position of **A** and **B**, the electron donating and withdrawing character of **A** and **D** and the donating force of **A** and **C**.

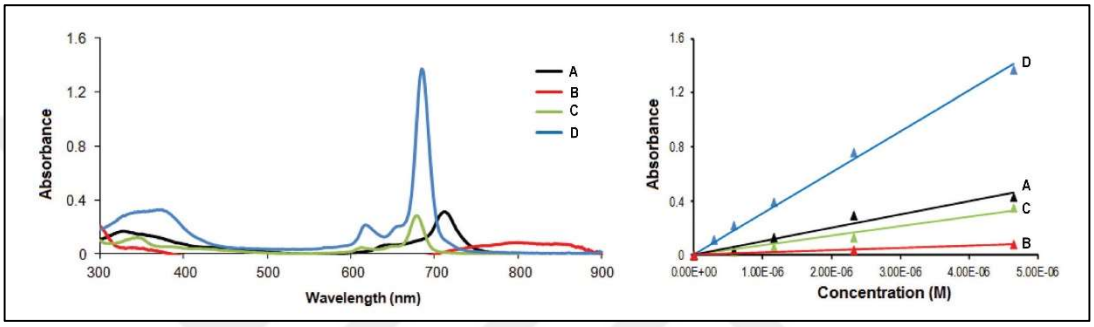

Figure 2.9: UV-Vis spectra of **A-D** in DCM (4.5 µM) and plot of absorbance vs concentration. (Adapted with the authorization of Royal Society of Chemistry).

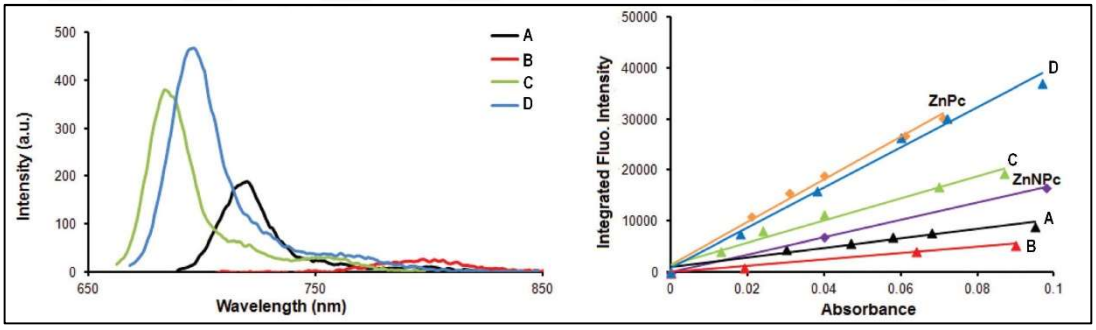

Figure 2.10: Fluorescence emission spectra of **A-D** in DCM (normalized absorbance values ~0.04) and plot of integrated fluorescence intensity vs absorbance. (Adapted with the authorization of Royal Society of Chemistry).

Shifted Q and Soret bands can be seen in Figure 2.9, difference in fluorescence emission spectra and their quantum values can be seen in Figure.2.10. Φ_Δ values are 0.66, 0.52, 0.32, 0.06 for **D** > **C** > **A** > **B** respectively, which demonstrates the strong effect of substitution pattern [35].

2.1.5 Applications of Phthalocyanines

As of 2012, over 95% of world production of all phthalocyanines are used as colorants [36] due to their exceptional chemical as well as thermal stability and thanks to their very vibrant, deep shades of green and blue colors [18]. Later researches have shown that they can be adopted to be used in other areas as well mostly due to their versatility in design. Thanks to their strong intermolecular π-π interactions, they have found usage as semiconductors [37]. They could also be tailored to be used as various kinds of sensors since in their metallated form, they show conductivity and they can form organized structures used as organic thin-film transistors [38]. If they coordinate a redox active metal ion, they can be used for catalytic oxidation of various organics such as, alkanes, olefins and aromatics [39-43]. They could be used as gas sensors since their films could be tailored to interact with various gases by the help of chemical affinity, chemical reaction or adsorption [44]. Other areas of applications include materials for non-linear optics [45-47], liquid crystals [48-50], electrophotography [51], optical data storage [52], fuel cells [53], photovoltaic cells [54], photo-electrochemical cells [55] and electrochromics [56].

Among these applications, the most of important aspect for this work is their high singlet oxygen and/or reactive oxygen species quantum yields, when appropriately metallated. Together with red-shifted Q-bands, this property makes phthalocyanines very good candidates as photosensitizers in photodynamic therapy [57]. PDT has proven to be effective against certain types of cancer and its now one of the well accepted treatments along with surgery, chemo therapy and radio therapy [58]. Third generation of photosensitizers is being researched to combine their properties with imaging, targeting, photodynamic action, synergic combinations with other therapeutics or two-photon excitation.

2.2. Silica Based Nanoparticles

2.2.1. Introduction to Silica Based Nanoparticles

Silica based nanoparticles can be divided into two main groups,

i) Mesoporous Silica Nanoparticles (MSN).
ii) Periodic Mesoporous Organosilica (PMO) nanomaterials.

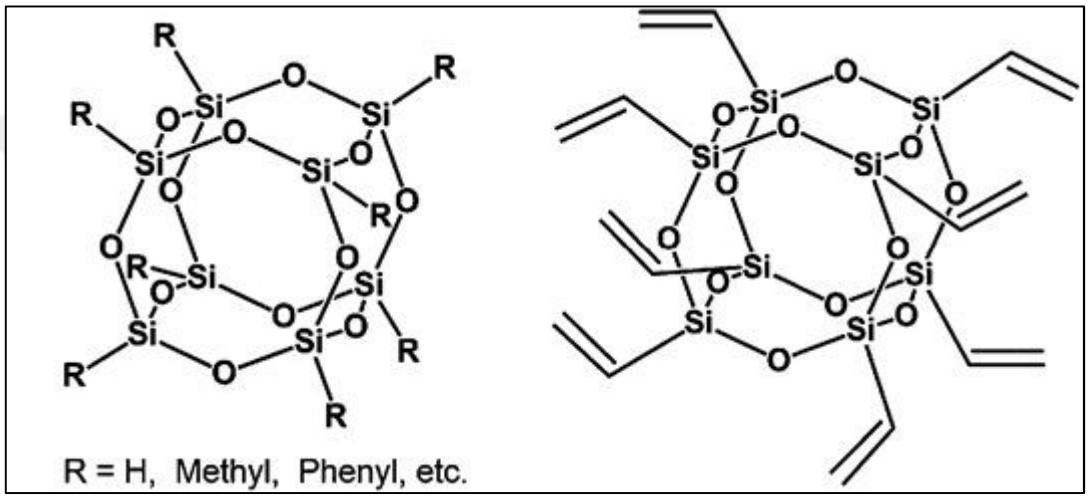

Figure 2.11: Silsesquioxane framework examples.

They are both mesoporous (pore sizes ranging from 2 nm - 50 nm.[59]) and their framework is based on silsesquioxanes (Fig. 2.11). The main difference between MSN and PMO is that the latter contains organic functional groups covalently linking siloxane groups (Fig. 2.12) [60]. Periodicity of PMOs comes from repeating units appearing at regular intervals, hence the name, periodic mesoporous organosilica.

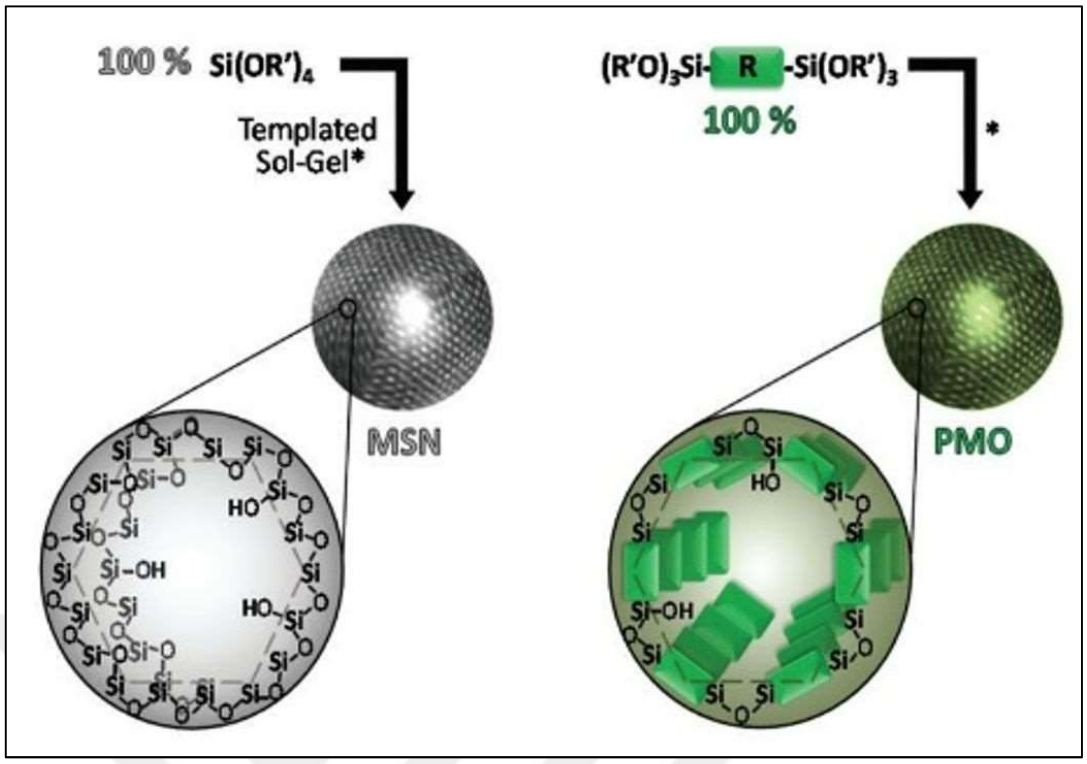

Figure 2.12: Difference between MSN and PMO. (Adapted with the authorization of Royal Society of Chemistry).

Main focus of this work will be PMOs but understanding MSNs is also important. MSN primal forms were first patented around 1970 [61], they mostly stay dormant more than 20 years until their reproduction in 1992 by Mobil Oil Company, being named Mobil Crystalline Material (MCM) [62, 63]. The most well-known example is hexagonal structured MCM-41 [64]. Soon after, there were other versions such as Michigan State University Matter-X (MSU-X) and Santa Barbara Amorphous (SBA) [62]. Mesoporous silica particles could be prepared in lots of different morphologies. To name a few, sphere forms [65, 66], hollow spheres [67], wormlike [68], crystal like [69, 70], toroid [71], rope like [72], and gyroid [73]. Their most important aspects for possible applications like drug delivery systems, chromatography or catalysis are the pore structure, morphology and monodispersity [73-78].

In 1999, just 7 years after first commercial MSN and only 1 year after the development of the SBA-type, three research groups (Inagaki [79], Ozin [80] and Stein [81]) independently described the first PMO materials.

2.2.2. Synthesis of PMOs

Although there are numerous ways of synthesizing PMO materials, all of the techniques depend on polycondensation of organics by surfactants exerting a structure-directing effect. They are obtained by the sol–gel process from organo-bridged alkoxysilanes (precursors) in the presence of surfactants (Fig. 2.13) [82].

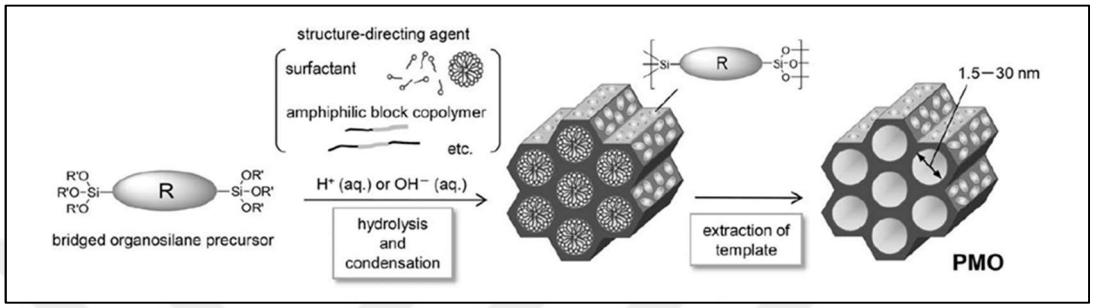

Figure 2.13: PMO synthesis from bridged organosilanes. (Reproduced with the authorization of Royal Society of Chemistry).

Surfactant-templated pores could be expanded with suitable organic molecules which would serve as auxiliary templating agents. Surfactants with longer hydrophobic chains or amphiphilic copolymers could be used to serve as pore-templating. Cetyltrimethylammonium bromide (CTAB) is very popular as surfactant. Figure 2.14 lists different surfactants used in PMO synthesis [83].

Broad array of precursors is available for design of PMOs. In early researches, it was handful of compounds such as ethylene or phenylene. Contemporary researches have widened the available organic bridging groups from hydrocarbons and heteroaromatics to metal complexes [83]. Figure 2.15 lists different precursors used in PMO synthesis [83]. Their high chemical stability thanks to silica framework, flexibility for shaping, controllability in sol-gel condensation and ease of precursor synthesis have made them studied extensively [84-86].

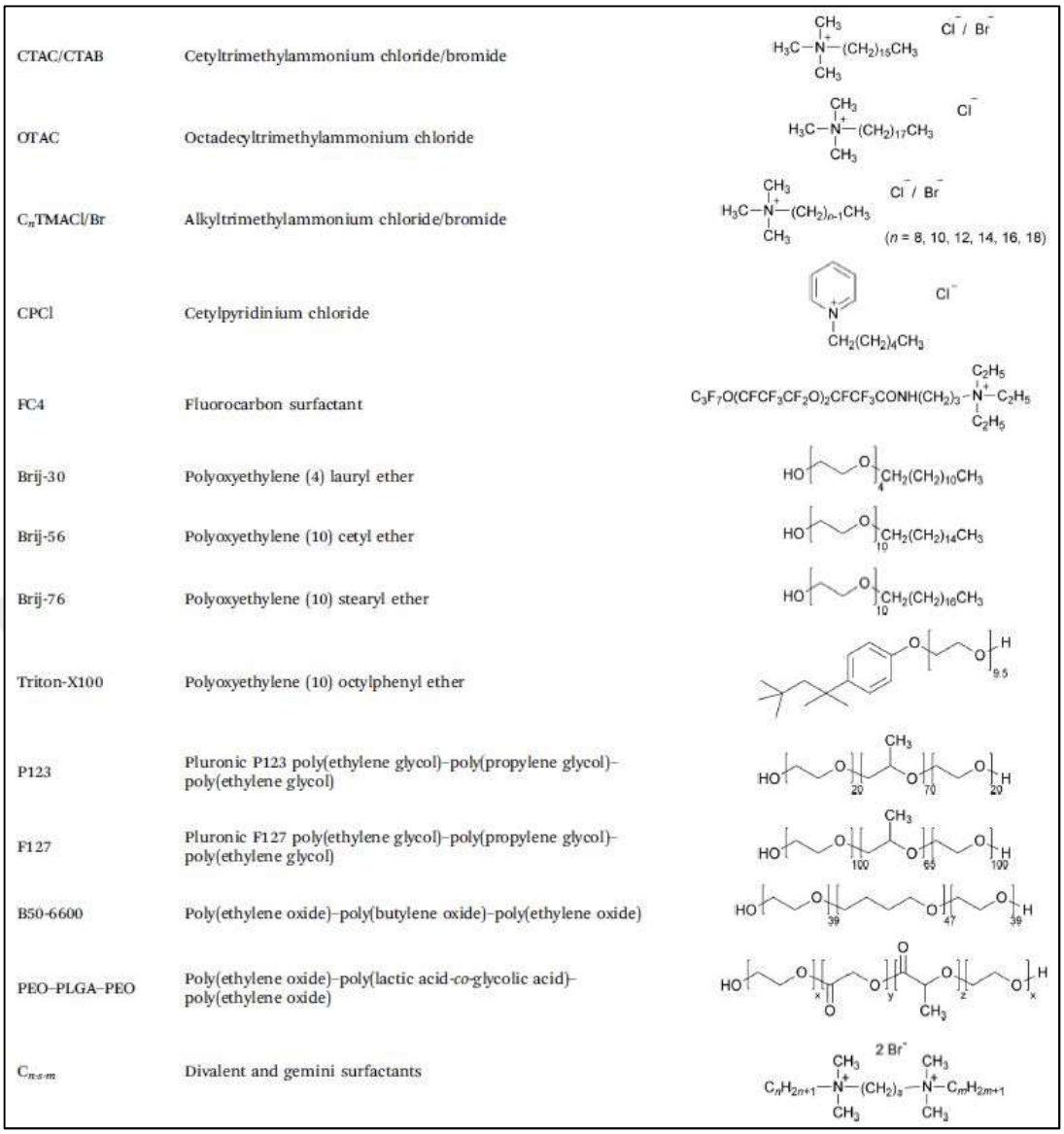

Figure 2.14: Examples of different surfactants used in PMO synthesis. (Reproduced with the authorization of Royal Society of Chemistry).

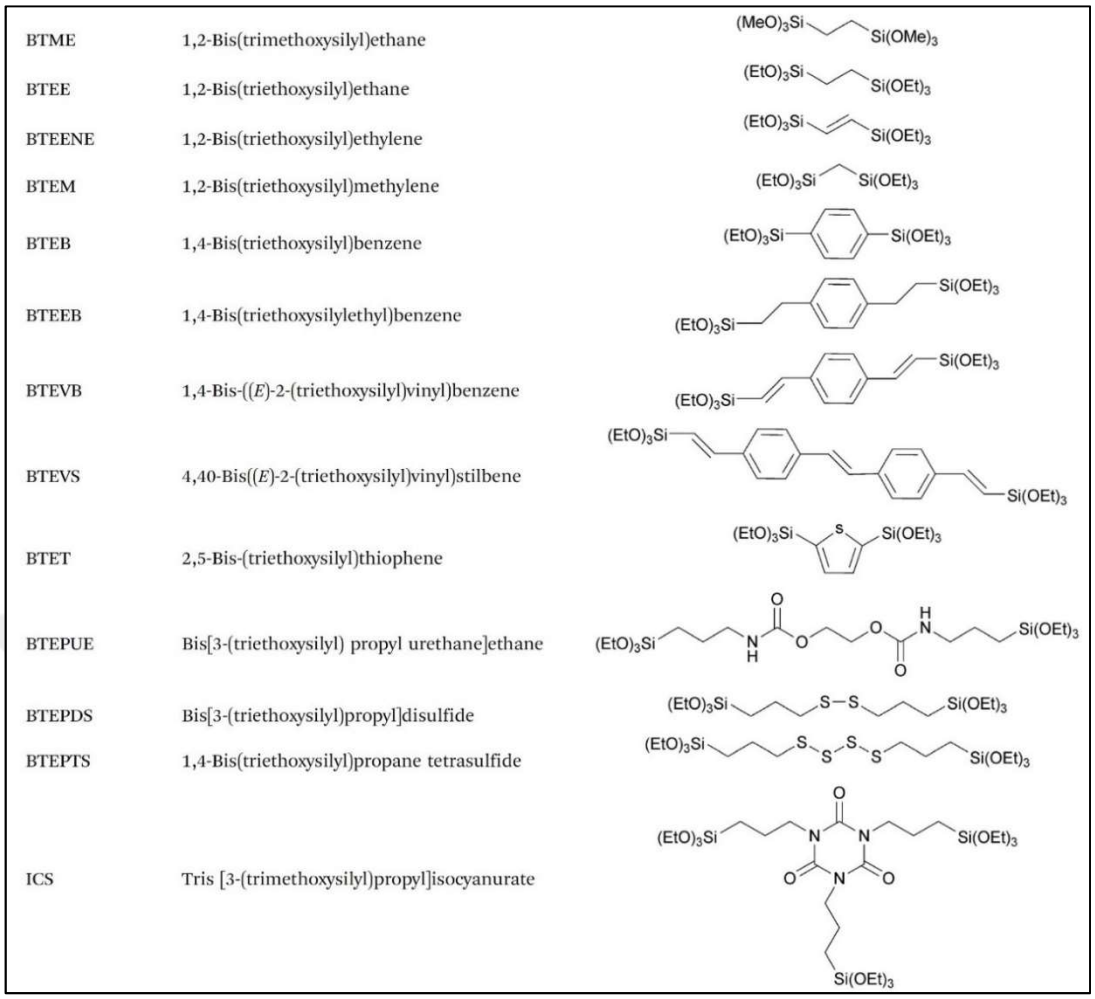

Figure 2.15: Examples of frequently used precursors in PMO synthesis. (Reproduced with the authorization of Royal Society of Chemistry).

$Si(OEt)_3$ or $Si(OMe)_3$ groups could be introduced to precursors in different ways. $Si(OR)_3$ attached thiol groups could be bonded to appropriate precursors [8], amine functionalized precursors could be further modified [12] or click reactions could be employed [87].

2.2.3. Post-Functionalization of PMOs

Bridging groups could be modified after synthesis, which makes PMOs very versatile. Lots of different post-functionalization options exist by use of aromatic or unsaturated bridges. Figure 2.16 lists some of the examples of post-functionalization options on PMO bridges [88]. Classical sulfonation reaction to phenyl groups producing acidic moieties on the PMO [89], sulfonation after a Diels-Alder reaction to a ethylene group [90], introduction of amine groups after a conventional nitro addition [91] or arenetricarbonyl complex addition by chemical vapor deposition method [92].

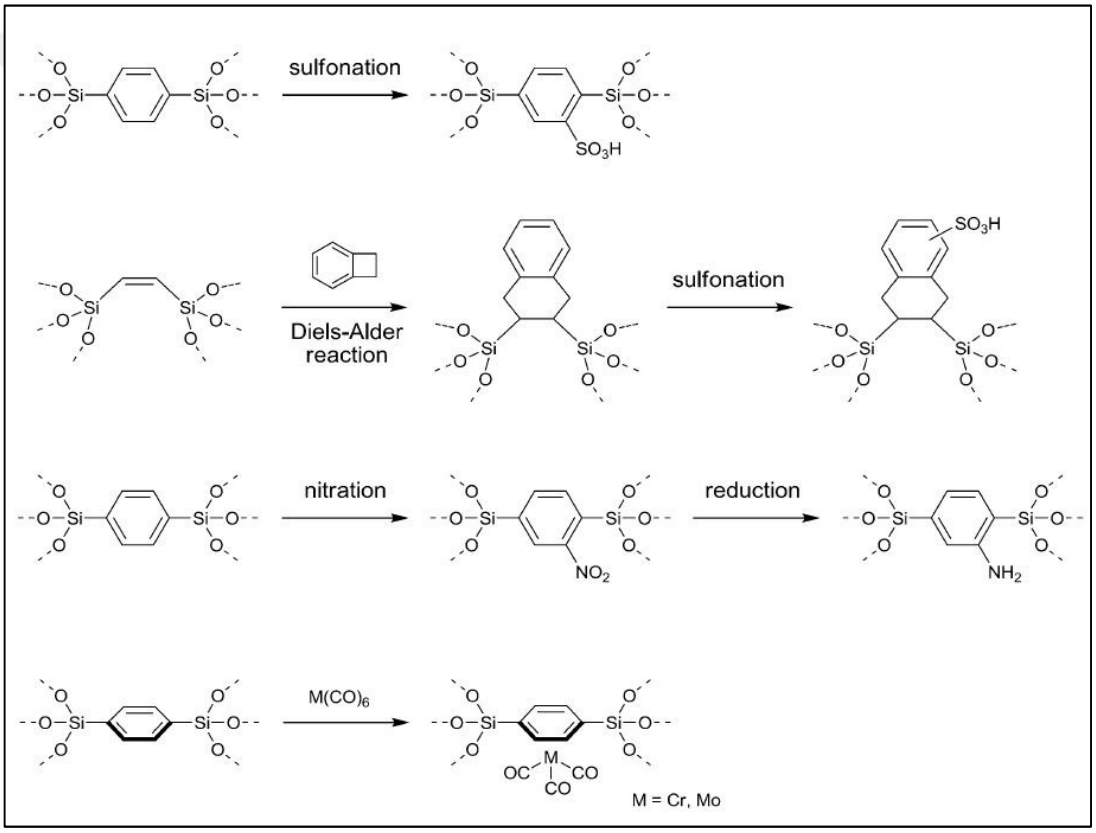

Figure 2.16: Post functionalization of PMOs. (Reproduced with the authorization of Royal Society of Chemistry).

2.2.4. The Uniqueness of PMOs

PMO materials are special among the silica based nanoparticles thanks to the combination of all the advantages of a robust porous organic framework, along with the intrinsic properties of the organic fragments [93-96].

On the one hand, PMO nanoparticles share the advantages of MSNs such as:

i) Porous channels useful for various applications in catalysis [97, 98], adsorption [99], drug delivery [100, 101], light-harvesting [102, 103].
ii) Tunable pore size organization [82, 104].
iii) Engineering of the nanoparticles outer and inner surface through the silicon chemistry, thus allowing the modulation of the nanoparticles surface functionalities as well as its dispersability in aqueous or organic solvents [82].
iv) Biocompatibility [105].

On the other hand, the organic moieties of PMO materials provide:

i) Virtually unlimited applications, according to the features of the organic groups selected to constitute the pores.
ii) The highest organic content in the material, thus maximizing the influence of the organic group on the overall properties of the material.
iii) The modulation of the hydrophilicity/hydrophobicity of the pores, which permitted for instance much higher drug loading capacities [106, 107].
iv) Additional features arising from crystal-like PMO materials, such as molecular rotors with phenylene [108].
v) The PMOs may be degraded under certain conditions when specific functional groups sensitive to acid–basic, redox, photochemical, or biochemical reactions are present in the structure of the organic framework [109, 110].
vi) Post-modification of the organic fragment by classical organic chemistry [88-92].

2.2.5. Synthesis of nanoPMOs

Although a wide variety of bulk PMO materials has been reported, reaching the nanoscale for such materials is much more challenging and has been less studied. Even so, there are many different methods of preparing nanoPMOs. In the next chapter, some of the methods will be listed according to shape and date.

2.2.5.1 Synthesis of Spherical nanoPMOs

In 2006, the first nanoPMO were reported with a hollow spherical morphology by the use of the FC-4 and CTAB (Fig.2.14) surfactants. Ethylene-bridged hollow PMO (HPMO) nanoparticles were prepared from 1,2-bis(trimethoxysilyl)ethane (Fig. 2.17) with a sodium hydroxide catalyzed sol–gel reaction at 80 °C [111]. This approach led, for the first time, to nanoPMOs with sizes ranging from 100 to 400 nm in diameter.

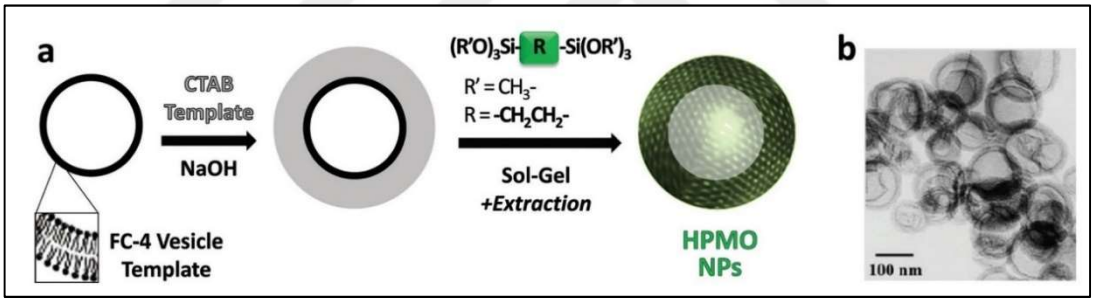

Figure 2.17: Schematic representation of the first spherical nanoPMO (a), and a Transmission Electron Microscopy (TEM) image of a resulting nanomaterial (b). (Reproduced with the authorization of Royal Society of Chemistry).

In 2009, phenylene-bridged, PMO nano-spheres were reported, with a diameter ranging from 50 to 1000 nm, and a worm-like porosity [112].

In 2011, colloidal solutions of monodisperse PMO nano-spheres of 20 nm in diameter were reported, for simple organic bridges such as methylene, ethylene and ethenylene [113].

2.2.5.2 Synthesis of Rod and Fiber shaped nanoPMOs

In 2005, Lu *et al*. first reported the controlled synthesis of PMO nanorods (200 × 1000–2000 nm) with ethylene bridges [114]. They used the pluronic P123 triblock copolymer (Fig.2.14) surfactant and obtained well-organized hexagonal pores of 8 nm.

In 2009, using the trisilylated octaethoxy-1,3,5-trisilapentane precursor, among different nano-objects PMO nanorods (700 × 200 nm) and nanofibers (100 × 2000 nm) were obtained with an adjustable aspect ratio from 2:1 to 20:1 by varying the concentration of the precursor [115, 116].

In 2014, Durand *et al*. reported mixed PMO nanoparticles, obtained from the co-condensation of bis(triethoxysilyl)-ethane (E) with bis(3-triethoxysilylpropyl)-disulfide (DIS), leading to porous nanorods with various aspect ratios, whereas the hydrolysis condensation of DIS alone yielded dense nanospheres (Fig. 2.18). The resulting mixed PMO nanoparticles displayed highly ordered 2 nm pores. Furthermore, the good mixing of the two precursors resulted in an efficient degradation upon disulfide cleavage by mercaptans. In a sense, NPs act as trojan horses for efficient in vitro cancer therapy [109].

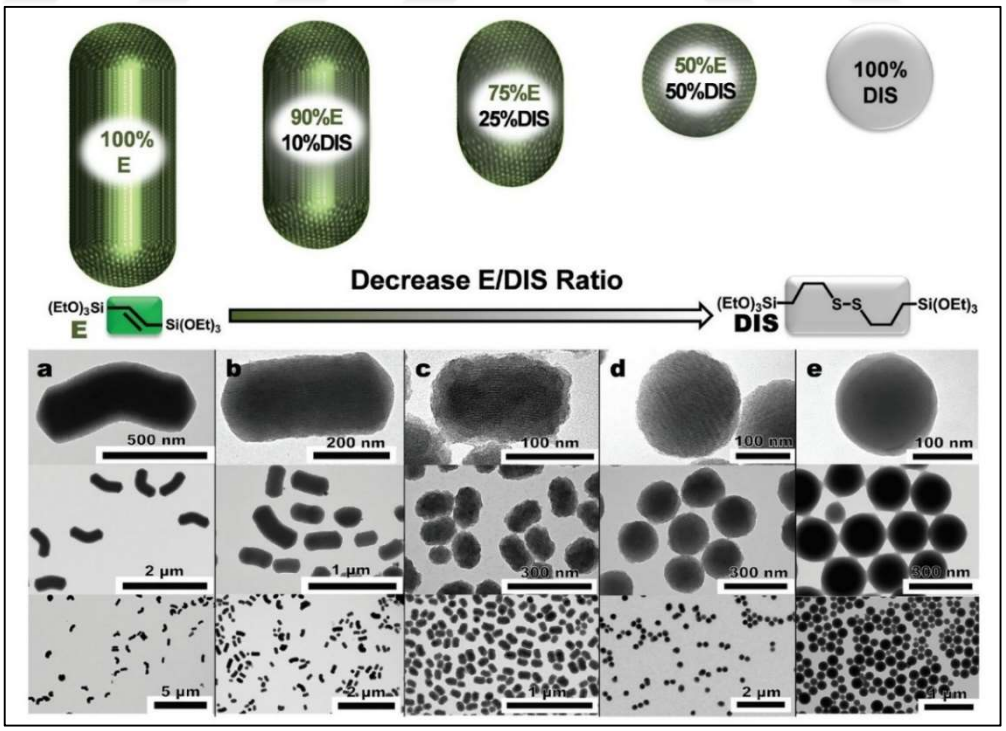

Figure 2.18: Size / morphology control of nanoPMO and their TEM images. (Reproduced with the authorization of Royal Society of Chemistry).

2.2.6. Applications of Silica-Based Nanoparticles

Although there are many different kinds of applications of MSNs and PMOs, such as optical materials and sensors [117], solid crystals [118] or absorbents [119], this work mainly focuses on biological applications. Table 2.1 and Table 2.2 lists all kinds of biological applications based on MSNs [119]. and Table 2.3 lists the bio-molecules and drugs immobilized onto PMOs [83].

Table 2.1: Biological applications of MSNs. (Reproduced with the authorization of Royal Society of Chemistry).

Type of material	Synthesis method	Characteristics	Comment	Application
LPMSN	CTAB-templated, postsynthetic hydrothermal treatment with TOPO	SA: 407 PD: 8 PS:180	Rough surface, Irregular porosity	PET
LPMSN/polymer composite	CTAB-templated, *in situ* TMB addition	SA: 1040 PD: 4.7 PS:100 ±15	MCM-41 type	Growth factor loading, neural tissue regeration
LPMSN/collagen composite	CTAB/TOMAB co-templated	SA: 1265 PD (bimodal): 15.9; 2.3 PS:300	Irregularly structured porosity	Protein/NGF adsorption, neural tissue engineering
Series of LPMSNs	Pluronic-templated, *in situ* TMB addition, fluorocarbon surfactant mediated	SA:575-821, PD: 5.2-19.5 PS:50-400	Cubic, hexagonal, mesocellular foam	/
LPMSN	octane/water/P123/TEOS	SA:565 PD: 13 PS:50-200	Rod-shaped, regular porosity	Adsorption of lysozyme
Series of LPMSNs	P123/TMOS, acidic conditions	SA:707-867 PD: 7.0-8.3 PS:10-200	SBA-15 type rods	Protein adsorption, cellular uptake
LPMSN	CTAB-templated, *in situ* TMB addition	SA: 1061 PD (bimodal): 5.4; 14.5 PS:50 - 900	MCM-41 type, Wide distribution of PS	Cytochrome c delivery to cancer cells
HMM (LPMSN)	CTAB/TEOS/polymerization of styrene/aminoacid catlyst/octane	SA: ca. 600, PD: 4-20 PS:20-150	Tunable particle suze and pore diameter	Delivery of drug telmisartan
LPMSN	Postsynthetic etching of MCM-41 type MSN with aqueous $NaBH_4$	SA: N/A, PD: 3.0-9.7 PS:100-500	No record of SA, partial loss of porosity and structuration	Delivery of paclitaxel to cancer cells
Ultra-LPMSN	Postsynthetic etching of MCM-41 type MSN with methanolic solution of calcium nitrate or magnesium nitrate	SA: 312, 425 PD(bimodal): 4- 50 PS: ca. 200	Irregular pore structure	Adsorption of large proteins and antibodies
Series of LPMSNs	CTA^+ with tosilate or bromide counterions with small organic amines for templating	SA: 435-837 PD: 1.6- 5.4 PS: 40-130	Tunable large scale synthesis, different porsity	/
LPMSN	Dimethylphosphonatoethyl-trimethoxysilane/TEOS/ base/CTAB pore-templating	SA: 772 PD: 11,1 PS: 70-90	Raspberry pore morphology	Adsorption of bovine serum albumin
Series of LPMSN	Tannic acid-templating in ethanol/NH_4OH	SA: 420-560 PD: 6-13 PS: 200	Measured encapsulated enzyme activity	Adsorption of differently sized proteins
Series of LPMSN	DMHA/CTAB/OTAB pore templating, F127 for regulation of particle size	SA: ca. 1000 PD: 2.7-4.6 PS: ca. 200	Regular porosity Increased cyt c loading with pore diameter	Adsorption of cytochrome c and delivery to cancer cells
LPMSN	TOMAB/CTAB-pore templating	SA: ca. 1280 PD: 17.4	Irregular porosity	Adsorption of cytochrome c

Table 2.2: Biological applications of MSNs, continued. (Reproduced with the authorization of Royal Society of Chemistry).

Series of LPMSN	pore-swelling alkanes/etanol/NH_4OH/H_2O/ CTAB	SA: ca. 1200 PD: 2.5 - 8.8 PS: 50-100	Enzyme activity improved upon confinement in mesopores	Adsorption of lysozyme, stability and activity
SBA-1 type LPMSN	hexadecyl pyridinium chloride-pore templating, complexed with poly(acrylic acid). TMB-pore expansion	SA: ca. 800 PD: 3.8 – 5.3 PS: 100-130	Cubic pore arrangement	Adsorption of lysozyme, activity against bacterial cell wall
LPMSN	pore-templating with Pluronic P104	SA: N/A PD: 6.5 PS: 300x500	Entrapped enzyme shows size selective activity	Porcine liver esterase loaded, gated nanodevice
LPMMSN	Magnetite nanoparticles/CTAB/TMB-pore expansion	SA: 959 PD: 12.4 PS: 80-750	Core/shell, radial porous structure	/
SBA-15 type LPMMSN	P123/NaCl/H_2O/EtOH/TEOS	SA: 46 PD: 7 PS: ca. 600	Very low SA and pore volume	Loading of large drug rapamycin
LPMMSN	CTAB templating, decane/TMB as pore expanders	SA: 700–1100 PD: 3.8–6.1 PS: 40–70	Core/shell, radial porous structure	loading of DNA, MRI, drug delivery
LPMMSN	Pluronic P123/CTAB-templating, acidic conditions	SA: 190 – 250 PD:4.3- 4.5 PS: ca. 300	High magnetization (29.3 emu/g)	removal of toxic microcystin-LR
SBA-15, FDU-12 type LPMSN, LPMMSN	macroporous carbon-PS templating, P123(or F127)/TEOS /(magnetite NP) in ethanol/water	SA: 790, 280 PD: 8, 7 PS: 450	Highly uniform spheres	Microcystin removal from water
LPMMSN	Hexadecyltrimethylammonium *p*-toluene-sulfonate-pore templating, triethanolamine	SA: 464-596 PD(bimodal): 3.4; 7.9-12.5 PS: 150	Uniform morphology, radial porosity	Drug delivery, cell uptake, hyperthermia, gene delivery
Series of LPMMSN	TEOS/Pluronic F127/TMB /HCl/H2O, fluorocarbon FC-4 for PS templating	SA: 201-716 PD: entr. 3.7-17.3, cav. 12.2-20.5 PS: 70-300	Smaller entrance size, bigger cavity, different porous structures	Plasmid DNA loading and stability against nucleases
Ultra-LPMSN	Postsynthetic treatment of MSN with TMB at 140°C for 4 days in autoclave	SA: 395 PD: 23 PS: 200	Irregular porous structure	Loading siRNA. Knockdown of GFP and VEGF genes *in vivo*
LPMSN, LPMMSN	TEOS/Pluronic F127/TMB /HCl/H2O, fluorocarbon FC-4 for PS templating	SA: 421-700 PD: 10.6 PS: 200	Impregnation of iron salts, in situ Fe_3O_4	Simultaneous drug and gene delivery
Series of LPMSN, LPMMSN	Polystyrene-b-poly (acrylic acid)/CTAB-pore templating H_2O/THF/EtOH/TEOS/NH_3	SA: 233-507 PD: 2.8-16 PS: 30-650	Uniform, hexagonal, cubic, lamellar, hollow porosity	Gene delivery, inhibition of VEGF, MRI
LPMSN	TEOS/APTES/CTAB/TMB/ decane/NH_3/ethylene glycol/H_2O	SA: 959 PD: 5.9 PS: 70	Radial porosity	Glutathione responsive delivery of oligonucleotides

Table 2.3: Bio-molecules and drugs immobilized onto PMOs. (Reproduced with the authorization of Royal Society of Chemistry).

Protein	Cytochrome *c*		
	Bovine heart	$-CH_2-CH_2-$	2D-hexagonal/rodlike
	Horse heart	$-C_6H_4-/-(C_6H_4)_2-$	Disordered/hollow spherical particles
	Serum albumin		
	Bovine	$-CH_2-CH_2-$	Cubic/hollow particles Hollow spheres
		$-CH_2-CH_2-$ functionalized with $-NH_2$ or $-COOH$	2D-hexagonal/rodlike
	Hemoglobin	$-CH_2-CH_2-$ functionalized with $-NH_2$ or $-COOH$	2D-hexagonal/rodlike
Enzyme	Lysozyme		
	Hen egg white	$-CH_2-CH_2-$	2D-hexagonal/rodlike
		$-(CH_2)_3-NH-(CH_2)_3-/-C_6H_4-/-(C_6H_4)_2-$	Hollow spherical particles
		$-CH_2-CH_2-$	Cubic/hollow particles
	Lipase		
	Rhizopus oryzae	$-CH_2-CH_2-$	n.a.
	Candida Antarctica fraction B	$-CH_2-CH_2-$	2D-hexagonal/rodlike
	Thermomyces lanuginosus	$-CH_2-CH_2-/-CH=CH-/-C_6H_4-$	—/Mesocellular cagelike
	Papain	$-CH_2-CH_2-$ functionalized with $-(CH_2)_3-O-CH_2-(CH)_2O$	2D-hexagonal
	Chloroperoxidase	$-(CH_2)_3-NH-(CH_2)_3-$	Disordered
	Horseradish peroxidase	$-(CH_2)_3-NH-CO-NH-(CH_2)_3-/-(CH_2)_3-NH-CO-S-(CH_2)_3-$	2D-hexagonal
		$-(CH_2)_3-S-CH_2-CHOH-CH_2-O-(CH_2)_3-$	2D-hexagonal
Amino-acids	Glycine, L-lysine, isoleucine	$-C_6H_4-$	Disordered/hollow spherical
		$-(C_6H_4)_2-/-(CH_2)_3-NH-(CH_2)_3-$	Worm-like/hollow spherical
Drug	Tetracycline	$-CH_2-CH_2-$	2D-hexagonal/spherical particles
	Cisplatin	$-CH_2-CH_2-$	2D-hexagonal
	Captopril	$-(CH_2)_3-NH-CO-NH-C_6H_4-SO_2-NH-CO-NH-(CH_2)_3-$	2D-hexagonal/rodlike
		$-(CH_2)_3-NH-CO-N((CH_2)_2)_2N-CO-NH-(CH_2)_3-$	2D-hexagonal/polyhedral bipyramidal crystals
	5-Fluorouracil	$-(CH_2)_3-NH-CO-NH-C_6H_4-SO_2-NH-CO-NH-(CH_2)_3-$	2D-hexagonal/rodlike
		$-(CH_2)_3-NH-CO-N((CH_2)_2)_2N-CO-NH-(CH_2)_3-$	2D-hexagonal/polyhedral bipyramidal crystals
		$-(CH_2)_3-NH-CO-NH-CCN=CCN-NH-CO-NH-(CH_2)_3-$	2D-hexagonal/shaped tubular-twisted columns-micro-elongated particles
	Ibuprofen	$-(CH_2)_3-NH-CO-NH-CCN=CCN-NH-CO-NH-(CH_2)_3-$	2D-hexagonal/shaped tubular-twisted columns-micro-elongated particles

2.2.7. Porphyrin-based silica nanoparticles for PDT

In literature, there are several examples of for one-[120-125] and two-photon [126] PDT applications. However, these works are describing a photosensitizer which is physically entrapped, not covalently bonded, inside the silica network. Entraption could lead to premature release of the photosensitizer from the silica network which in fact leads to reduced efficiency of treatment. It could also cause some side effects. To overcome these drawbacks, photosensitizer could be attached to the silica matrix by covalent bonds [127-130] through trialkoxysilane groups. Furthermore, surface of cancer cells is overexpressed with specific bioreceptors [131] and functionalizing the nanoparticles in order to target these receptors would enhance the uptake of the nanoparticles. The first example of silica-based nanoparticles functionalized to target breast cancer cells for PDT applications were described in 2007 by Zang *et al.* [132]. Merocyanine was used as a photosensitizer. Two years later, Durand *et al.* described a second nanoparticle, in this case the photosensitizer was porphyrin derivative (Fig. 2.19) [12].

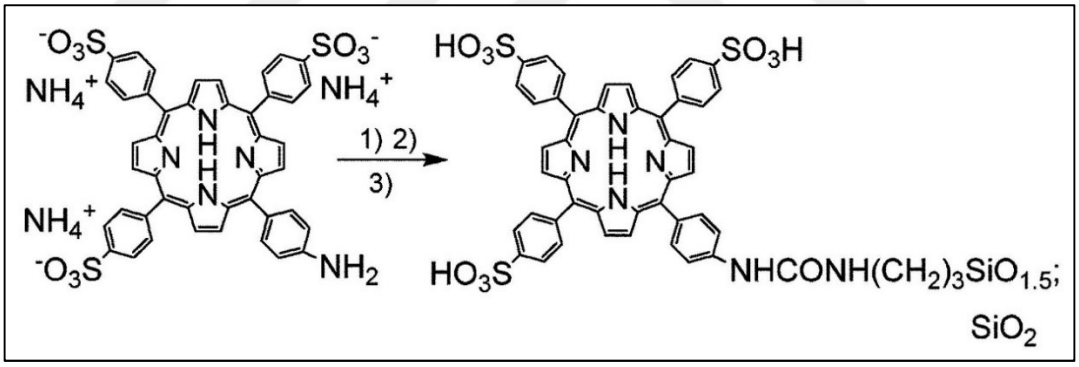

Figure 2.19: First covalently attached porphyrin derivative to MSN. (Reproduced with the authorization of Royal Society of Chemistry).

Water-soluble anionic porphyrin covalently attached to the mesoporous silica network by use of isocyanatopropyltriethoxysilane moiety. Durand *et al.* demonstrated that surface functionalization of nanoparticles with mannose (Fig. 2.20) is essential to get a high PDT efficiency. Through the involvement of overexpressed mannose receptors in cancer cells which increases active endocytosis, breast cancer cells (MDA-MB-231) were targeted with mannose moieties.

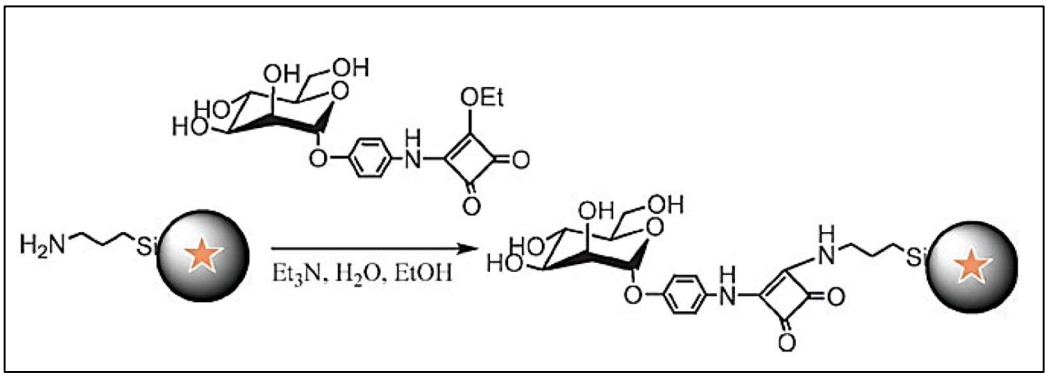

Figure 2.20: Mannose functionalization of the surface of MSN. (Reproduced with the authorization of Royal Society of Chemistry).

There are other porphyrin-based silica nanoparticles reported in the literature [6-11] by Durand *et al*. which follow his initial work. In Figure 2.21, first of their kind, porphyrin-based silica nanoparticles for two-photon induced PDT can be seen. Multi-functionalized porous silicon nanoparticles (pSiNPs) with therapeutically active side groups and/or targeting units (mannose) utilize the EPR effect to target exactly the tumor. They were again, designed by Durand *et al*., in 2014 [11] and results are very promising. They have showed that pSiNPs are effective in killing MCF-7 cancer cells.

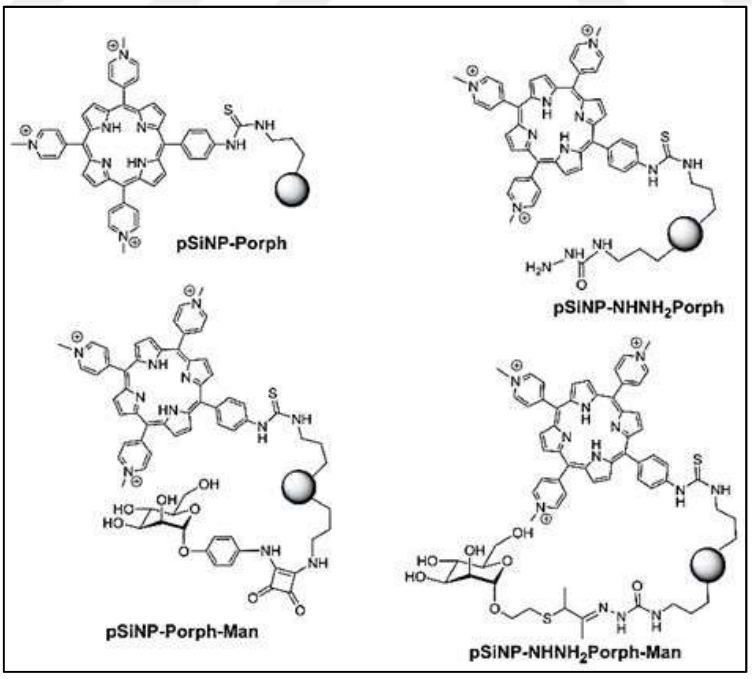

Figure 2.21: Examples of first porous silicon nanoparticles used in two-photon induced PDT. (Reproduced with the authorization of Wiley Online Library).

In literature, there are other nanoparticles that give two-photon adsorption such as gold nanorods, carbon dots or Cd-Se quantum dots but they are non-biodegradable or highly toxic [133, 134]. This limits their use in clinical experiments. On the other hand, pSiNPs are proved to be biodegradable [135, 136] into harmless silicic acid that is rapidly discarded by renal clearance. pSiNPs are also useful for imaging since they have intrinsic luminescence.

Biodegradable nanoparticles are of particular interest since they favor a safe and efficient excretion of the nanodevice [137-139]. In Figure 2.22, it can be seen examples of Disulfide / Porphyrin based biodegradable bridged silsesquioxane nanoparticles for two-photon induced PDT. Durand showed that glutathione cleaves disulfide linkers in the nanoparticles frameworks and they were efficient in fluorescence imaging and killing MCF-7 cancer cells [87].

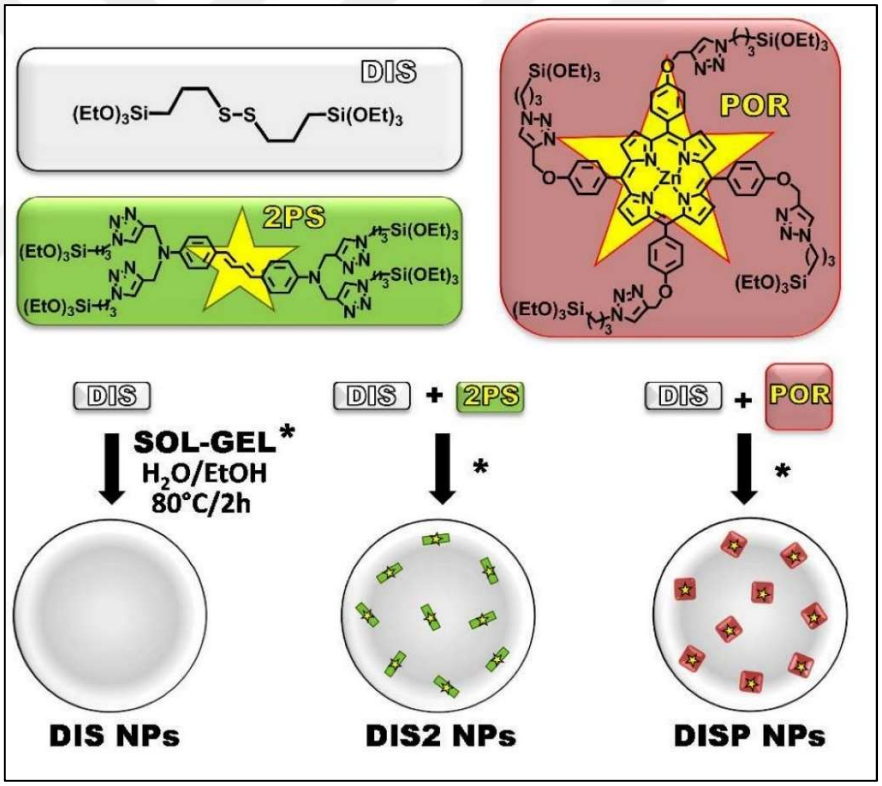

Figure 2.22: Disulfide / Porphyrin based biodegradable bridged silsesquioxane NPs. (Reproduced with the authorization of Royal Society of Chemistry).

In Figure 2.23, it can be seen examples of porphyrin-based mesoporous silica nanoparticles [8]. Durand and his team covalently incorporated the porphyrin photosensitizer to 20 nm mesoporous silica nanoparticles prepared by the sol-gel procedure in the presence of CTAB and TEOS. They were interested in developing

small-sized silica nanoparticles able to cross biological membranes. They successfully managed to image retinoblastoma cells and showed results on breast cancer cells.

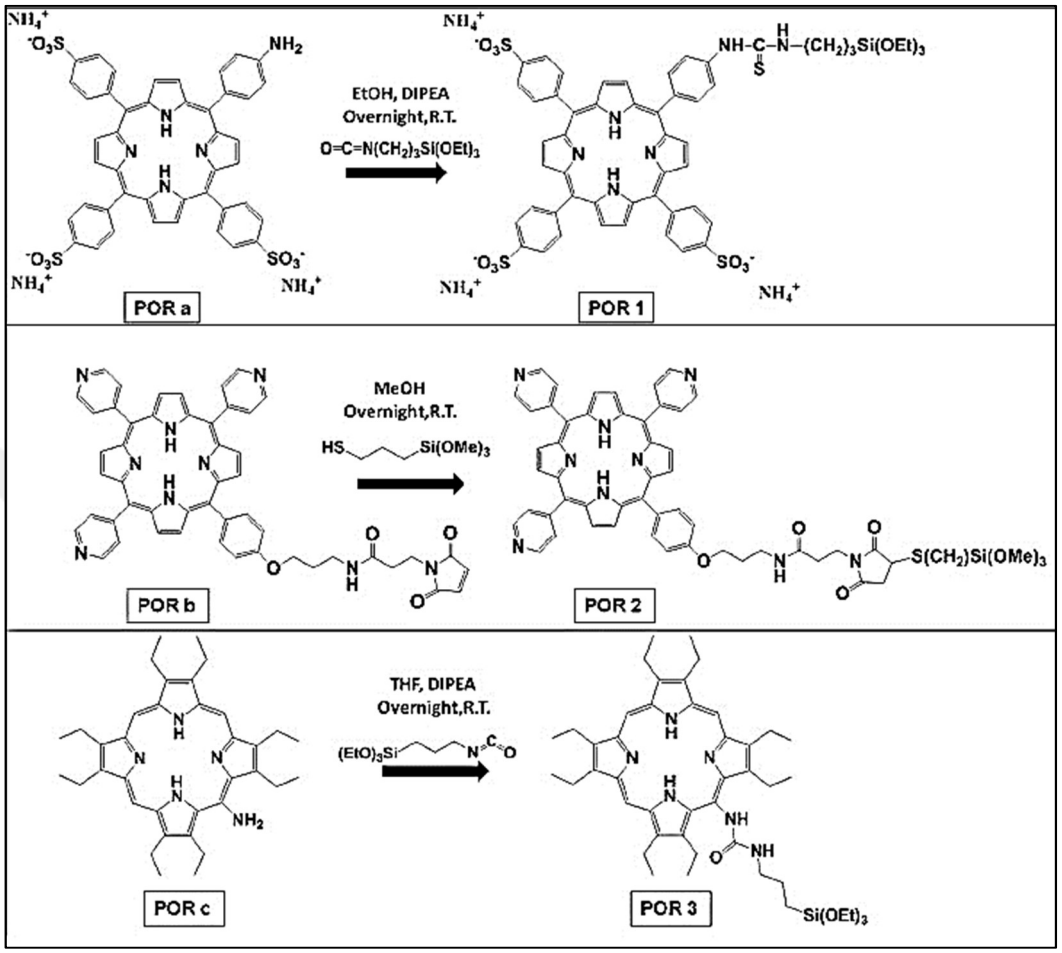

Figure 2.23: Porphyrin based precursors for mesoporous silica nanoparticles. (Reproduced with the authorization of Springer Link).

3. DESIGN STRATEGY

Since the goal of this work is to synthesize symmetric A_4 phthalocyanines bearing terminal alkyne groups with different spacers and different positions to be used as building blocks of Periodic Mesoporous Organosilica Nanoparticles (nanoPMOs) towards photodynamic applications, it has been envisioned 2 different approaches to obtain the targeted phthalocyanines. Both of them starts from an appropriately substituted phthalonitrile bearing a terminal hydroxy group (Fig. 3.1), then by following the below strategies A and B, targeted phthalocyanines will be prepared.

- Route A: Grafting the propargyl molecule to the hydroxylated phthalonitrile then synthesize the corresponding phthalocyanine.
- Route B: Synthesis of the phthalocyanine directly from the hydroxylated phthalonitrile then grafting of propargyl molecule.

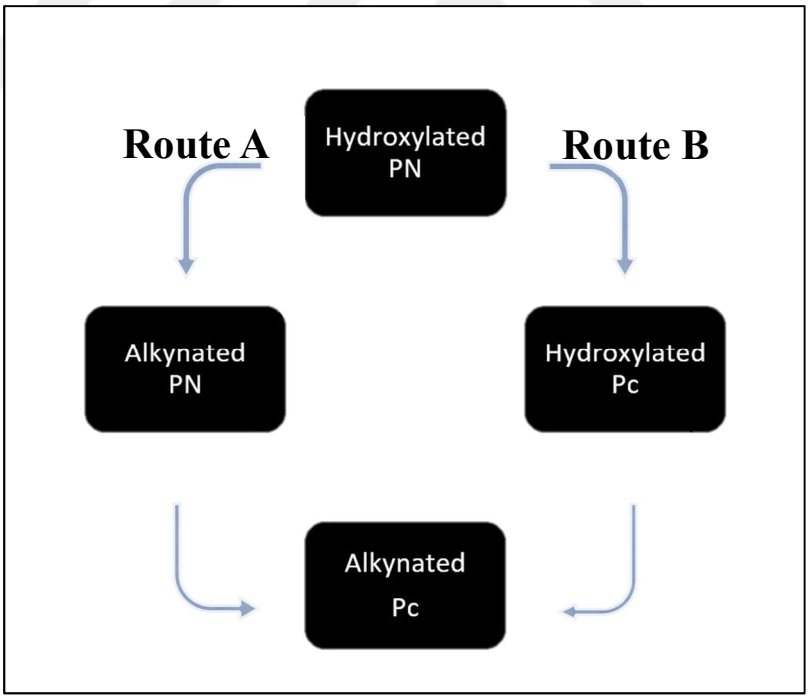

Figure 3.1: Synthesis routes.

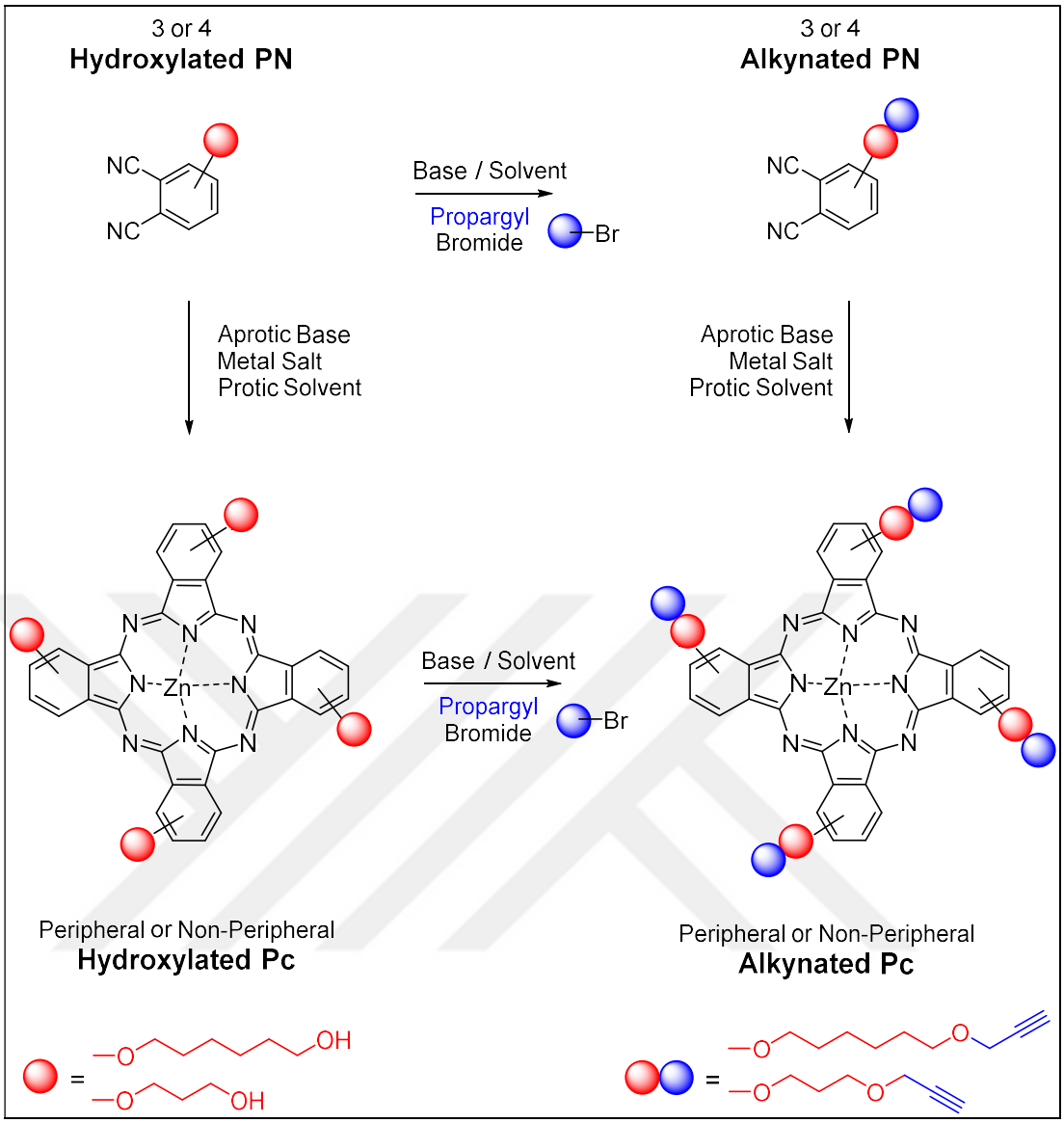

Figure 3.2: Synthesis routes in detail.

4. RESULTS AND DISCUSSION

4.1. Phthalonitriles

4.1.1. Starting Phthalonitriles's Synthesis

Starting compounds for all the phthalocyanines in this work are either 4-nitrophthalonitrile (**4**) or 3-nitrophthalonitrile (**8**). Even though both of the starting phthalonitriles are commercially available, they can also be synthesized at laboratory rather easily through three step reactions (Fig. 4.1 - 4.2) [140, 141]. Compound **4** and **8** can then be modified via substitution reaction to yield the desired phthalonitrile.

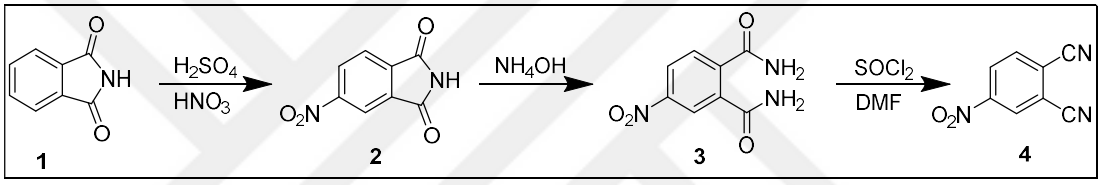

Figure 4.1: 4-Nitrophthalonitrile (**4**) synthesis.

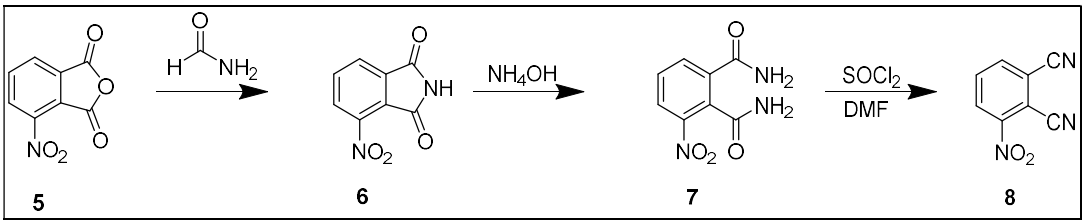

Figure 4.2: 3-Nitrophthalonitrile (**8**) synthesis.

4.1.2. Hydroxylated Phthalonitriles Synthesis

Since the aim of this work is to determine the effect of spacer length and position on the nanoPMO, 1,6-hexanediol and 1,3-propanediol were chosen as spacers of different length. Both diols have two terminal hydroxy groups available for substitution with the starting phthalonitriles (**4** and **8**) nitro groups. So, to favor the single substitution reaction of the nitro groups with the hydroxy groups and avoid the formation of dimeric phthalonitriles, diols are used in excess (5 eq.). K_2CO_3 also is used in excess (25 eq.) for better activation of hydroxy groups. Instead of excess usage of diols, mono protection groups on diols could be employed [142].

Initial phthalonitrile synthesis were done in acetone for the purpose of ease of removal of solvent and possible precipitation issues (Fig. 4.3). Both of the reaction mixtures, were separated using chromatographic techniques including preparative TLC and characterized by MALDI-TOF MS, IR and TLC. Even though our group has done similar synthesis before using acetone as solvent and have gotten satisfactory results, it was observed that it wasn't the case for compounds **11** and **12**. Even after three separate silica gel column chromatographies and two separate preparative TLC, it wasn't possible to purify the desired compounds.

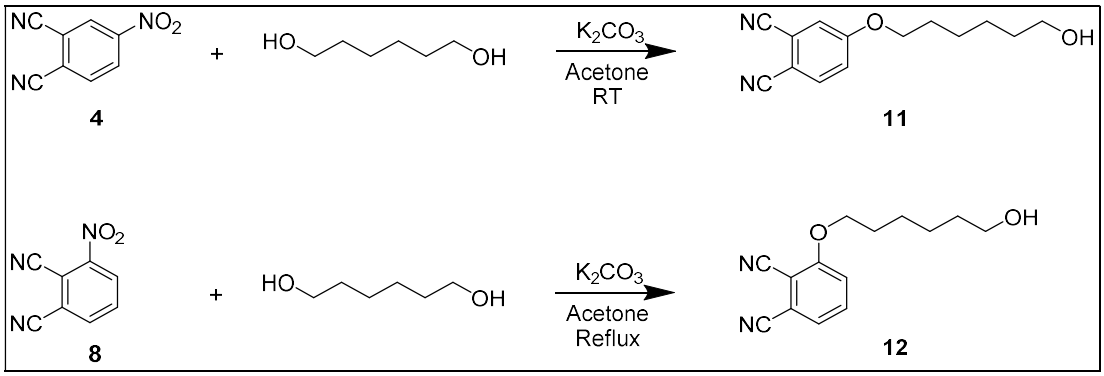

Figure 4.3: Hydroxylated phthalonitriles **11, 12** synthesis in acetone.

Acetone as solvent was only tried with hexanediol on 2 separate reactions at different temperatures with different nitro group positions. These findings have obliged us to search for different solvent. Classical conditions DMF/K_2CO_3 yielded satisfactory results, with no issue during the precipitation as possibly anticipated.

Synthesis of hydroxylated phthalonitriles **9**, **10**, **11** and **12** can be seen in Figure 4.4 and their corresponding yields can be seen at Table 4.1.

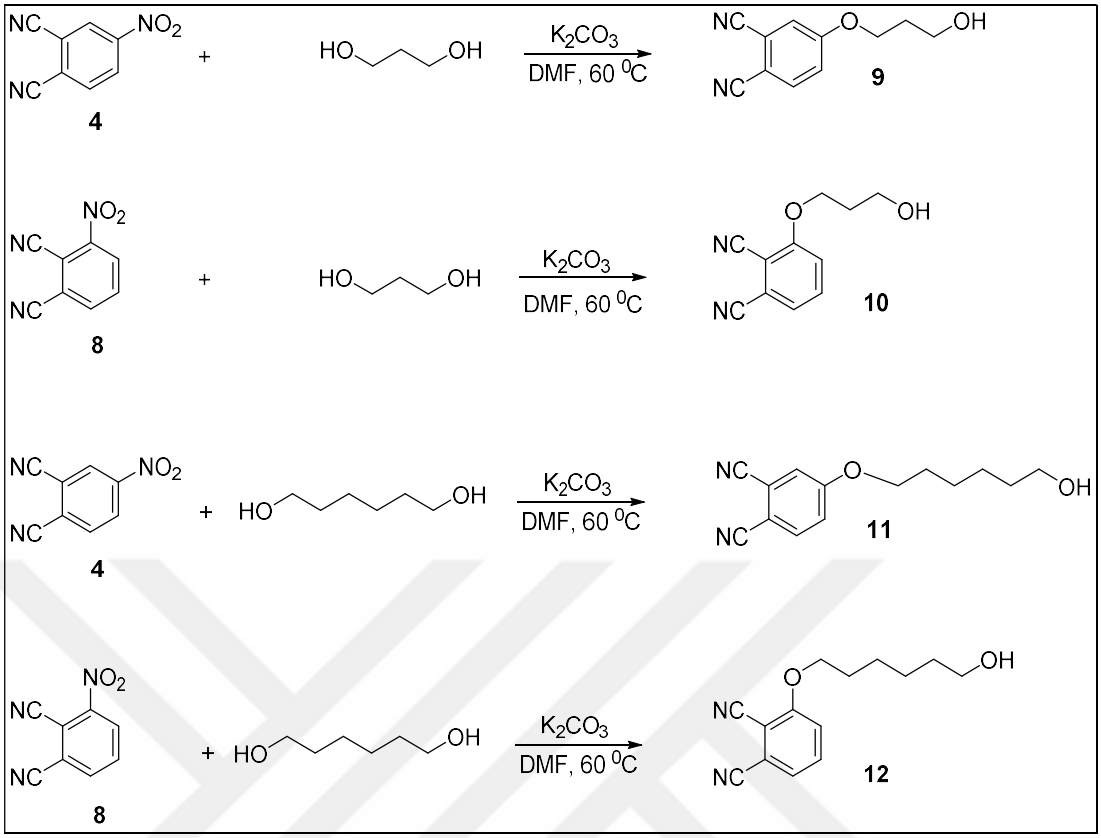

Figure 4.4: Hydroxylated phthalonitriles **9-12** synthesis in DMF.

Table 4.1: Experimental yields of hydroxylated phthalonitriles.

Compound	Yield (%)
9	56
10	33
11	27
12	45

4.1.3 Hydroxylated Phthalonitriles Characterization

All hydroxylated phthalonitriles were characterized by MALDI-TOF mass spectrometry, ^{1}H and ^{13}C NMR and FT-IR spectroscopy.

4.1.3.1. MALDI-TOF Mass Spectra of Hydroxylated Phthalonitriles

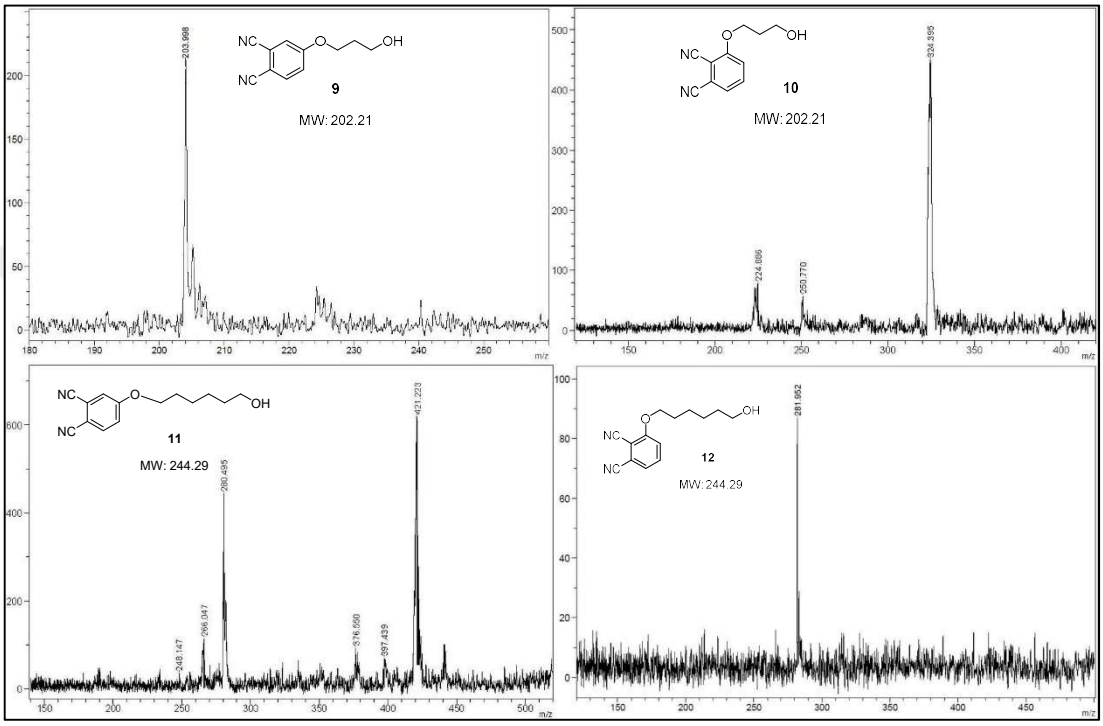

Figure 4.5: MALDI-TOF mass spectra of hydroxylated phthalonitriles.

All mass spectra were recorded with MALDI-TOF MS. Spectra can be seen in Figure 4.5 with their corresponding hydroxylated phthalonitrile structures as insets. In Table 4.2 comparison of corresponding hydroxylated phthalonitriles, *m/z* values with the matrixes can be seen.

Table 4.2: Calculated and found MALDI-TOF MS values of hydroxylated PNs.

Compound	Molecular Formula	Matrix Used	Molecular Weight (g/mol)	Found *m/z*
9	$C_{11}H_{10}N_2O_2$	DHB	202.21	203.998 $[M+H]^+$
10	$C_{11}H_{10}N_2O_2$	DIT	202.21	224.886 $[M+Na]^+$
11	$C_{14}H_{16}N_2O_2$	DHB	244.29	266.047 $[M+Na]^+$
12	$C_{14}H_{16}N_2O_2$	No Matrix	244.29	281.952 $[M+K]^+$

4.1.3.2. ^{1}H and ^{13}C NMR Spectra of Hydroxylated Phthalonitriles

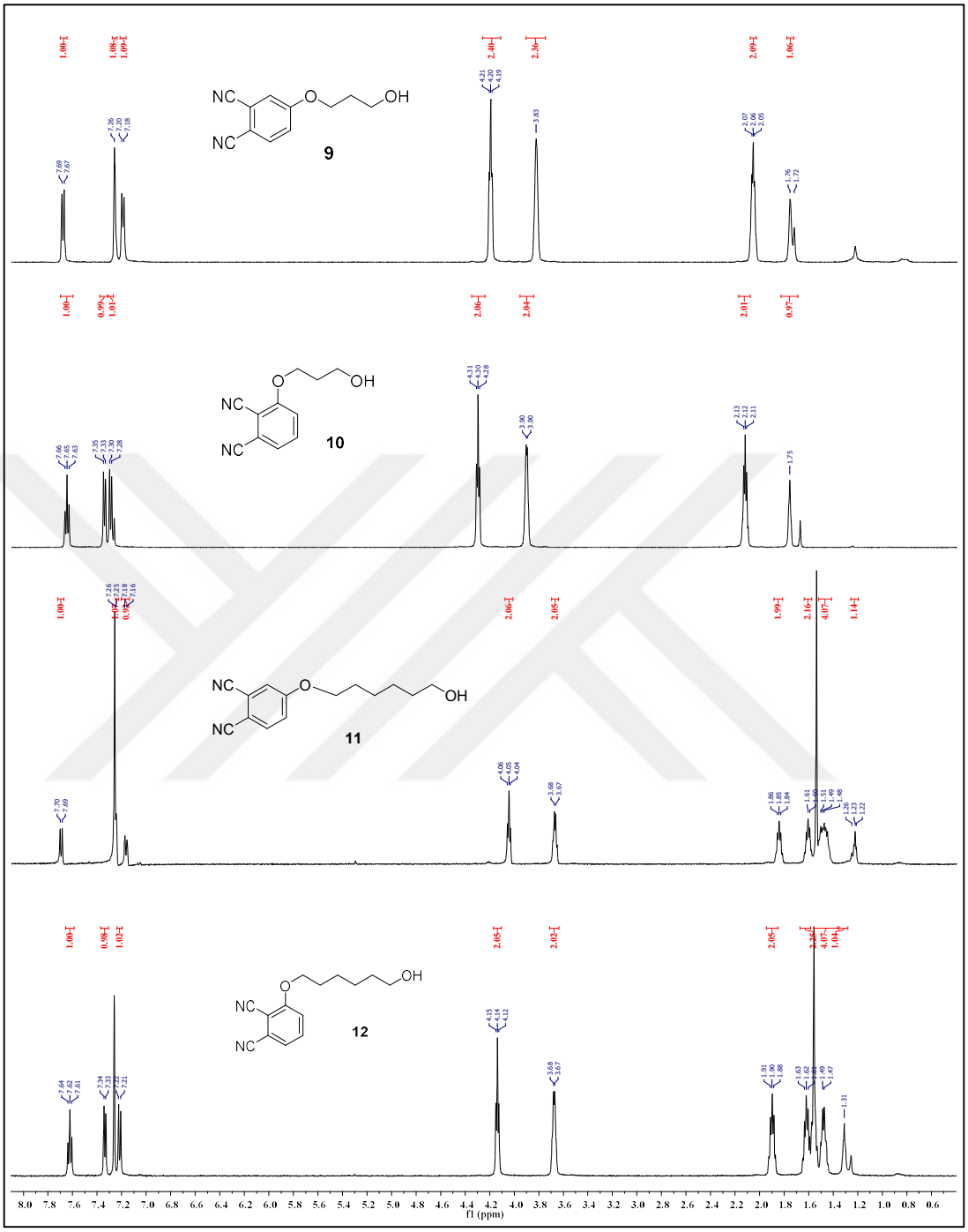

Figure 4.6: ^{1}H NMR spectra of hydroxylated phthalonitriles in $CDCl_3$.

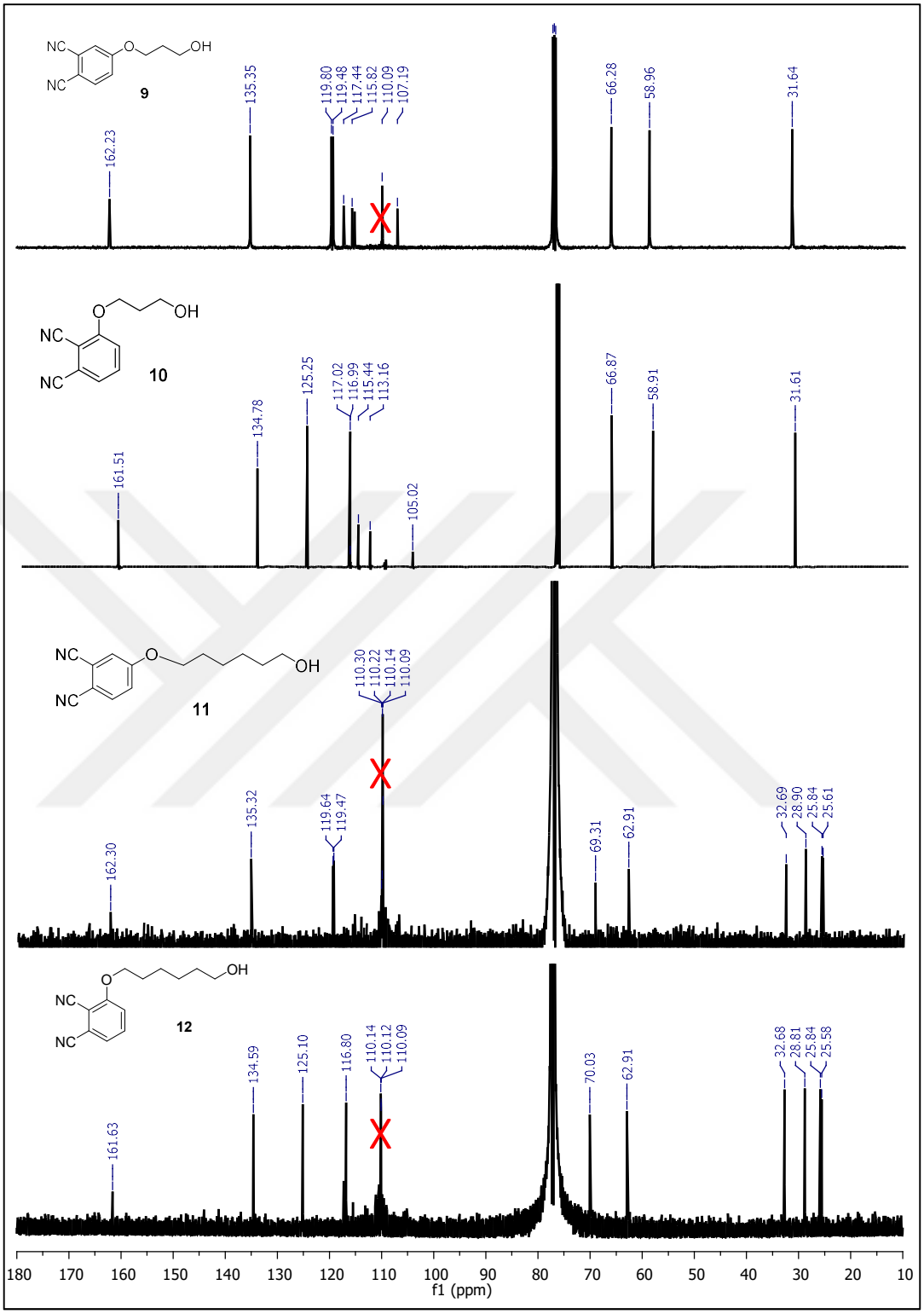

Figure 4.7: ^{13}C NMR of hydroxylated phthalonitriles in $CDCl_3$.

4.1.3.3. FT-IR Spectra of Hydroxylated Phthalonitriles

FT-IR spectra of hydroxylated phthalonitriles **9**, **10**, **11**, **12** are given in Figure 4.8 and Figure 4.9. In each spectra, C≡N bonds (around 2230 cm^{-1}), aliphatic C-H bonds (between 2950-2860 cm^{-1}), aromatic C-H bonds (around 3085 cm^{-1}), C=C bonds (around 1580 cm^{-1}) and -OH bonds as broad peaks (between 3310-3330 cm^{-1}) can be seen. There is no significant effect of position or spacer length on FT-IR spectra. Unexpectedly, the band corresponding to hydroxyl is not observed for **11**.

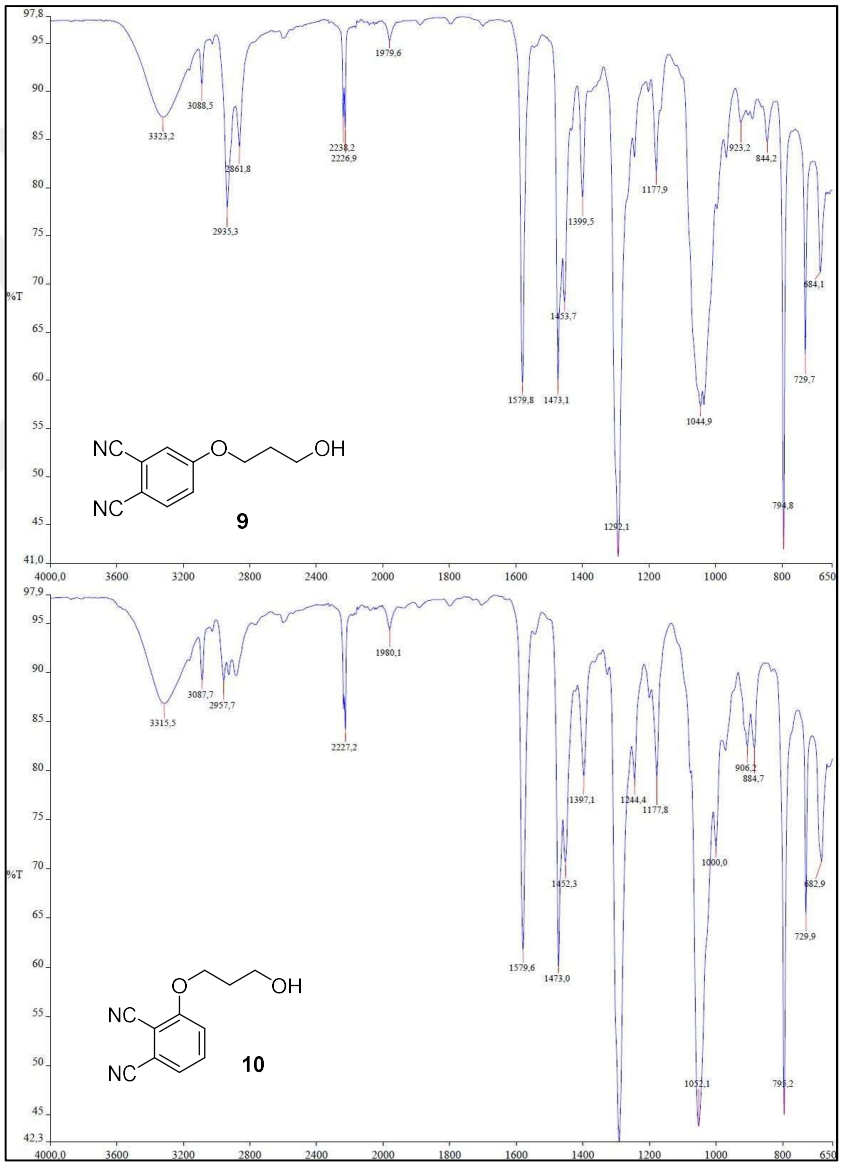

Figure 4.8: FT-IR spectra of hydroxylated phthalonitriles **9** and **10**.

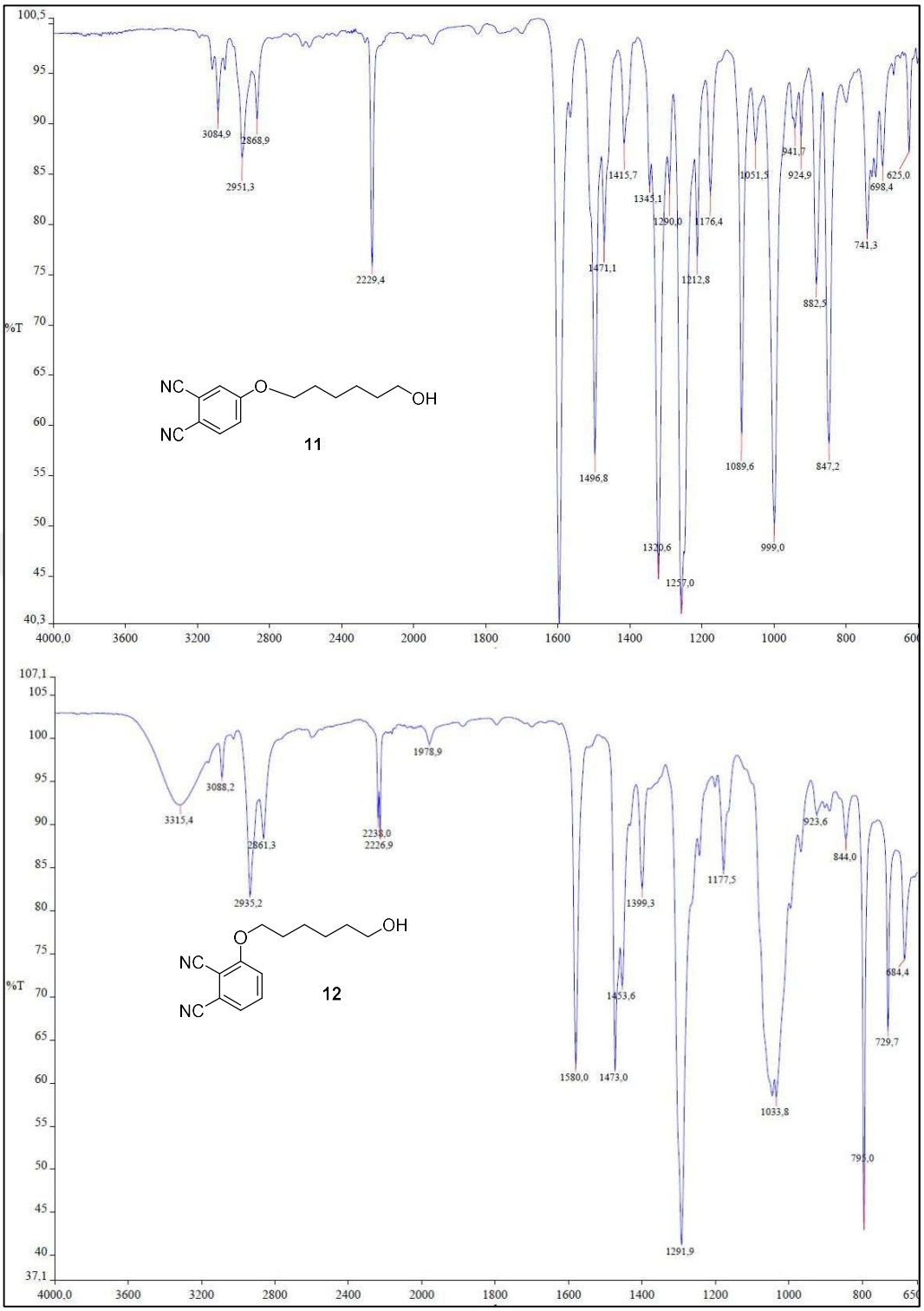

Figure 4.9: FT-IR spectra of hydroxylated phthalonitriles **11** and **12**.

4.1.4 Alkynated Phthalonitriles Synthesis

While performing a multi-step phthalocyanine synthesis, it is generally preferred to make all the necessary modifications to the phthalonitrile instead of post-modification of phthalocyanine which was synthesized from intermediate phthalonitrile.

All of the targeted phthalocyanines being symmetric A_4, have four possible sites of reaction so any post-modification attempt on an intermediate phthalocyanine would theoretically yield four different phthalocyanines (without considering structural isomers) those being mono, di, tri and tetra substituted phthalocyanines. So, a great deal of effort was spent on synthesizing alkynated phthalocyanines from alkynated phthalonitriles (Fig. 4.10), hence to prepare alkynated phthalonitriles.

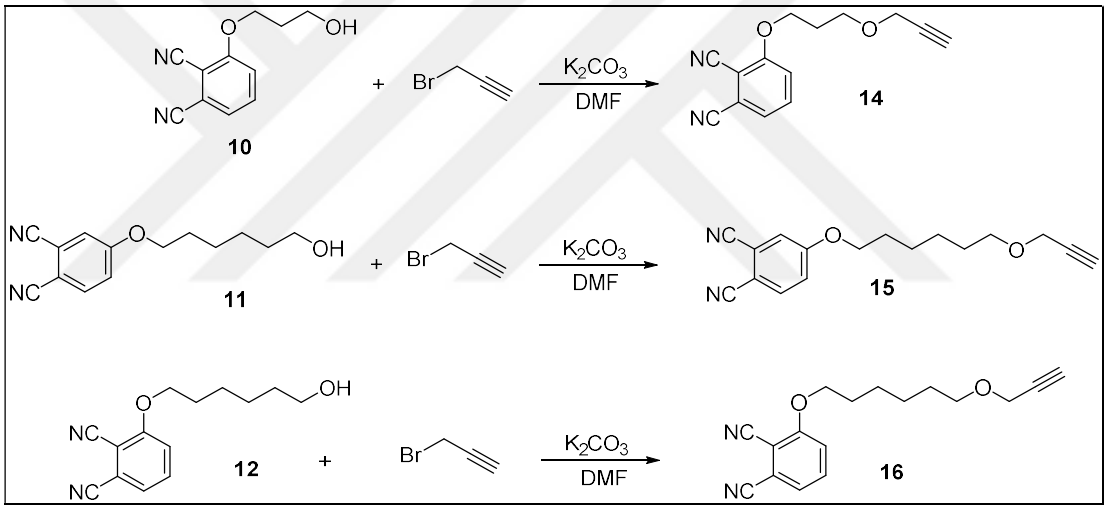

Figure 4.10: Alkynated phthalonitriles **14-16** synthesis.

Each compound was purified using chromatographic techniques including preparative TLC and characterized by MALDI-TOF MS, IR, NMR and TLC. It has been seen that not only their purifications were very tedious (for some cases three separate silica gel column chromatography and four separate preparative TLC) but also it has been seen only trace amounts or none at all, of targeted phthalocyanine peak at MALDI-TOF MS from its corresponding alkynated phthalonitrile. Conclusion was to discard the whole idea of synthesizing this line of phthalonitriles under above conditions.

4.2. Phthalocyanines

4.2.1. Hydroxylated Phthalocyanines Synthesis

Hydroxylated phthalocyanines **17**, **18**, **19**, **20** are prepared from hydroxylated phthalonitriles **9**, **10**, **11**, **12** respectively. Zinc acetate (2 eq.) is used as metal salt with DBU/*n*-Pentanol (Fig. 4.11). Greening of the reaction flask has been observed in all reactions after 2 minutes approximately.

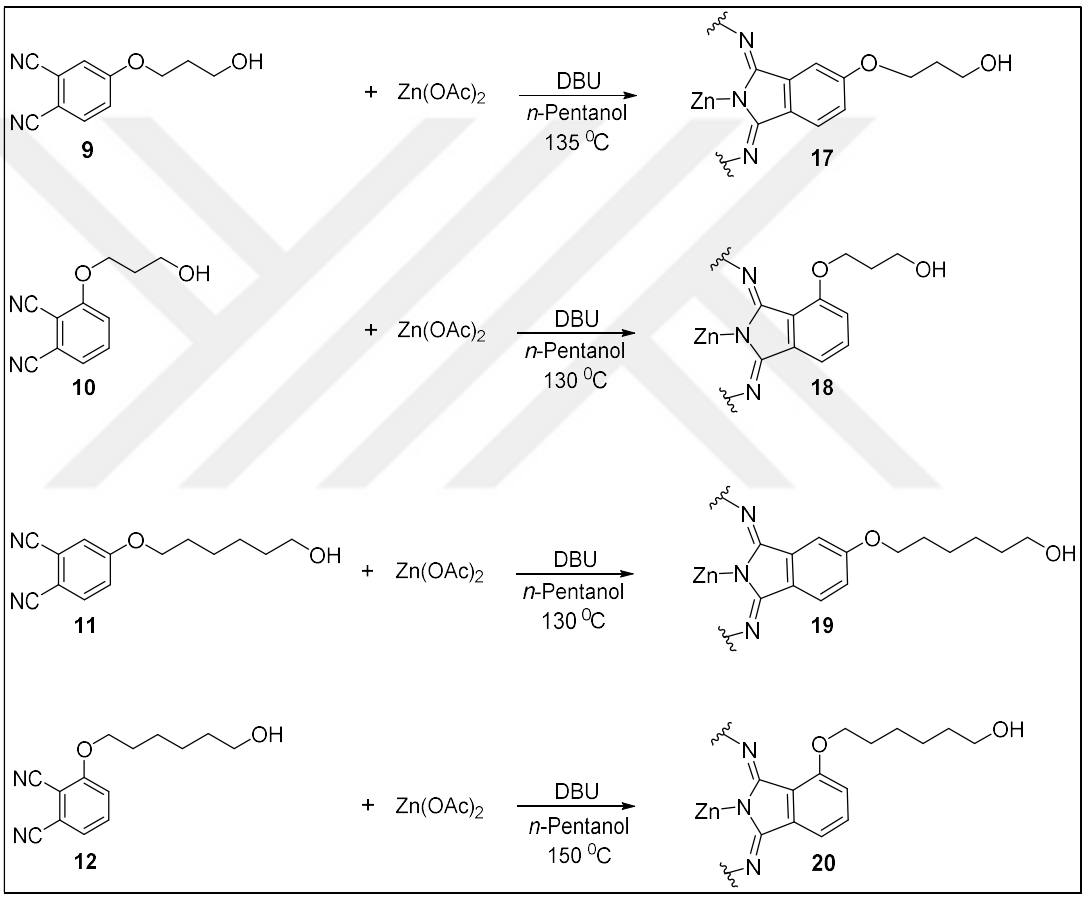

Figure 4.11: Hydroxylated phthalocyanines **17**-**20** synthesis.

Experimental yields (Table: 4.3) obtained are a bit low even though they are all eluted in 5:1, DCM:ethanol respectively, over 2 weeks. Reason being is that hydroxylated phthalocyanines have very high polarity so they have high tendency to interact with the silica gel.

Table 4.3: Experimental yields of hydroxylated phthalocyanines.

Compound	Yield (%)
17	30
18	24
19	34
20	32

4.2.2. Hydroxylated Phthalocyanines Characterization

All hydroxylated phthalocyanines were characterized by MALDI-TOF mass spectrometry, ^{1}H and ^{13}C NMR and UV-Vis spectroscopy.

4.2.2.1. MALDI-TOF Mass Spectra of Hydroxylated Pcs

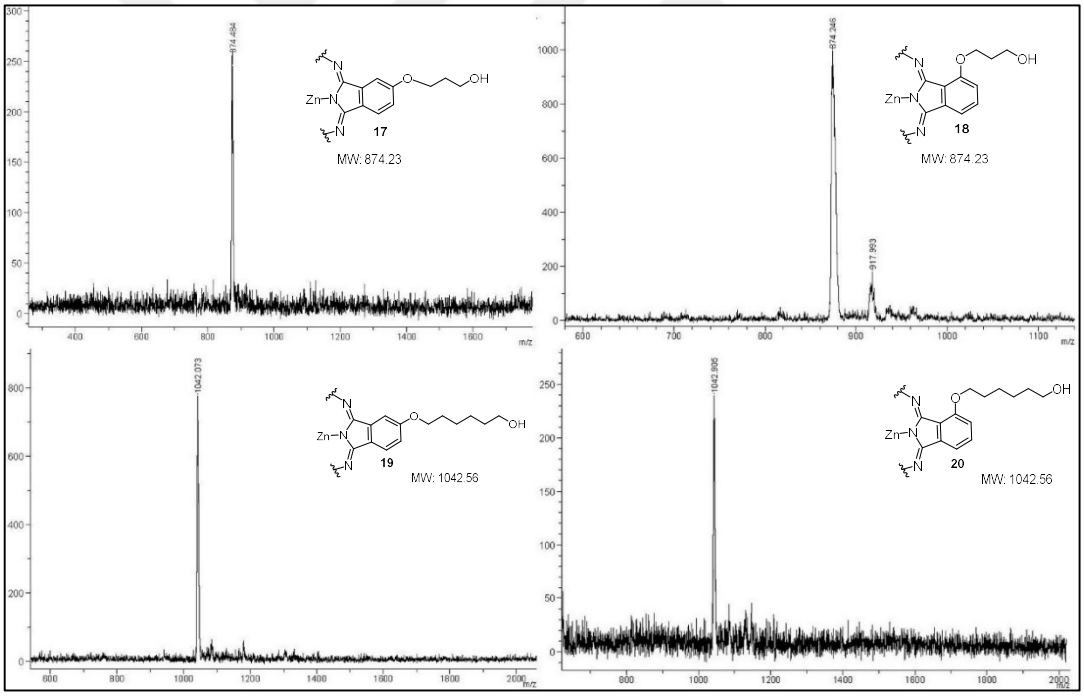

Figure 4.12: MALDI-TOF mass spectra of hydroxylated phthalocyanines.

All mass spectra were recorded with MALDI-TOF MS. Spectra can be seen in Figure 4.12 with their corresponding hydroxylated phthalocyanine structures as insets. In Table 4.4 comparison of corresponding hydroxylated phthalocyanines, *m/z* values with the matrixes can be seen.

Table 4.4: Calculated and found MALDI-TOF MS values of hydroxylated Pcs.

Compound	Molecular Formula	Matrix Used	Molecular Weight (g/mol)	Found m/z
17	$C_{44}H_{40}N_8O_8Zn$	DIT	874.23	874.484 $[M]^+$
18	$C_{44}H_{40}N_8O_8Zn$	DIT	874.23	874.246 $[M]^+$
19	$C_{56}H_{64}N_8O_8Zn$	DHB	1042.56	1042.073 $[M]^+$
20	$C_{56}H_{64}N_8O_8Zn$	DIT	1042.56	1042.905 $[M]^+$

4.2.2.2. ^{1}H and ^{13}C NMR Spectra of Hydroxylated Phthalocyanines

All hydroxylated phthalocyanines are aggregated in DMSO at concentrations necessary to record NMR spectra (Fig 4.13 and Fig 4.14). Other deuterated solvents did not prove more suitable to record these spectra.

Due to the fact that phthalocyanines have been obtained as regioisomeric mixtures (because they have been prepared from monosubstituted phthalonitriles), the aromatic protons appear as multiplets. Aromatic carbons are not always detectable in our conditions, but similarly several peaks appear, once again due to the regioisomeric mixtures.

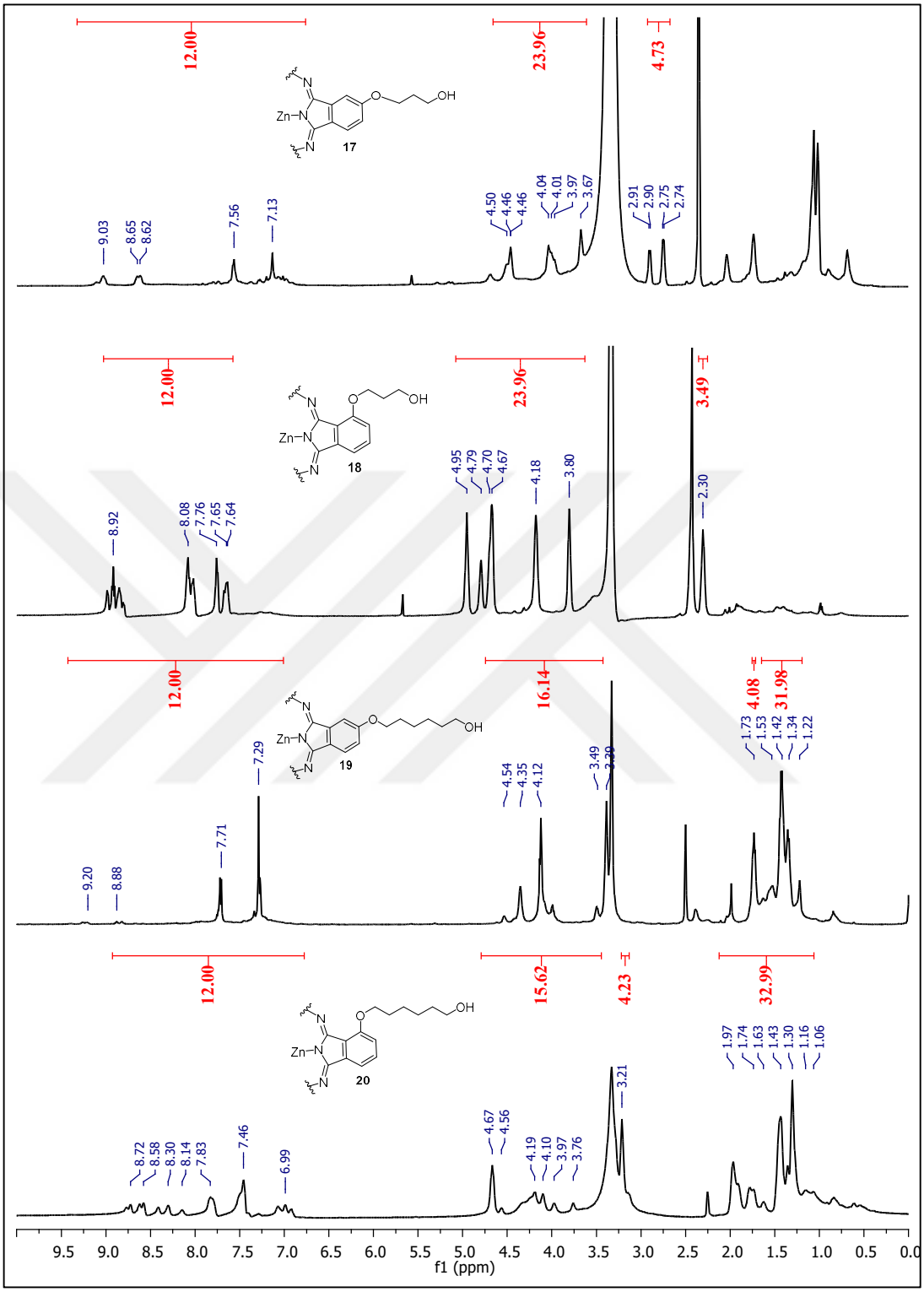

Figure 4.13: ^{1}H NMR spectra of hydroxylated phthalocyanines in DMSO-d_6.

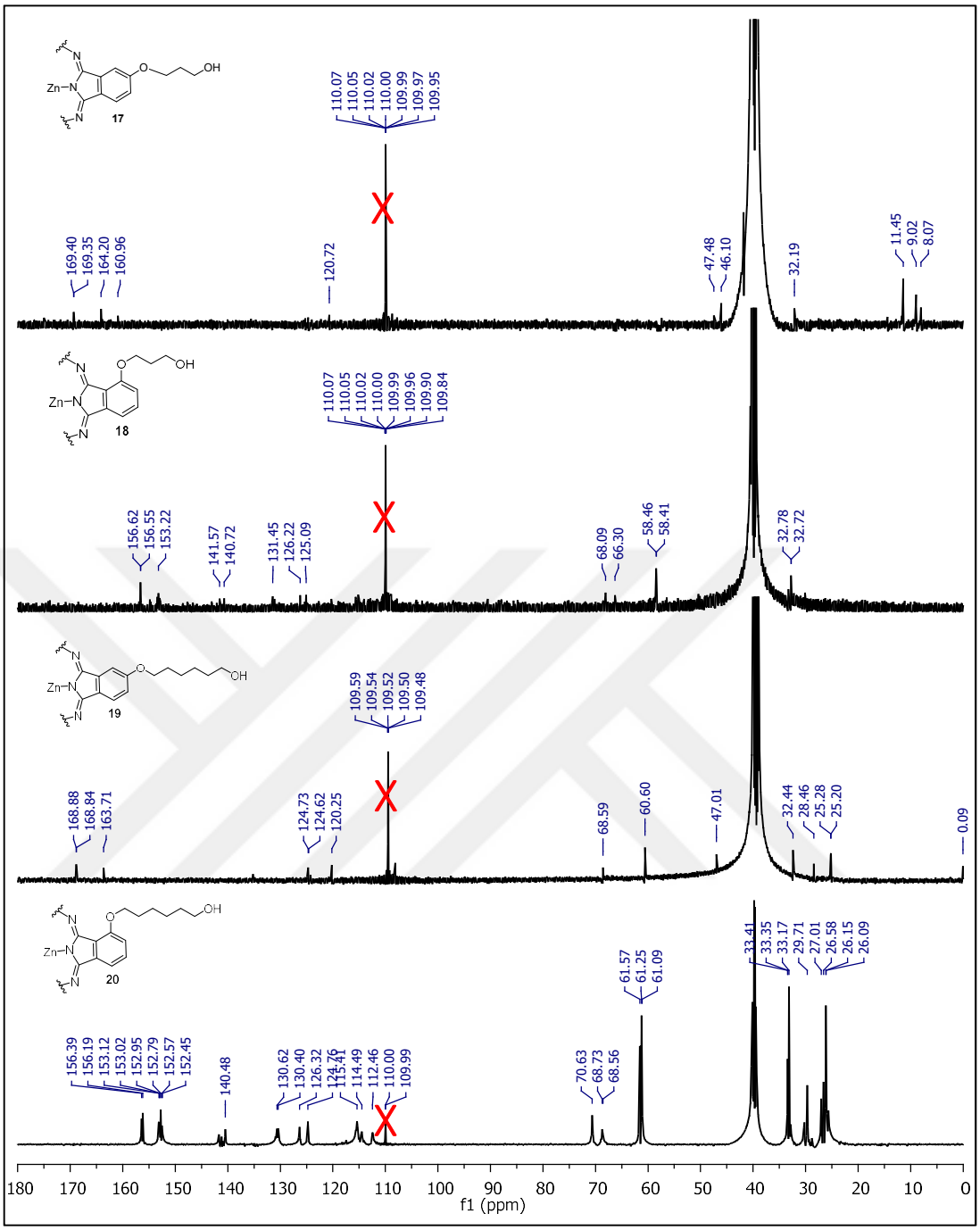

Figure 4.14: ^{13}C NMR spectra of hydroxylated phthalocyanines DMSO-d_6.

4.2.2.3. UV-Vis Spectra of Hydroxylated Phthalocyanines

Maximum absorbance of Q bands of the non-peripheral hydroxylated phthalocyanines (in DMSO) **17** and **19** is at 683 nm (Fig. 4.15 and Fig. 4.17), whereas those of peripheral derivatives **18** and **20** is at 706 nm (Fig. 4.16 and Fig. 4.18). Non-peripheral hydroxylated phthalocyanines Q bands, compared to peripheral ones, are shifted to longer wavelength, as expected, by approximately 23 nm. There is no significant effect of spacer length.

Table 4.5: Found max. absorbance λ and calculated log Ɛ of hydroxylated Pcs.

Compound	λ (nm)	Log Ɛ
17	683	4.61
18	706	5.18
19	683	3.93
20	706	5.27

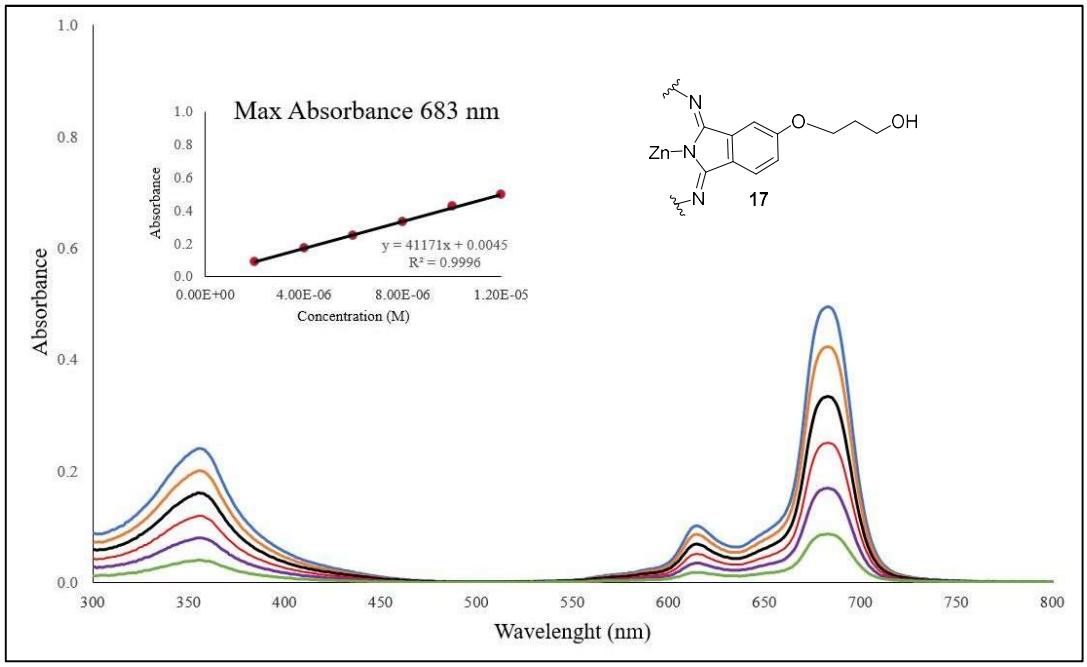

Figure 4.15: UV-Vis spectra of **17** (inset: plot of absorbance vs concentration) (DMSO, 2-12 μM).

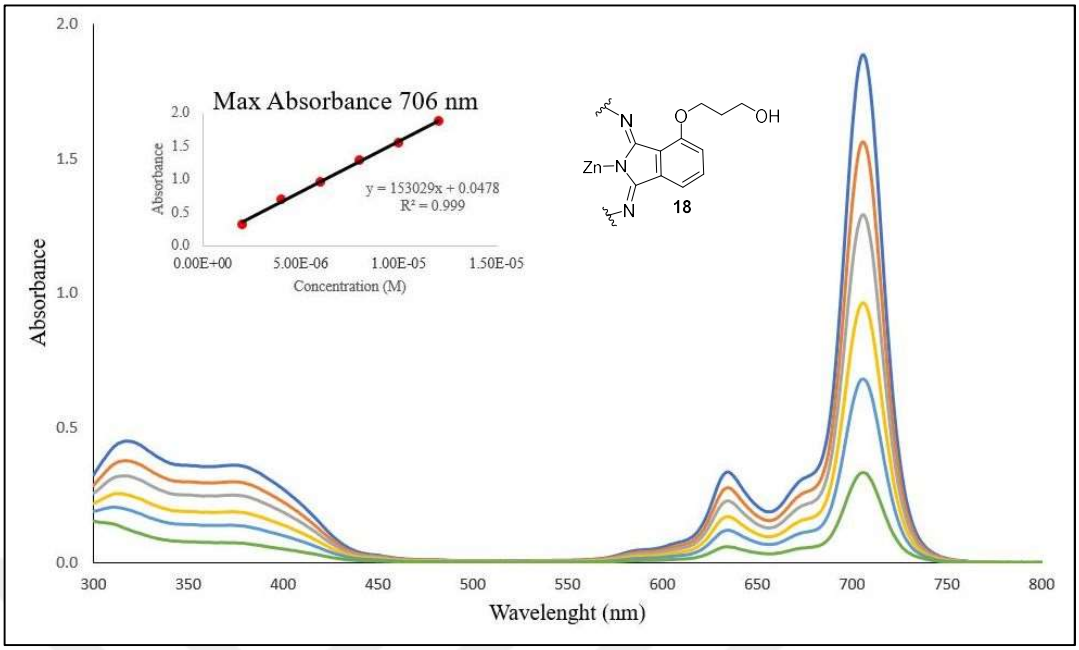

Figure 4.16: UV-Vis spectra of **18** (inset: plot of absorbance vs concentration) (DMSO, 2-12 μM).

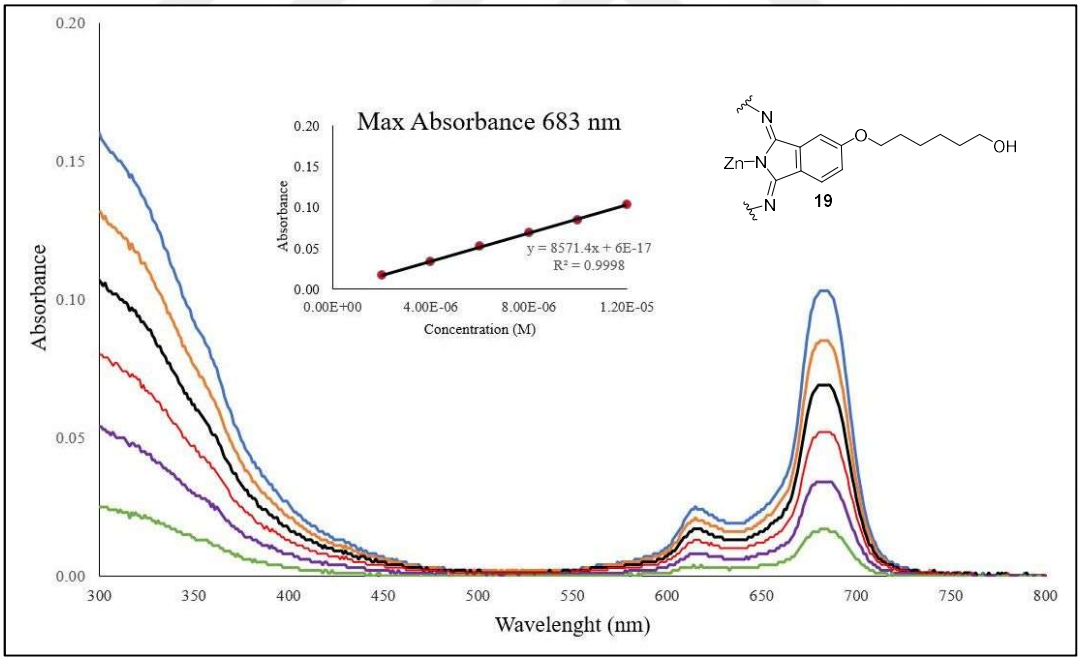

Figure 4.17: UV-Vis spectra of **19** (inset: plot of absorbance vs concentration) (DMSO, 2-12 μM).

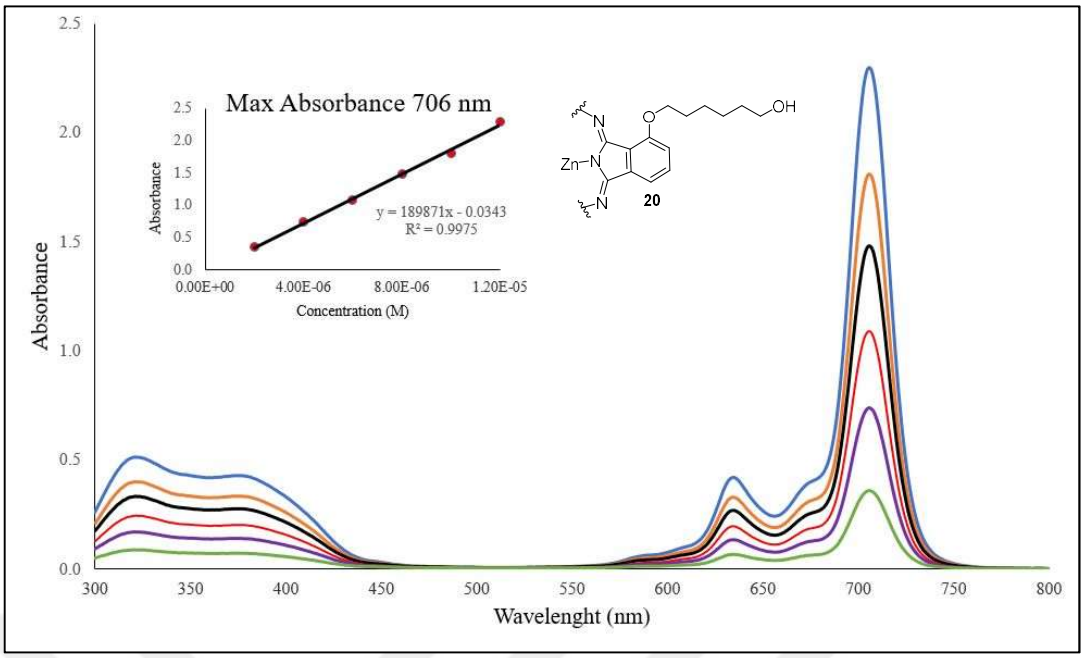

Figure 4.18: UV-Vis spectra of **20** (inset: plot of absorbance vs concentration) (DMSO, 2-12 μM).

4.2.3. Alkynated Phthalocyanines Synthesis

These are the final targeted molecules of this work which will be used as building blocks for the preparation of nanoPMOs. First attempts were done in K_2CO_3/DMF base/solvent pair. Different reaction temperatures and spans were tried. Also, various equivalents of K_2CO_3/DMF base/solvent pairs as well as propargyl bromide were tried. TLC and MALDI-TOF MS results of these first attempts were not satisfactory as in either trace amount of fully propargylated phthalocyanine formation or none at all. It has been found that 100 eq. of NaH base coupled with freshly distilled dry THF yields the targeted fully propargylated phthalocyanine in satisfactory yields. As it can be seen from below (Fig. 4.19), alkynated phthalocyanines **21**, **22**, **23**, **24** are prepared from hydroxylated phthalocyanines **17**, **18**, **19**, **20** respectively. Experimental yields (Table: 4.5) obtained can be seen below. Experimental yield for **21** could not be obtained because some of it had spilled during quenching of excess NaH, also experimental yield for **24** could not be obtained since it was synthesized from crude compound **20**.

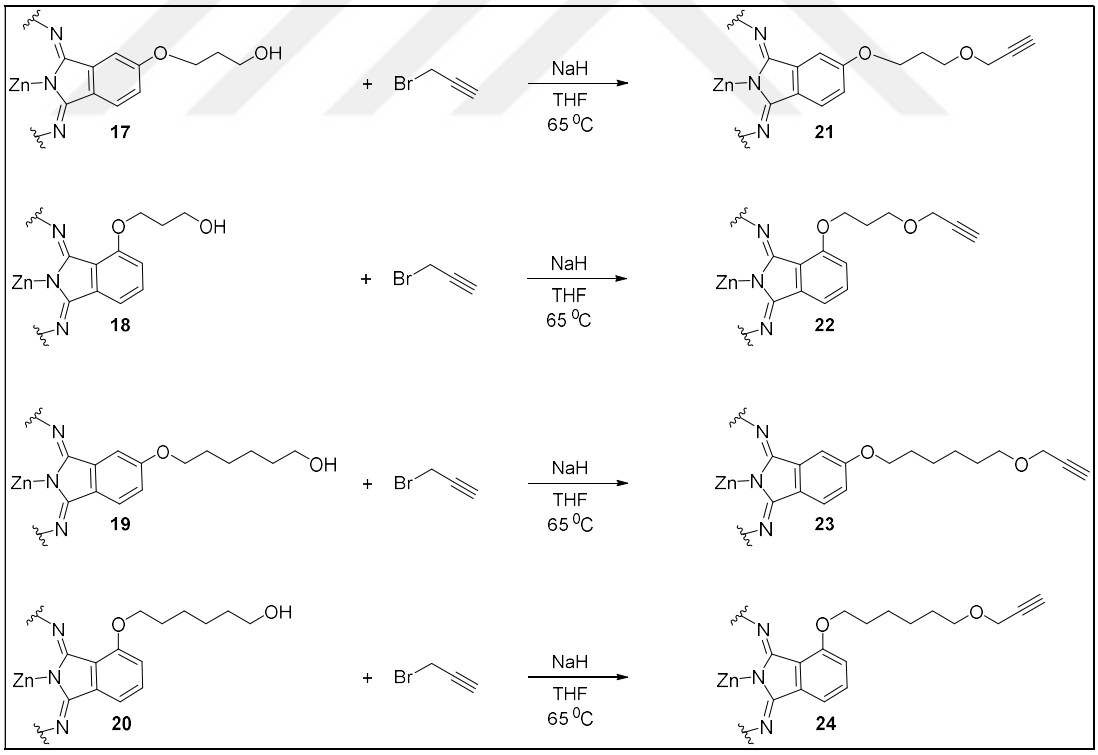

Figure 4.19: Alkynated phthalocyanines **21**-**24** synthesis.

Table 4.6: Experimental yields of alkynated phthalocyanines.

Compound	Yield (%)
21	---
22	54
23	52
24	---

4.2.4. Alkynated Phthalocyanines Characterization

All alkynated phthalocyanines were characterized by MALDI-TOF mass spectrometry, ^{1}H and ^{13}C NMR and UV-Vis spectroscopy.

4.2.4.1. MALDI-TOF Mass Spectra of Alkynated Pcs

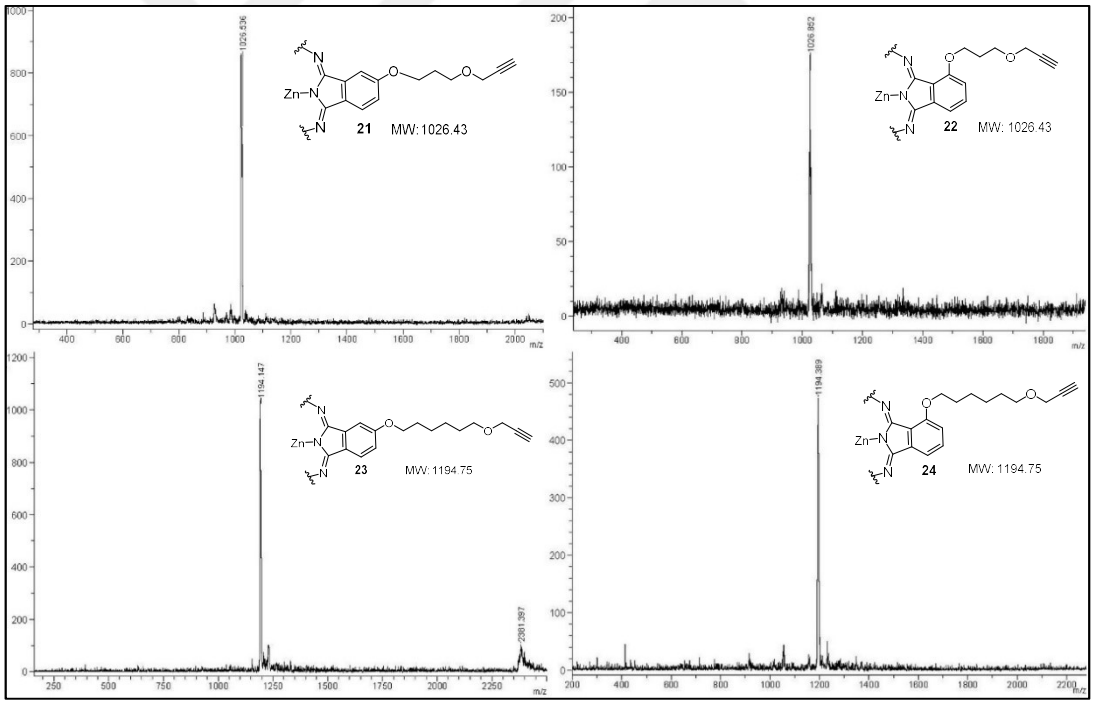

Figure 4.20: MALDI-TOF mass spectra of alkynated phthalocyanines.

All mass spectra were recorded with MALDI-TOF MS. Spectra can be seen in Figure 4.20 with their corresponding alkynated phthalocyanine structures as insets. In Table 4.6 comparison of corresponding alkynated phthalocyanines, *m/z* values with the matrixes can be seen.

Table 4.7: Calculated and found MALDI-TOF MS values of alkynated Pcs.

Compound	Molecular Formula	Matrix Used	Molecular Weight (g/mol)	Found m/z
21	$C_{56}H_{48}N_8O_8Zn$	DHB	1026.43	1026.536 $[M]^+$
22	$C_{56}H_{48}N_8O_8Zn$	DIT	1026.43	1026.852 $[M]^+$
23	$C_{68}H_{72}N_8O_8Zn$	DIT	1194.75	1194.147 $[M]^+$
24	$C_{68}H_{72}N_8O_8Zn$	DHB	1194.75	1194.389 $[M]^+$

4.2.4.2. ^{1}H and ^{13}C NMR Spectra of Alkynated Phthalocyanines

The spectra (Fig 4.21 and Fig 4.22) have been recorded in DMSO which proved to be the solvent avoiding best the aggregation, although not entirely satisfactorily as NMR recording request quite concentrated solutions.

As for the hydroxylated phthalocyanines described earlier on in this thesis, the phthalocyanines are isomeric mixtures, aromatic protons appear as multiplets. The multiplicity of the aromatic peaks, as expected, is not affected by the length of the spacer, but rather by the position of the substituent.

On the ^{13}C NMR spectra, one can observe that even the peaks corresponding to the substituents can be splitted. This is due again to the fact that these tetrasubstituted phthalocyanines have been obtained as regioisomeric mixtures. As reported previously for other phthalocyanines prepared by other groups [143], for some compounds, not all aromatic peaks are discernible. This is the case in particular for some quaternary carbons which are less intense than primary, secondary and tertiary (respectively) carbons. Nevertheless, for each compound, the expected peak corresponding to the alkynyl function are observed, all with roughly the same chemical shift (77 and 81 ppm).

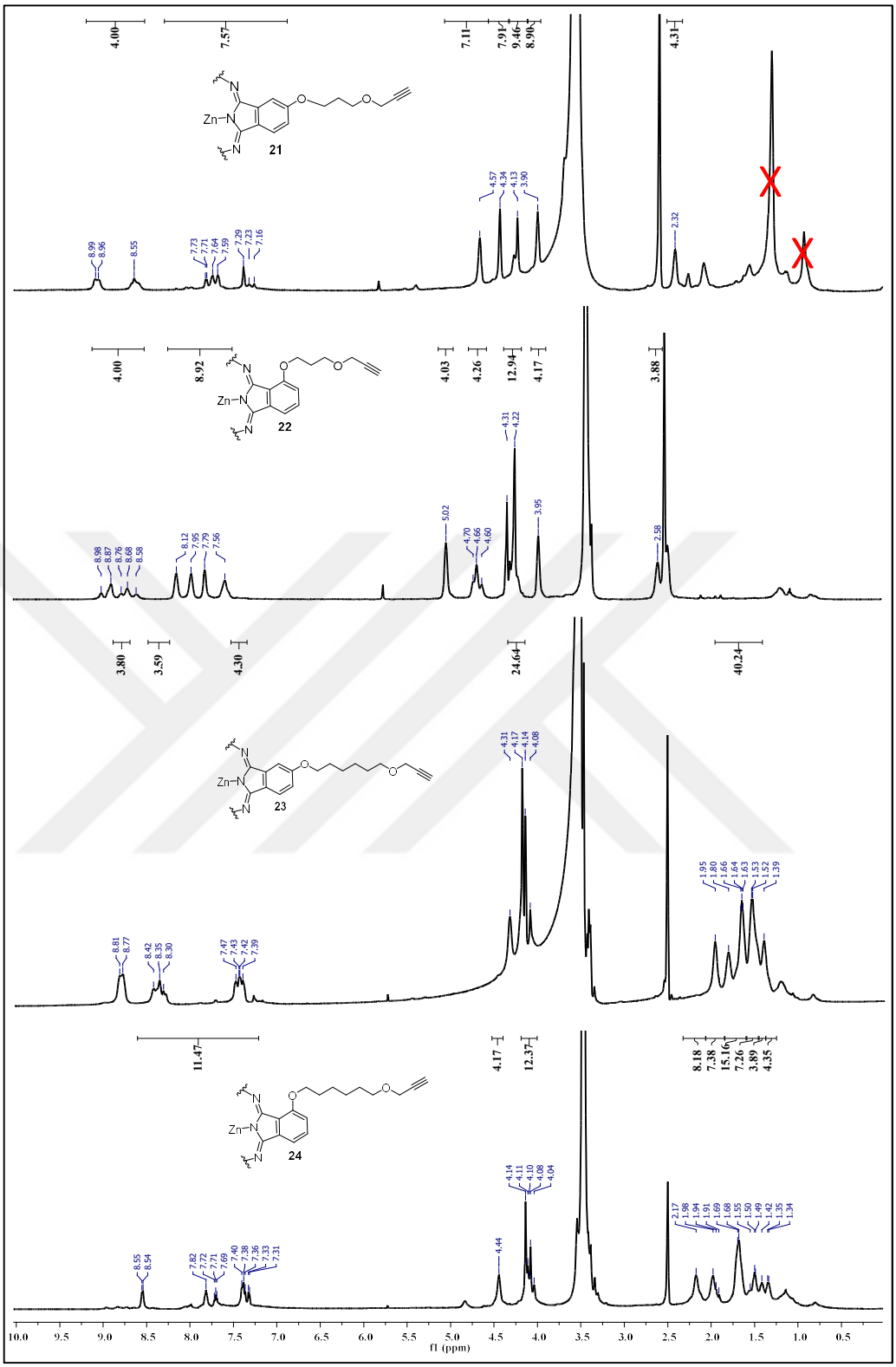

Figure 4.21: ^{1}H NMR spectra of alkynated phthalocyanines DMSO-d_6.

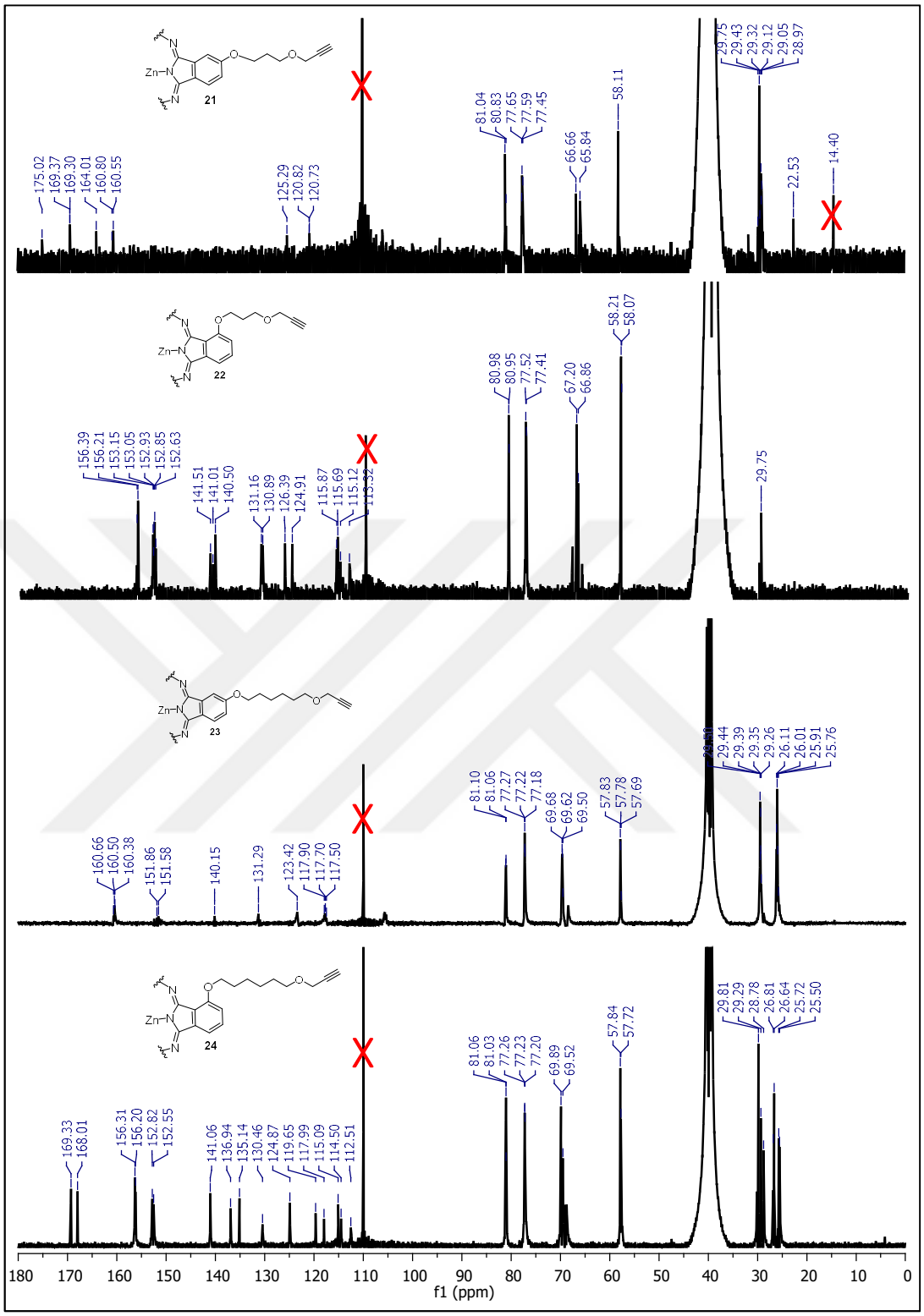

Figure 4.22: ^{13}C NMR spectra of alkynated phthalocyanines DMSO-d_6.

4.2.4.3. UV-Vis Spectra of Alkynated Phthalocyanines

Maximum absorbance of Q bands of the non-peripheral alkynated phthalocyanines (in DMSO) **21** and **23** is at 683 nm (Fig. 4.24 and Fig. 4.26), whereas those of peripheral derivatives **22** and **24** is at 705 nm (Fig. 4.25 and Fig. 4.27). Non-peripheral hydroxylated phthalocyanines Q bands, compared to peripheral ones, are shifted to longer wavelength, as expected, by approximately 22 nm. There is no significant effect of spacer length.

Table 4.8: Found max. absorbance λ and calculated log Ɛ of alkynated Pcs.

Compound	λ (nm)	Log Ɛ
21	683	4.83
22	705	5.31
23	683	5.08
24	705	4.85

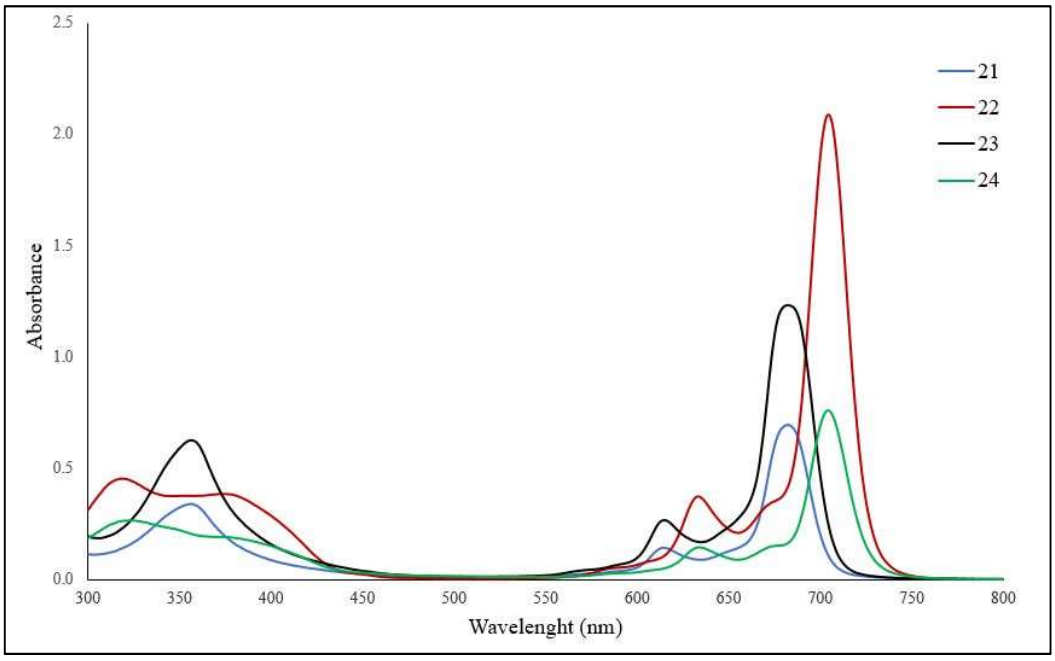

Figure 4.23: Superimposed UV-Vis spectra of alkynated phthalocyanines **21-24** (DMSO, 10 μM).

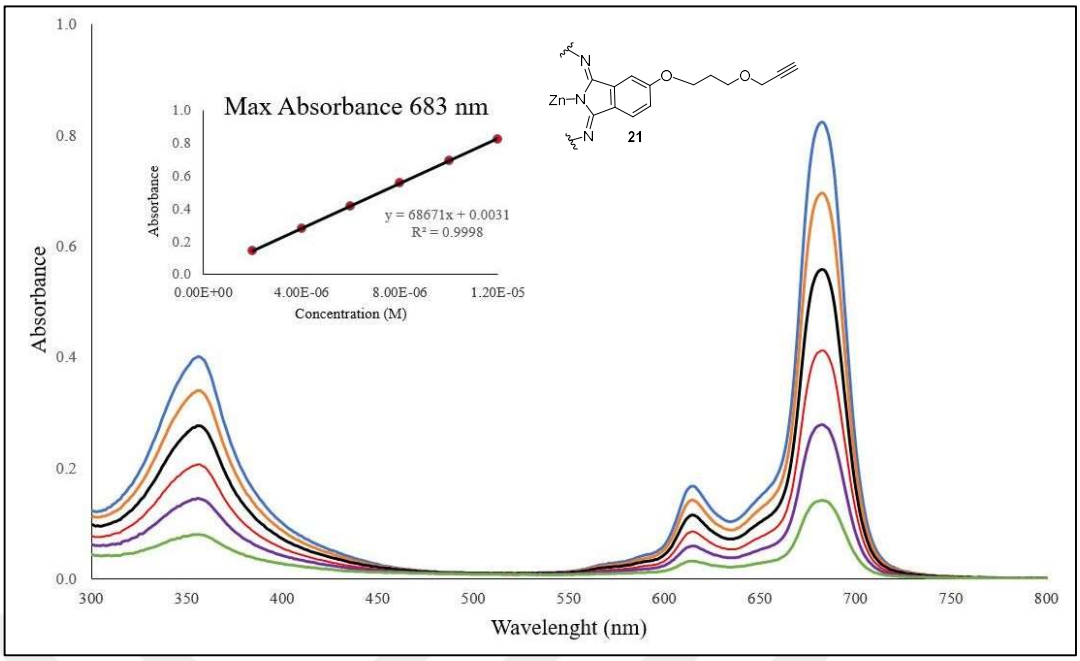

Figure 4.24: UV-Vis spectra of **21** (inset: plot of absorbance vs concentration) (DMSO, 2-12 µM).

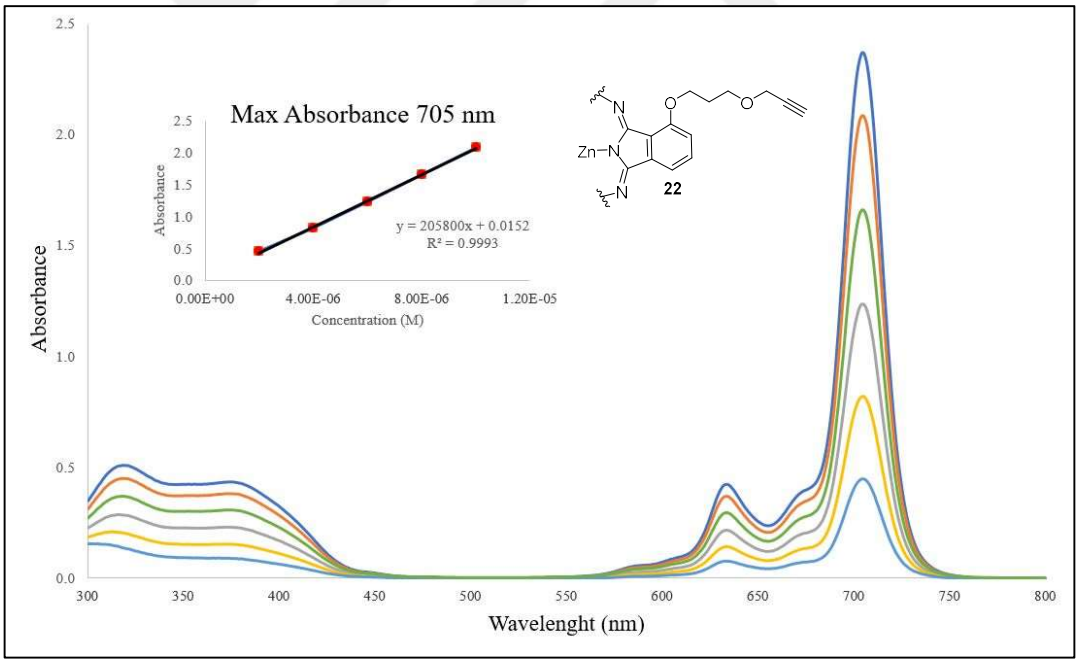

Figure 4.25: UV-Vis spectra of **22** (inset: plot of absorbance vs concentration) (DMSO, 2-12 µM).

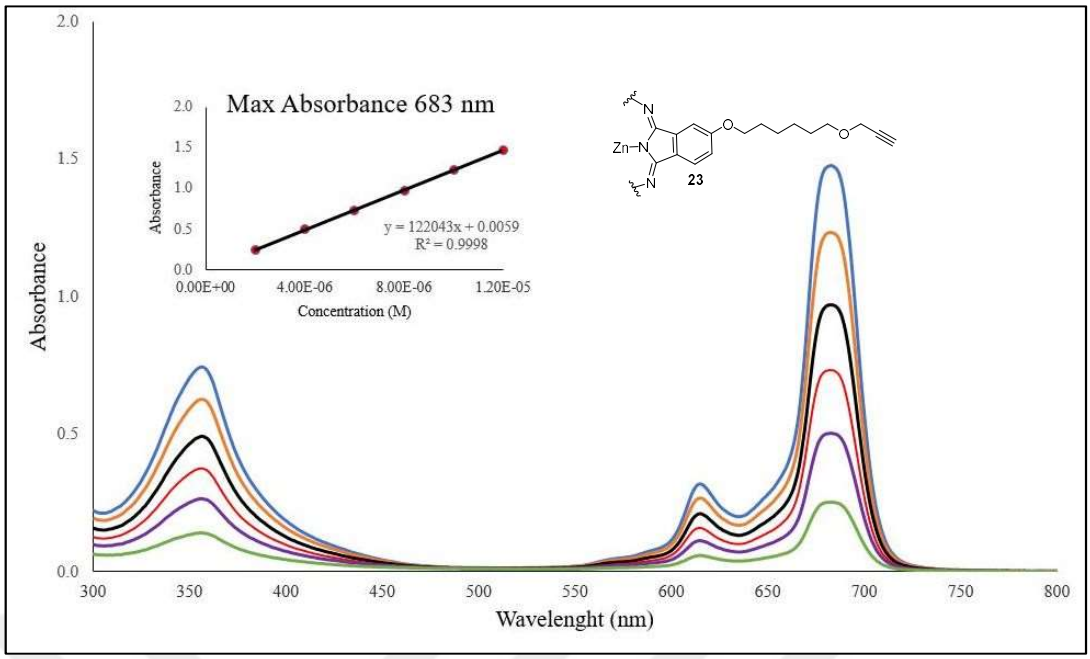

Figure 4.26: UV-Vis spectra of **23** (inset: plot of absorbance vs concentration) (DMSO, 2-12 μM).

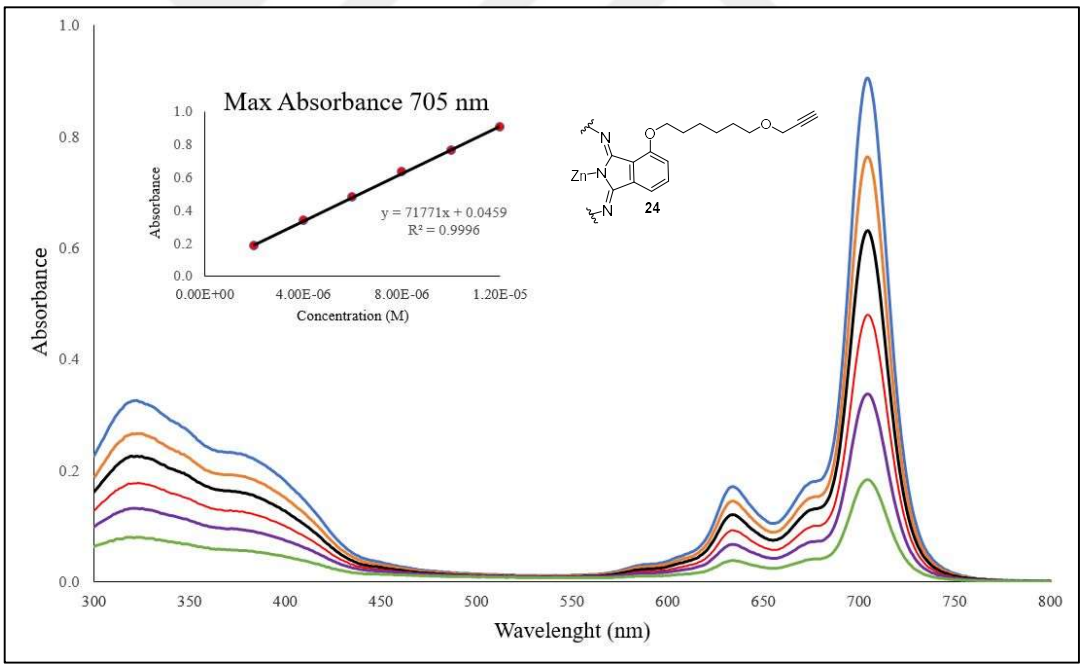

Figure 4.27: UV-Vis spectra of **24** (inset: plot of absorbance vs concentration) (DMSO, 2-12 μM).

4.2.5. Fluorescence Quantum Yields of Alkynated Phthalocyanines

All fluorescence quantum yields have been determined in DMSO. They are all of approximately the same value (0.07-0.013). This evidences that neither the position of the substituent, nor the length of the spacer, has a significant effect of this value.

Table 4.9: Fluorescence emission / excitation wavelengths and fluorescence quantum yields of alkynated Pcs.

Compound	Emission λ_{max} (nm)	Excitation λ_{max} (nm)	Φ_F
21	695	686	0.09
22	717	709	0.13
23	697	689	0.13
24	714	707	0.07

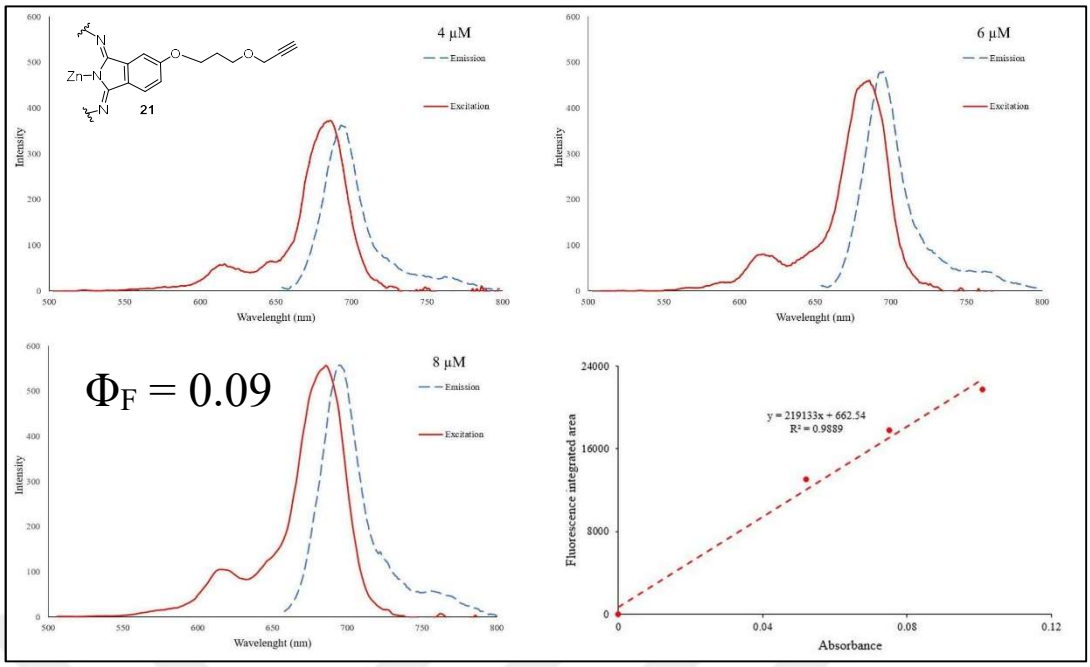

Figure 4.28: Fluorescence emission / excitation spectra of alkynated phthalocyanine **21** (DMSO, 4-8 µM) and fluorescence area integration vs absorbance.

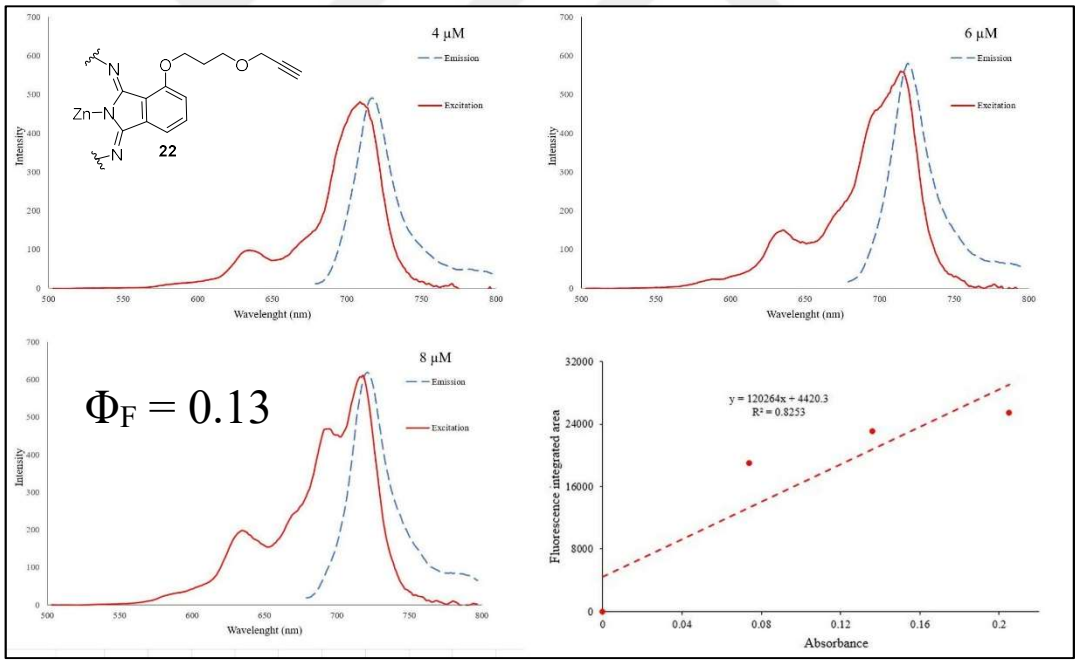

Figure 4.29: Fluorescence emission / excitation spectra of alkynated phthalocyanine **22** (DMSO, 4-8 µM) and fluorescence area integration vs absorbance.

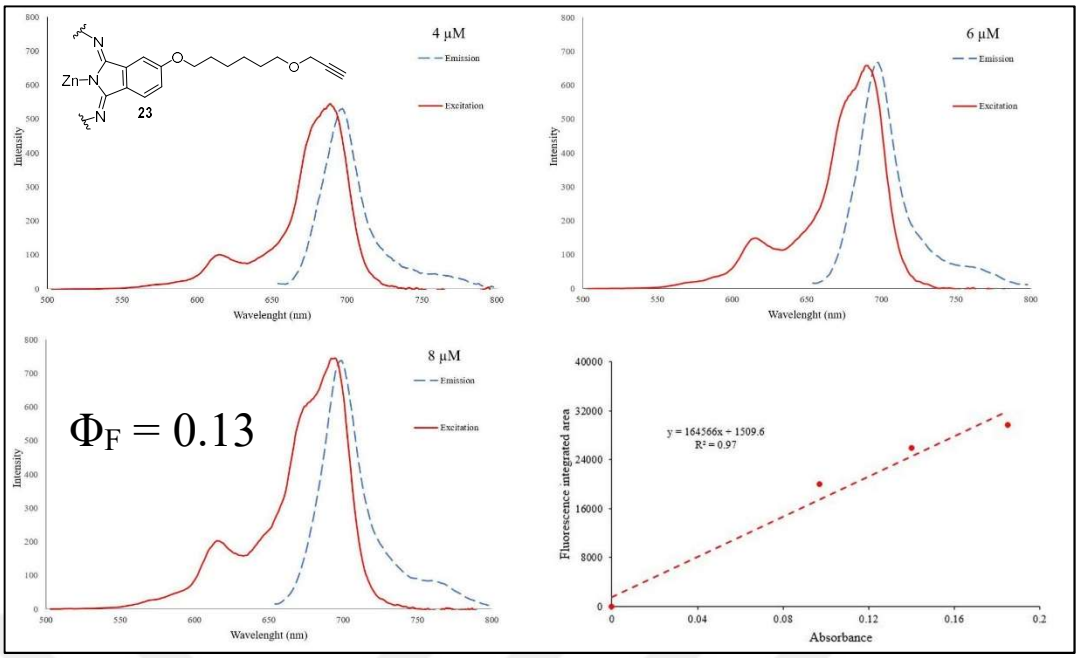

Figure 4.30: Fluorescence emission / excitation spectra of alkynated phthalocyanine **23** (DMSO, 4-8 µM) and fluorescence area integration vs absorbance.

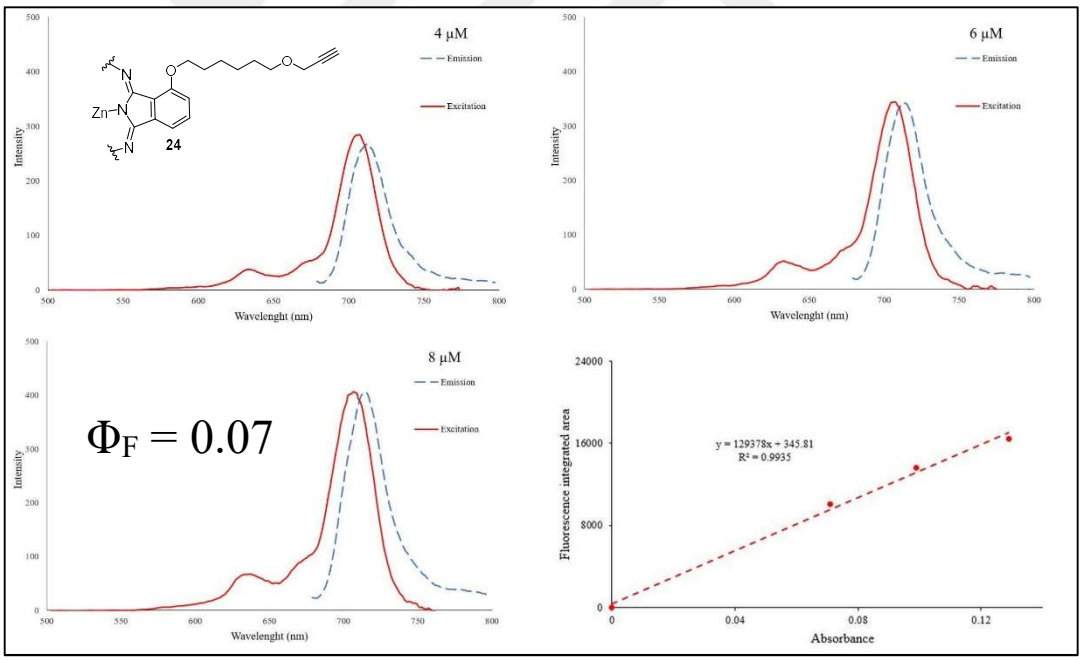

Figure 4.31: Fluorescence emission / excitation spectra of alkynated phthalocyanine **24** (DMSO, 4-8 µM) and fluorescence area integration vs absorbance.

4.2.6. Singlet O_2 Quantum Yields of Alkynated Phthalocyanines

All SOG quantum yields have been determined in DMSO. They are all of approximately the same value (66-71%). This evidences that neither the position of the substituent, nor the length of the spacer, has a significant effect of this value. All phthalocyanines generate singlet oxygen in range appropriate for photodynamic therapy, and close to those of unsubstituted ZnPc (0.67 in DMSO) [144]. These measurements confirm that the photosensitizing properties of the phthalocyanine macrocycle core are retained and not affected by the substituents.

Table 4.10: Singlet O_2 quantum yields of alkynated Pcs.

Compound	Φ_Δ
21	0.66
22	0.70
23	0.70
24	0.71

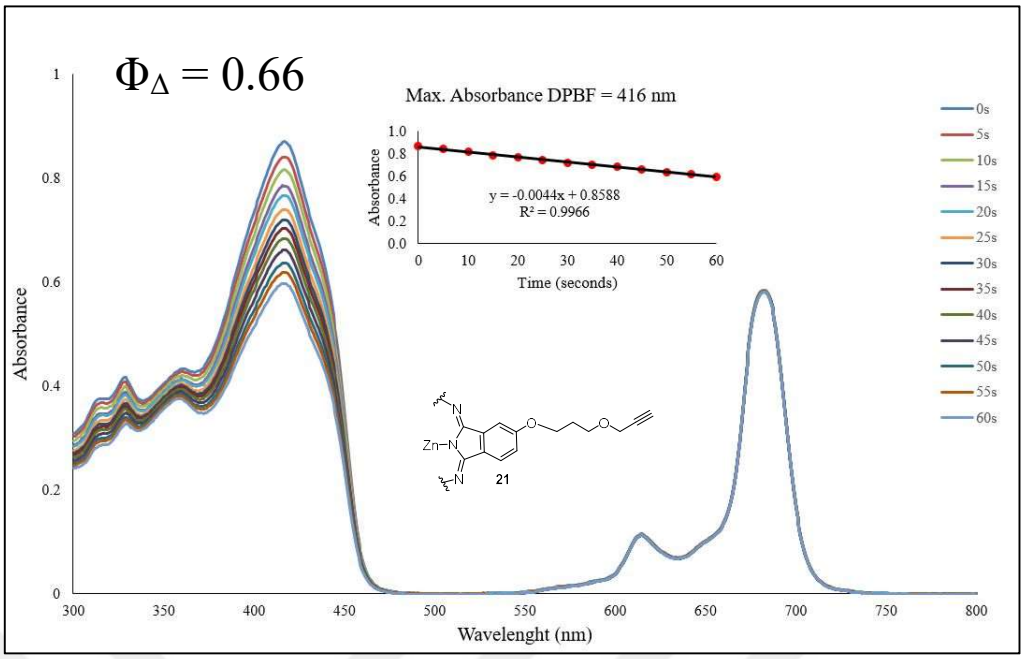

Figure 4.32: Singlet O_2 generation of alkynated phthalocyanine **21** (inset: plot of absorbance vs time) (DMSO, 8 µM).

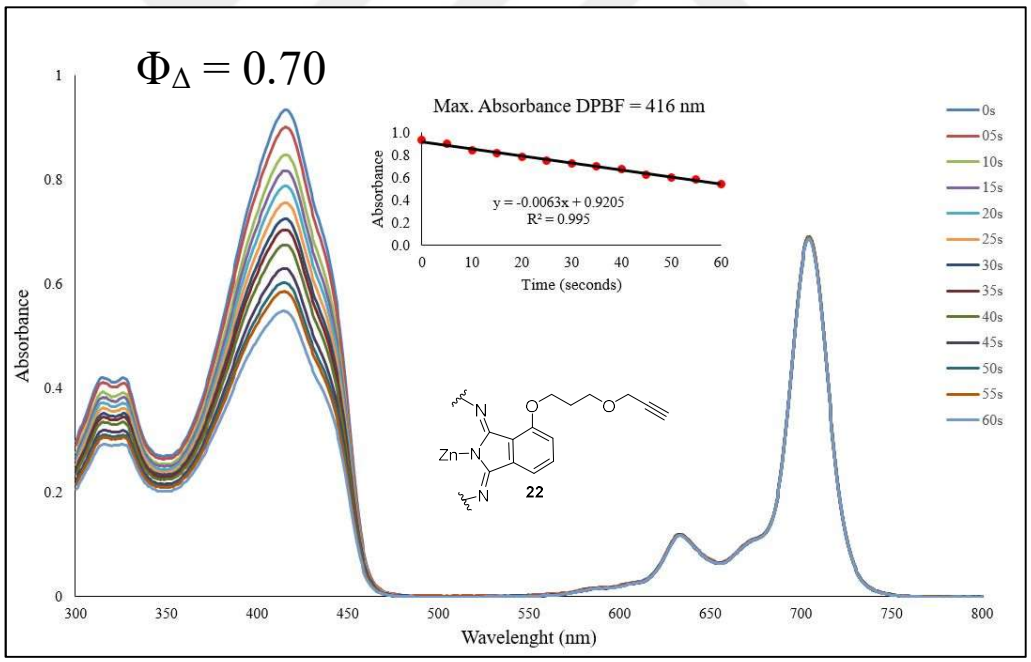

Figure 4.33: Singlet O_2 generation of alkynated phthalocyanine **22** (inset: plot of absorbance vs time) (DMSO, 4 µM).

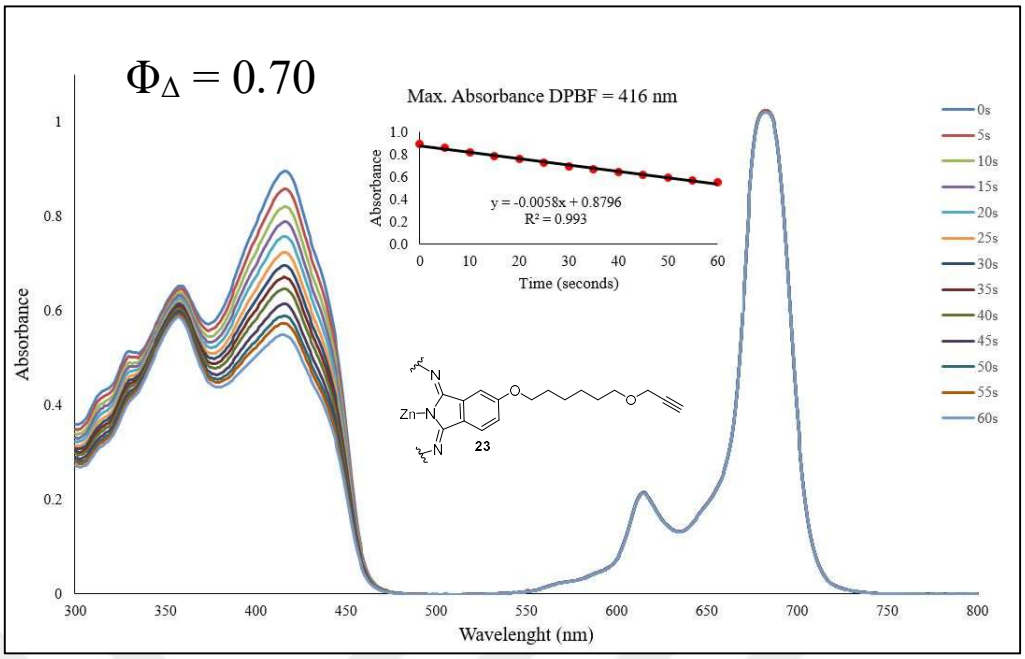

Figure 4.34: Singlet O_2 generation of alkynated phthalocyanine **23** (inset: plot of absorbance vs time) (DMSO, 8 µM).

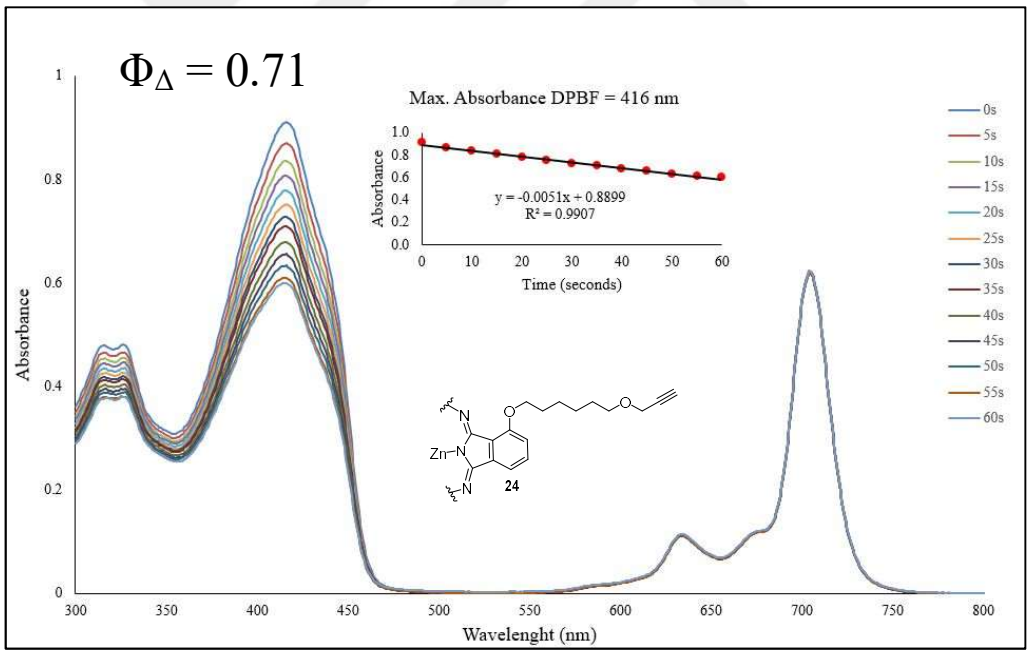

Figure 4.35: Singlet O_2 generation of alkynated phthalocyanine **24** (inset: plot of absorbance vs time) (DMSO, 8 µM).

5. EXPERIMENTAL PART

5.1. Numeration of Synthesized Compounds

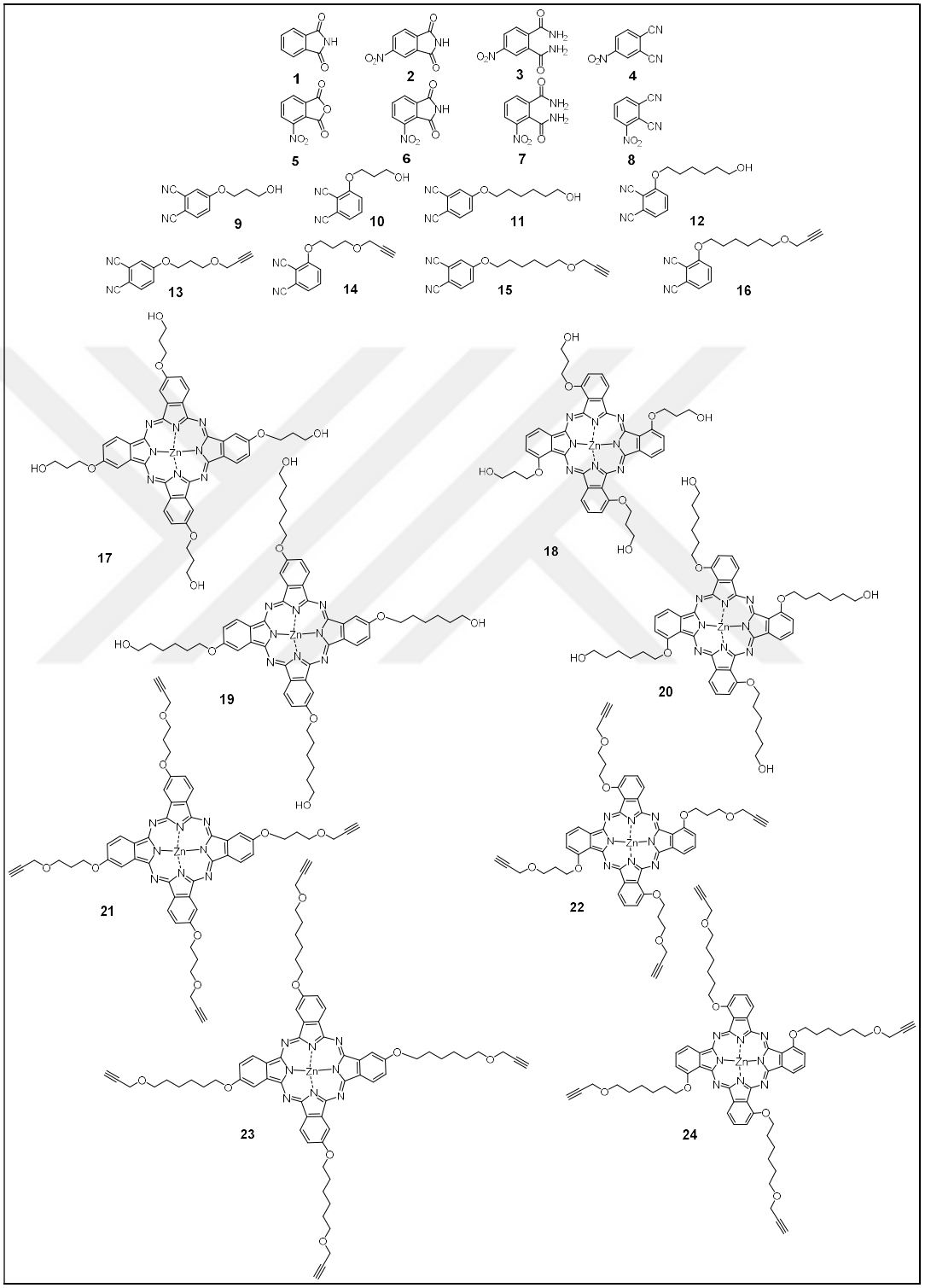

Figure 5.1: Numeration of synthesized compounds.

5.2. Materials and Methods

Table 5.1: Chemicals used for synthesis, purifications and separations.

Name	Cas Number	Manufacturer
Formamide	75-12-7	Merck
Zincacetate	557-34-6	Alfa Aeser
Ammonium Hydroxide	1336-21-6	Merck
Sodium Sulfate	7757-82-6	Sigma
DBU	6674-22-2	Fruka
DMF	69-12-2	Merck
1,6 Hexandiol	629-11-8	Sigma
1,3 Propandiol	504-63-2	Sigma
DMSO-d_6	2206-27-1	Merck
Chloroform-*d*	869-49-6	Merck
3-Nitrophtalic anhydride	641-70-3	Merck
n-Pentanol	71-41-0	Fruka
Propargyl bromide	106-96-7	Acros
Sodium hydride	7646-69-7	Sigma
THF	109-99-9	Sigma
$SOCl_2$	7-09-7719	Merck
Na	7440-23-5	
Benzophenone	119-61-9	Acros
Potassium Carbonate	584-08-7	Sigma
Silica (Column)	7631-86-9	Merck
Silica (Preparative TLC)	112926-00-8	Merck
Dichloromethane	-	Technical Grade
Hexane	-	Technical Grade
Ethyl Acetate	-	Technical Grade
Acetone	-	Technical Grade
Ethanol	-	Technical Grade
HNO_3	7697-37-2	Merck
H_2SO_4	7664-93-9	Merck
K_2CO_3	584-08-7	Sigma

Table 5.2: Instruments used for characterization.

Name	Model	Place
MALDI-TOF Mass Spectrometry	Bruker Microflex LT	GTU
NMR Spectrometry*	Varian Unity INOVA 500 MHz	GTU
FT-IR infrared Spectrometry	PerkinElmer Spectrum 100	GTU
UV-Vis Spectrometry	Shimadzu UV-2600	GTU
Spectro fluorometer	Varian Eclipse	GTU

* In some ^{13}C NMR spectra, the peak around 110 ppm is an artifact from our NMR apparatus. This is why it is marked with a cross (X).

5.3. Synthesis of 4-nitrophthalimide (2)

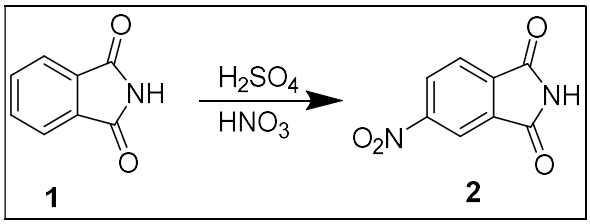

Figure 5.2: Synthesis of 4-nitrophthalimide **(2)**.

Mixture of H_2SO_4 (200 mL) and HNO_3 (65%, 50 mL) was prepared in ice bath and cooled down to 15 °C. Phthalimide (**1**) (40 g, 0.272 mol) was slowly added to the acid mixture over an hour while continuously stirring. It was stirred for another hour at 35 °C then it was cooled down to 0 °C and it was poured onto approximately 1 kg of ice while maintaining a temperature lower than 15 °C. The precipitation was washed with cold water, and crystallized in ethanol (1.5 L). Yellow crystals were dried under vacuum at 110 °C [141].

- Yield 77%
- Melting Point: 194 °C
- $C_8H_4N_2O_4$, MW: 192.13 g/mol

5.4. Synthesis of 4-nitrophthalamide (3)

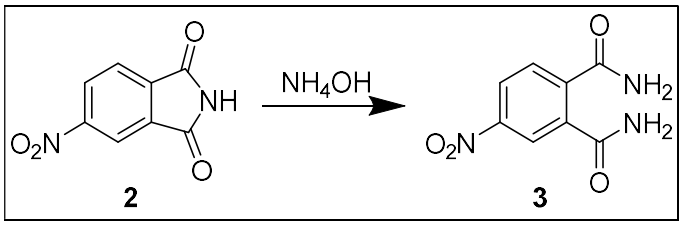

Figure 5.3: Synthesis of 4-nitrophthalamide **(3)**.

4-nitrophthalimide (**2**) (5 g, 0.026 mol) was stirred in 25% ammonia (35 mL) solution at room temperature for 24 hours. The precipitate was filtered and washed with water until it is neutral. The white precipitate was washed with ethanol (150 mL). The white solid was dried under vacuum at 110 °C [141].

- Yield 75%
- Melting Point: 198 °C
- $C_8H_7N_3O_4$, MW: 209.16 g/mol

5.5. Synthesis of 4-nitrophthalonitrile (4)

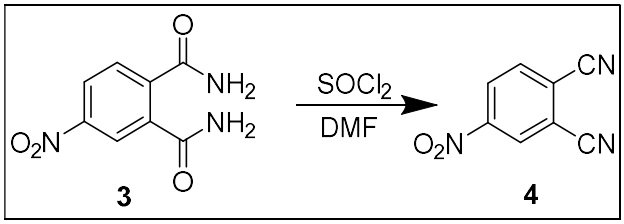

Figure 5.4: Synthesis of 4-nitrophthalonitrile **(4)**.

Dry DMF (140 mL) was cooled down to 0 °C in ice bath under argon atmosphere. $SOCl_2$ (14.2 mL) was added very slowly, drop by drop while maintaining reaction mixture temperature not exceeding 5 °C. The mixture was stirred for additional 10 minutes. 4-nitrophthalamide (**3**) (16.9 g, 0.093 mol) was then added slowly while maintaining reaction mixture temperature not exceeding 5 °C. After the addition of **3**, the ice bath was removed and the reaction mixture was stirred at room temperature for 3 hours and then poured onto ice slowly. The precipitate was filtered and washed with cold water until it was neutral. Pale yellow compound **4** was then dried under vacuum at 65 °C [141].

- Yield 68%
- Melting Point: 139 °C
- $C_8H_3N_3O_2$, MW: 173.13 g/mol

5.6. Synthesis of 3-nitrophthalimide (6)

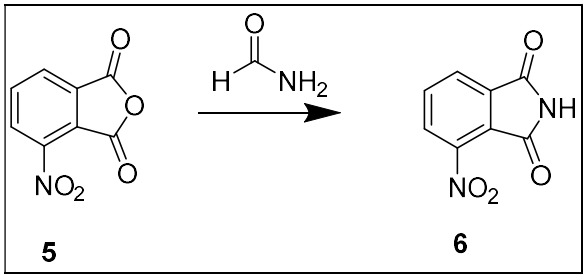

Figure 5.5: Synthesis of 3-nitrophthalimide **(6)**.

3-nitrophthalic anhydride (**5**) (22.2 g, 0.115 mol) was stirred and refluxed at 145 °C in formamide (35 mL) for 3 hours with a condenser attached. After stirring, mixture was cooled down to room temperature, then filtrated. The precipitate was washed with water until its pH is 7. Resulting yellow solid was then dried under vacuum [140].

- Yield 92%
- Melting Point: 203 °C
- $C_8H_4N_2O_4$, MW: 192.13 g/mol

5.7. Synthesis of 3-nitrophthalamide (7)

3-nitrophthalimide (**6**) (23.6 g, 0.123 mol) was added to 25% ammonia (60 mL) solution at room temperature while stirring. Brownish yellow reaction mixture was then heated slowly to 45 °C and stirred for 5 hours. After stirring, mixture was cooled down to room temperature, then filtrated. The precipitate was washed with cold water until its pH is 7. Obtained white solid was then dried under vacuum at 110 °C [140].

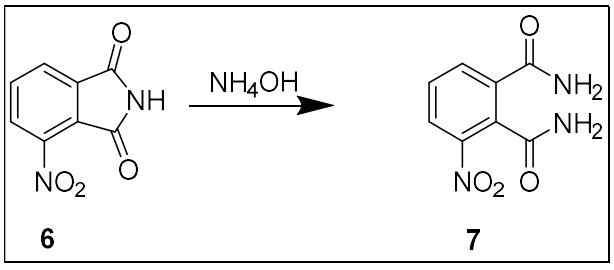

Figure 5.6: Synthesis of 3-nitrophthalamide **(7)**.

- Yield 76%
- Melting Point: 223 °C
- $C_8H_7N_3O_4$, MW: 209.16 g/mol

5.8. Synthesis of 3-nitrophthalonitrile (8)

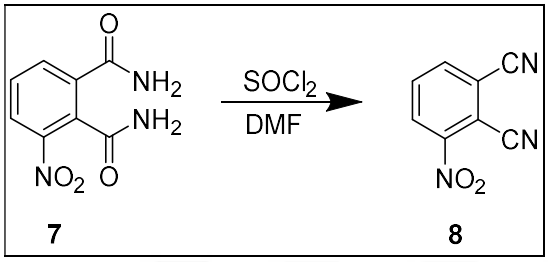

Figure 5.7: Synthesis of 3-nitrophthalonitrile **(8)**.

Dry DMF (40 mL) was cooled down to 0 °C in ice bath under argon atmosphere. $SOCl_2$ (25 mL) was added very slowly, drop by drop while maintaining reaction mixture temperature below 5 °C. The mixture was stirred for additional 3 hours under room temperature. 3-nitrophthalamide (**7**) (7.01 g, 0.033 mol) was then added slowly while maintaining reaction mixture temperature not exceeding 5 °C. After the addition of **7**, the ice bath was removed and the reaction mixture was stirred at room temperature for another 3 hours and then poured onto ice slowly. The precipitate was filtered and washed with cold water until it was neutral. Pale yellow compound **8** was then dried under vacuum at 65 °C [141].

- Yield 72%
- Melting Point: 163 °C
- $C_8H_3N_3O_2$, MW: 173.13 g/mol

5.9. Synthesis of 4-(3-hydroxypropoxy)phthalonitrile (9)

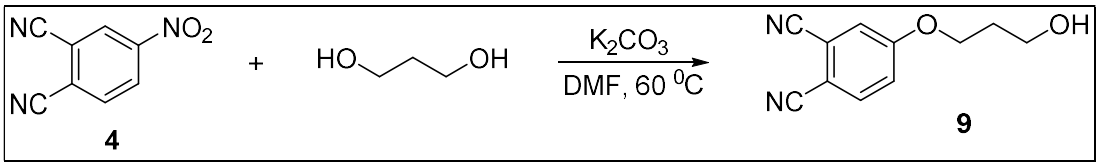

Figure 5.8: Synthesis of **9**.

4-nitrophthalonitrile (**4**), (2.6 g, 15 mmol) 1,3 propanediol (5.70 g, 75 mmol), and K_2CO_3 (41 g, 300 mmol) was heated to 60 °C with DMF (100 mL) and stirred for 24 hours. After stirring, mixture was cooled down to room temperature and extracted with ethyl acetate. It was purified with silica gel colon chromatography (50 DCM / 1 ethanol) and obtained white solid.

- Yield 56% (1.7 g)
- $C_{11}H_{10}N_2O_2$, MW: 202.21 g/mol
- MS-MALDI-TOF (*m/z*): 203.998 $[M+H]^+$ (Matrix: DHB).
- FT-IR (cm^{-1}): 3323, 3088, 2935, 2861, 2238, 2226, 1979, 1579, 1473, 1453, 1399, 1292, 1177, 1044, 923, 844, 794, 729, 684.
- ^1H NMR ($CDCl_3$, δ, ppm): 7.69 (d, 1H), 7.26 (s, 1H), 7.20 (d, 1H), 4.21 (t, 2H), 3.83 (s, 3H), 2.07 (t, 2H), 1.76 (s, 1H)
- ^{13}C NMR ($CDCl_3$, δ, ppm): 162.23, 135.35, 119.80, 119.48, 117.44, 115.82, 107.19, 66.28, 58.96, 31.64

5.10. Synthesis of 3-(3-hydroxypropoxy)phthalonitrile (10)

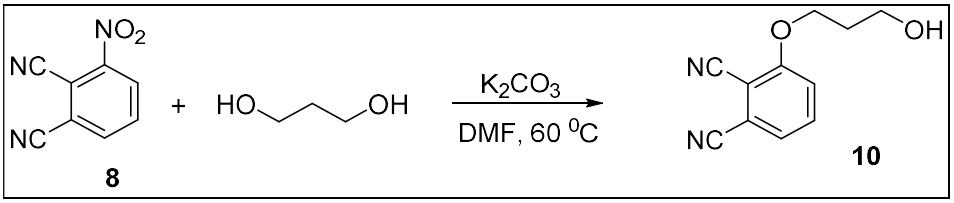

Figure 5.9: Synthesis of **10**.

3-nitrophthalonitrile (**8**) (5.2 g, 30 mmol), 1,3 propanediol (11.40 g, 150 mmol) and K_2CO_3 (103 g, 750 mmol) was heated to 60 °C with DMF (225 mL) and stirred for 24 hours. After stirring, mixture was cooled down to room temperature and added water (800 mL). The resulting white precipitate filtrated and purified with silica gel colon chromatography (50 DCM / 1 ethanol).

- Yield 33% (2 g)
- $C_{11}H_{10}N_2O_2$, MW: 202.21 g/mol
- MS-MALDI-TOF (*m/z*): 224.886 $[M+Na]^+$ (Matrix: DIT)
- FT-IR (cm^{-1}): 3315, 3087, 2957, 2227, 1980, 1579, 1473, 1452, 1397,1244, 1177, 1052, 1000, 906, 884, 795, 729, 682
- ^1H NMR ($CDCl_3$, δ, ppm): 7.66 (t, 1H), 7.35 (d, 1H), 7.30 (d, 1H), 4.31 (t, 2H), 3.90 (d, 2H), 2.13 (t, 2H), 1.75 (s, 1H)
- ^{13}C NMR ($CDCl_3$, δ, ppm): 161.51, 134.78, 125.25, 117.02, 116.99, 115.44, 113.16, 105.02, 66.87, 58.91, 31.61

5.11. Synthesis of 4-((6-hydroxyhexyl)oxy)phthalonitrile (11)

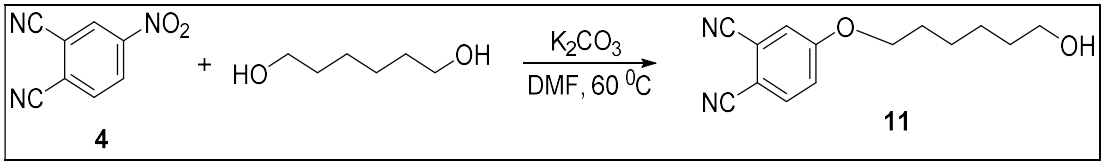

Figure 5.10: Synthesis of **11**.

4-nitrophthalonitrile (**4**) (3.46 g, 20 mmol), 1,6 hexanediol (12 g, 100 mmol) and K_2CO_3 (69 g, 500 mmol) was heated to 60 °C with DMF (150 mL) and stirred for 17 hours. After stirring, mixture was cooled down to room temperature and added water (500 mL) along with NaCl (50 g). The resulting white/green precipitate filtrated and purified with silica gel colon chromatography (50 DCM / 1 ethanol).

- Yield 23% (1.13 g)
- $C_{14}H_{16}N_2O_2$, MW: 244.29 g/mol
- MS-MALDI-TOF (*m/z*): 266.047 $[M+Na]^+$ (Matrix: DHB).
- FT-IR (cm^{-1}): 3084, 2951, 2868, 2294, 1496, 1471, 1415, 1345, 1320, 1290, 1257, 1212, 1176, 1051, 999, 941, 924, 882, 847, 741, 698, 625
- ^1H NMR ($CDCl_3$, δ, ppm): 7.69 (d, 1H), 7.25 (s, 1H), 7.18 (d, 1H), 4.05 (t, 2H), 3.68 (q, 2H), 1.85 (p,2H), 1.61 (p, 2H), 1.48 (m, 4H), 1.23 (m, 1H)
- ^{13}C NMR ($CDCl_3$, δ, ppm): 162.30, 135.32, 119.64, 119.47, 69.31, 62.91, 32.69, 28.90, 25.84, 25.61

5.12. Synthesis of 3-((6-hydroxyhexyl)oxy)phthalonitrile (12)

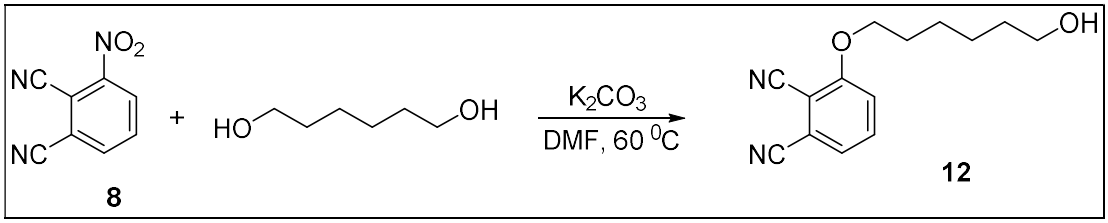

Figure 5.11: Synthesis of **12**.

3-nitrophthalonitrile (**8**) (3.46 g, 20 mmol), 1,6 hexanediol (12 g, 100 mmol) and K_2CO_3 (69 g, 500 mmol) was heated to 60 °C with DMF (150 mL) and stirred for 17 hours. After stirring, mixture was cooled down to room temperature and added water (500 mL). The resulting white precipitate filtrated and purified with silica gel colon chromatography (50 DCM / 1 ethanol).

- Yield 53% (2.6 g)
- $C_{14}H_{16}N_2O_2$, MW: 244.29 g/mol
- MS-MALDI-TOF (*m/z*): 281.952 $[M+K]^+$ (No Matrix).
- FT-IR (cm^{-1}): 3315, 3088, 2935, 2861, 2238, 2226, 1978, 1580, 1473, 1453, 1399, 1177, 1033, 923, 844, 795, 729, 684
- ^1H NMR ($CDCl_3$, δ, ppm): 7.62 (t, 1H), 7.33 (d, 1H), 7.21 (d, 1H), 4.14 (t, 2H), 3.67 (t, 2H), 1.90 (p, 2H), 1.63 (t, 2H), 1.49 (d, 4H), 1.31 (s, 1H)
- ^{13}C NMR ($CDCl_3$, δ, ppm): 161.63, 134.59, 125.10, 116.80, 70.03, 62.91, 32.68, 28.81, 25.84, 25.58

5.13. Synthesis of Phthalocyanine 17

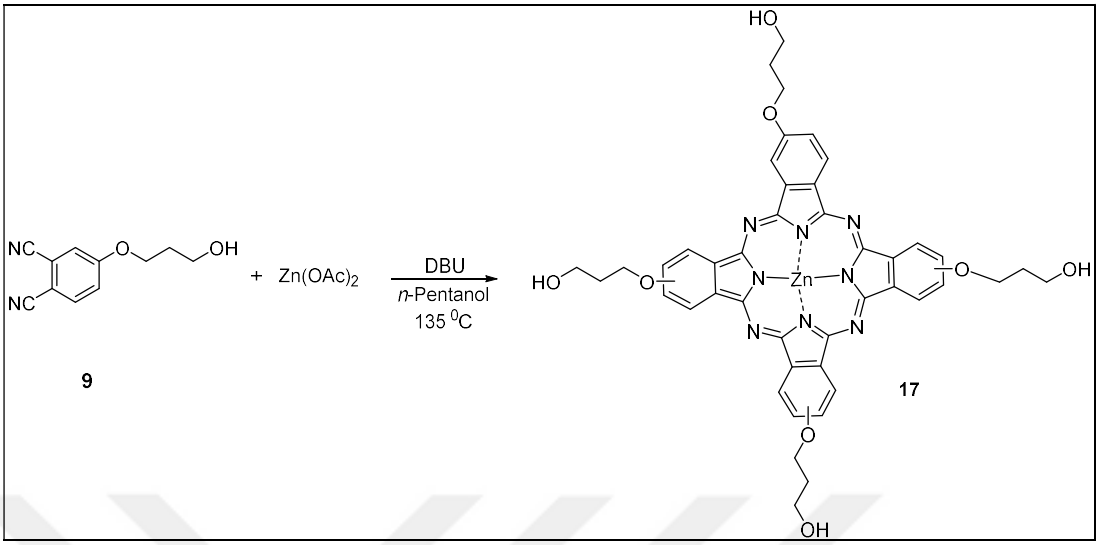

Figure 5.12: Synthesis of **17**.

Compound **9** (809 mg, 4 mmol), zinc acetate (367 mg, 2 mmol) and DBU (0.5 mL) was heated to 140 °C under argon atmosphere with *n*-pentanol (7 mL) and stirred for 18 hours. After stirring, mixture was cooled down to room temperature and water (600 mL) was added along with NaCl (60 g). The resulting green precipitate was filtrated, solubilized with acetone / ethanol (70mL / 30 mL) mixture then precipitated again in ethyl acetate (400 mL) and refiltrated. It was purified with silica gel colon chromatography (5 DCM / 1 ethanol).

- Yield: 30% (250 mg)
- $C_{44}H_{40}N_8O_8Zn$, MW: 874.23 g/mol
- MS-MALDI-TOF (*m/z*): 874.484 $[M]^+$ (Matrix: DIT).
- FT-IR (cm^{-1}): 3340, 2921, 2852, 1739, 1717, 1608, 1464, 1377, 1258, 1052, 748
- ^1H NMR (DMSO-d_6, δ, ppm): 9.03–7.13 (m, 121H), 4.50-3.67 (m, 24H), 2.91-2.74 (m, 4H)
- ^{13}C NMR (DMSO-d_6, δ, ppm): 169.40, 169.35, 164.20, 160.96, 120.72, 47.48, 46.10, 32.19, 11.45, 9.02, 8.07

5.14. Synthesis of Phthalocyanine 18

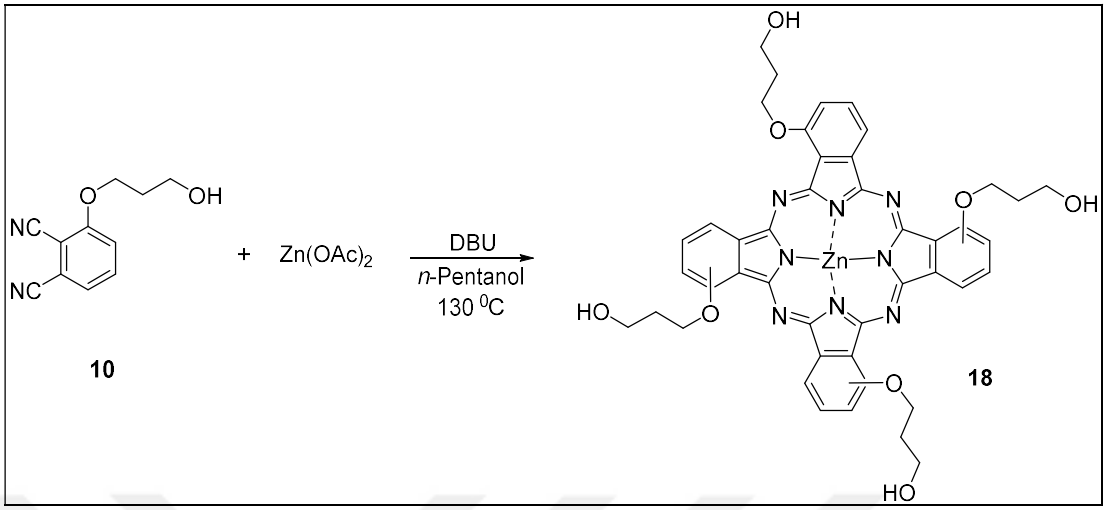

Figure 5.13: Synthesis of **18**.

Compound **10** (809 mg, 4 mmol), zinc acetate (367 mg, 2 mmol) and DBU (0.5 mL) was heated to 130 °C under argon atmosphere with *n*-pentanol (7 mL) and stirred for 18 hours. After stirring, mixture was cooled down to room temperature and added water (400 mL). The resulting green precipitate was filtrated, solubilized with acetone / ethanol (70mL / 30 mL) mixture then precipitated again in ethyl acetate (400 mL) and refiltrated. It was purified with silica gel colon chromatography (5 DCM / 1 ethanol).

- Yield: 24% (210 mg)
- $C_{44}H_{40}N_8O_8Zn$, MW: 874.23 g/mol
- MS-MALDI-TOF (*m/z*): 874.246 $[M]^+$ (Matrix: DIT).
- FT-IR (cm^{-1}): 3338, 2931, 1586, 1488, 1333, 1266, 1224, 1120, 1060, 918, 876, 801
- ^1H NMR (DMSO-d_6, δ, ppm): 8.92-7.64 (m, 12H), 4.95-3.80 (24H), 2.30 (s, 4H)
- ^{13}C NMR (DMSO-d_6, δ, ppm): 156.62, 156.55, 153.22, 141.57, 140.72, 131.45, 126.22, 125.09, 68.09, 66.30, 58.46, 58.41, 32.78, 32.72

5.15. Synthesis of Phthalocyanine 19

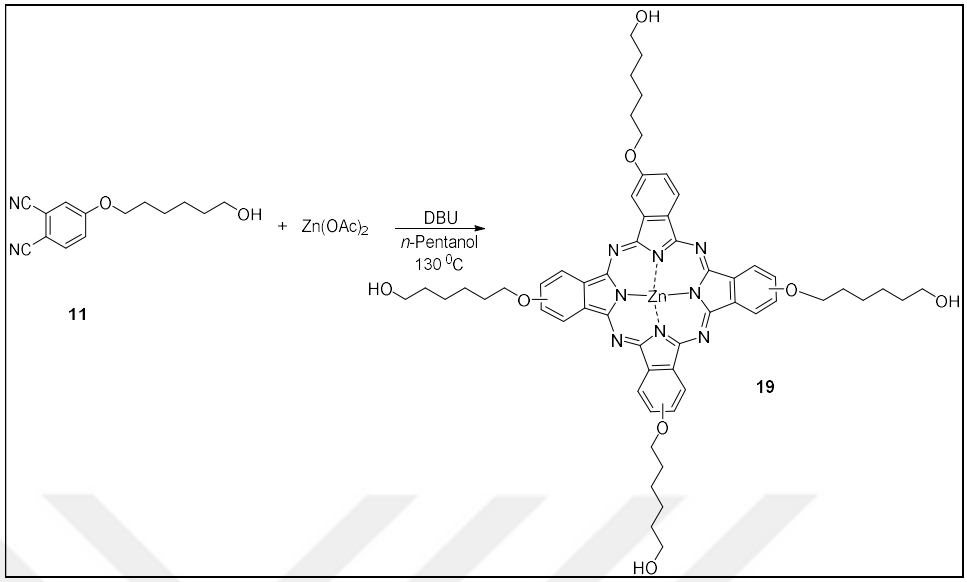

Figure 5.14: Synthesis of **19**.

Compound **11** (490 mg, 2 mmol), zinc acetate (183 mg, 1 mmol) and DBU (1 mL) was heated to 130 °C under argon atmosphere of *n*-pentanol (4 mL) and stirred for 15 hours. After stirring, mixture was cooled down to room temperature, added water (400 mL) and ethanol (50 mL). The resulting green precipitate was filtrated and dried under vacuum. It was purified with silica gel colon chromatography (5 DCM / 1 ethanol).

- Yield: 34% (180 mg)
- $C_{56}H_{64}N_8O_8Zn$, MW: 1042.56 g/mol
- MS-MALDI-TOF (*m/z*): 1042.073 $[M]^+$ (Matrix: DHB).
- FT-IR (cm^{-1}): 3333, 2932, 2859, 1605, 1488, 1386, 1337, 1228, 1085, 1045, 871, 825, 730
- ^1H NMR (DMSO-d_6, δ, ppm): 9.20-7.29 (m, 12H), 4.54-3.39 (16H), 1.73 (s, 4H), 1.53-1.22 (m, 32H)
- ^{13}C NMR (DMSO-d_6, δ, ppm): 168.88, 168.84, 163.71, 124.73, 124.62, 120.25, 68.59, 60.60, 47.01, 32.44, 28.46, 25.28, 25.20

5.16. Synthesis of Phthalocyanine 20

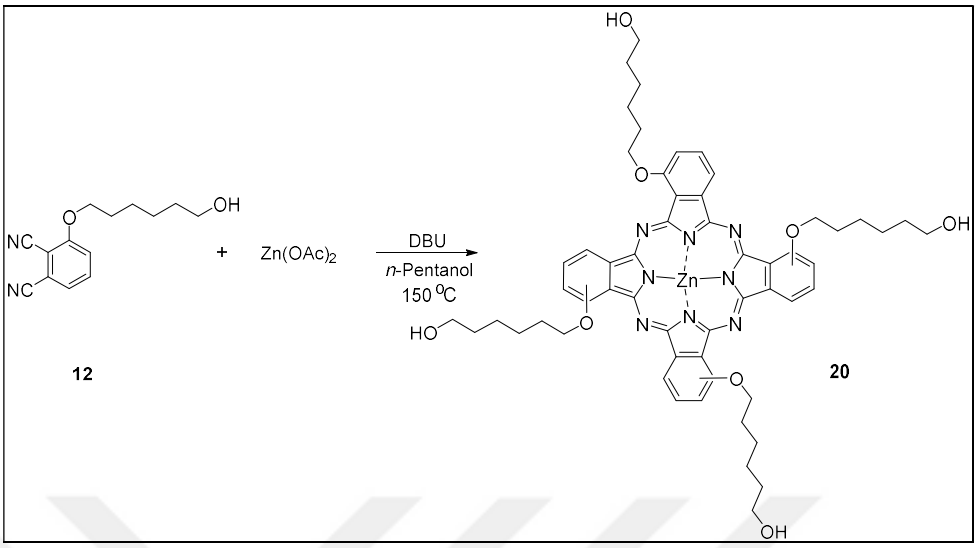

Figure 5.15: Synthesis of **20**.

Compound **12** (2 g, 8,2 mmol), zinc acetate (752 mg, 4.1 mmol) and DBU (3 mL) was heated to 150 °C under argon atmosphere with *n*-pentanol (6 mL) and stirred for 2 hours. Then, mixture was cooled down to room temperature and added water (700 mL). The resulting green precipitate was filtrated, solubilized with acetone / ethanol (200 mL / 50 mL) mixture then precipitated again in ethyl acetate (500 mL) and refiltrated. It was purified with silica gel colon chromatography (5 DCM / 1 ethanol).

- Yield: 32% (335 mg)
- $C_{56}H_{64}N_8O_8Zn$, MW: 1042.56 g/mol
- MS-MALDI-TOF (*m/z*): 1042.905 $[M]^+$ (Matrix: DIT).
- FT-IR (cm^{-1}): 3647, 3301, 2949, 2867, 1589, 1488, 1430, 1391, 1360, 1335, 1267, 1231, 1156, 1120 1083, 885, 860, 802, 768, 744
- ^1H NMR (DMSO-d_6, δ, ppm): 8.72-6.99 (m, 12H), 4.67-3.76 (m, 16H), 3.21 (s, 4H), 1.97-1.06 (m, 32H)
- ^{13}C NMR (DMSO-d_6, δ, ppm): 156.39, 156.19, 153.12, 152.95, 152.79, 152.57, 152.45, 140.48, 130.62, 130.40, 126.32, 124.76, 115.41, 112.46, 70.63, 68.73, 68.56, 61.57, 61.25, 33.41, 33.17, 29.71, 26.58, 26.15, 26.09

5.17. Synthesis of Phthalocyanine 21

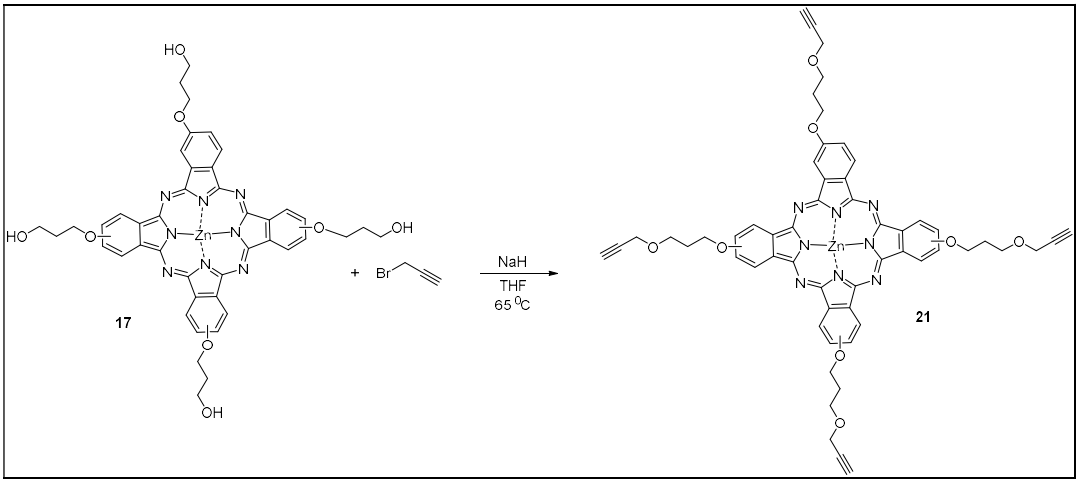

Figure 5.16: Synthesis of **21**.

Compound **17** (90 mg, 0.10 mmol), propargyl bromide (612 mg, 5 mmol) and NaH (48 mg, 2 mmol) was heated to 65 °C under argon atmosphere with dry THF (50 mL) and stirred for 5 hours. Then the mixture was cooled down to room temperature and ethanol (30 mL) was added drop by drop to quench the excess NaH while still stirring. After quenching, water (500 mL) was added to reaction mixture. The resulting deep green precipitate was filtrated and was purified with preparative thin layer chromatography (50 DCM / 1 ethanol).

- Yield: 10 mg
- $C_{56}H_{48}N_8O_8Zn$, MW: 1026.43 g/mol
- MS-MALDI-TOF (*m/z*): 1026.536 $[M]^+$ (Matrix: DHB).
- FT-IR (cm^{-1}): 3281, 2922, 2852, 1738, 1607, 1464, 1375, 1259, 1090, 1014, 795
- ^1H NMR (DMSO-d_6, δ, ppm): 8.99-8.55 (m, 4H), 7.73-7.16 (m, 8H), 4.57 (s, 8H), 4.34 (s, 8H), 4.13 (s, 8H), 3.90 (s, 8H), 2.32 (s, 4H)
- ^{13}C NMR (DMSO-d_6, δ, ppm): 175.02, 169.37, 169.30, 164.01, 160.80, 125.29, 120.82, 120.73, 81.04, 80.83, 77.65, 77.59, 77.45, 66.66, 58.11, 29.75, 29.43, 29.12, 28.97, 22.53, 14.10

5.18. Synthesis of Phthalocyanine 22

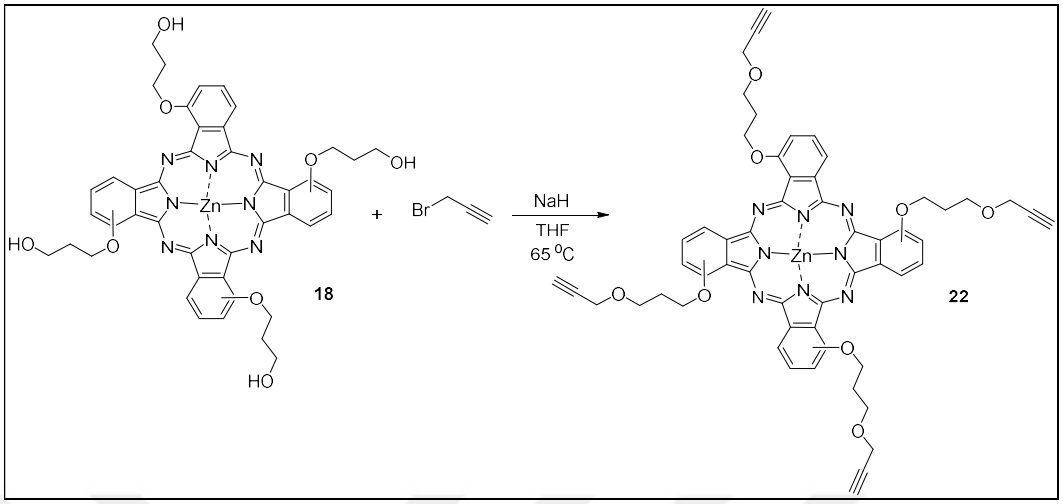

Figure 5.17: Synthesis of **22**.

Compound **18** (80 mg, 0.0915 mmol), propargyl bromide (543 mg, 4.57 mmol) and NaH (220 mg, 9.15 mmol) was heated to 65 °C under argon atmosphere with dry THF (75 mL) and stirred for 5 hours. Then the mixture was cooled down to room temperature and ethanol (30 mL) was added drop by drop to quench the excess NaH while still stirring. After quenching, water (300 mL) was added to reaction mixture. The resulting deep green precipitate was filtrated and was purified with preparative thin layer chromatography (50 DCM / 1 ethanol).

- Yield: 54% (50 mg)
- $C_{56}H_{48}N_8O_8Zn$, MW: 1026.43 g/mol
- MS-MALDI-TOF (*m/z*): 1026.852 $[M]^+$ (Matrix: DIT).
- FT-IR (cm^{-1}): 3281, 2870, 2113, 1587, 1488, 1398, 1333, 1265, 1233, 1175, 1079, 923, 875, 800, 741, 659
- ^1H NMR (DMSO-d_6, δ, ppm): 8.98-8.58 (m, 4H), 8.12-7.56 (m, 8H), 5.02 (s, 4H), 4.66 (t, 4H), 4.31-4.22 (m, 12H), 3.95 (s, 4H), 2.58 (s, 4H)
- ^{13}C NMR (DMSO-d_6, δ, ppm): 156.39, 156.21, 153.15, 153.05, 152.85, 152.63, 141.51, 141.01, 140.50, 131.16, 130.89, 126.39, 124.91, 115.87, 115.69, 115.12, 113.32, 80.98, 80.95, 77.52, 77.41, 67.20, 66.86, 58.21, 58.07, 29.75

5.19. Synthesis of Phthalocyanine 23

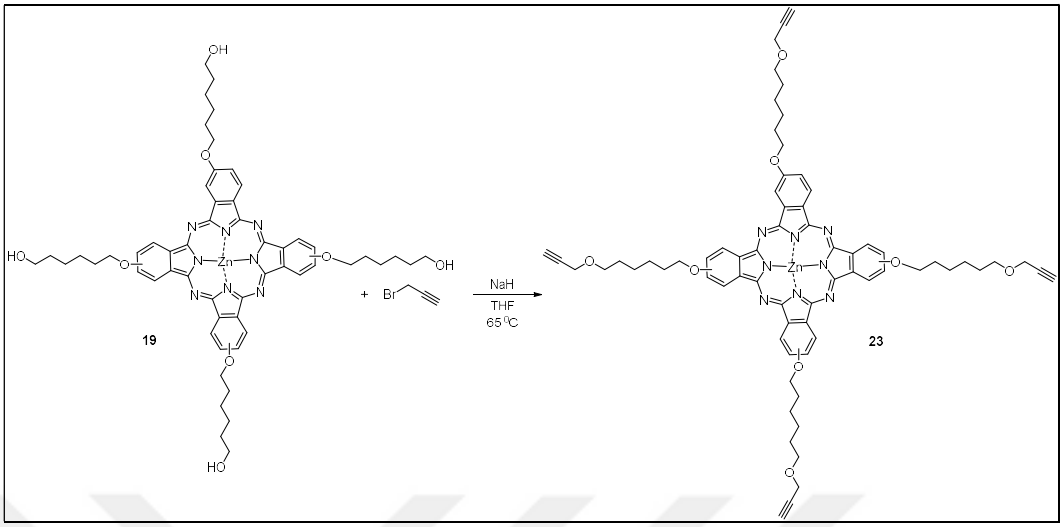

Figure 5.18: Synthesis of **23**.

Compound **19** (50 mg, 0.048 mmol), propargyl bromide (286 mg, 2.4 mmol) and NaH (115 mg, 4.8 mmol) was heated to 65 °C under argon atmosphere with dry THF (30 mL), stirred for one hour at 65 °C and 14 hours at room temperature. Ethanol (30 mL) was added drop by drop to quench the excess NaH while still stirring. After quenching, water (200 mL) was added to reaction mixture. The resulting deep green precipitate was filtrated and was purified with preparative thin layer chromatography (50 DCM / 1 ethanol).

- Yield: 52% (30 mg)
- $C_{68}H_{72}N_8O_8Zn$, MW: 1194.75 g/mol
- MS-MALDI-TOF (*m/z*): 1194.147 $[M]^+$ (Matrix: DHB).
- FT-IR (cm^{-1}): 3285, 2937, 1718, 1606, 1490, 1467, 1387, 1338, 1258, 1239, 1086, 1045, 1012, 863, 790, 744, 660
- ^1H NMR (DMSO-d_6, δ, ppm): 8.81 (d, 4H), 8.42-8.30 (m, 4H), 7.47-7.39 (m, 4H), 4.31-4.08 (m, 24H), 1.95-1.39 (m, 40H)
- ^{13}C NMR (DMSO-d_6, δ, ppm): 160.66, 160.38, 151.58, 140.15, 131.29, 123.42, 117.90, 117.70, 117.50, 81.10, 81.06, 77.27, 77.18, 69.68, 69.62, 69.50, 57.83, 57.78, 57.76, 29.44, 29.39, 29.26, 26.11, 26.01, 25.91, 25.76

5.20. Synthesis of Phthalocyanine 24

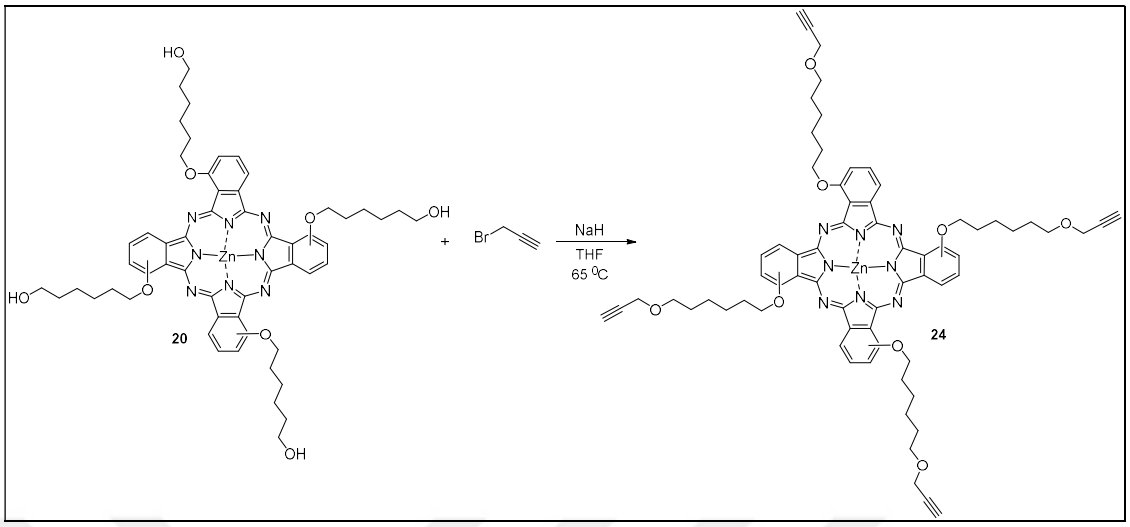

Figure 5.19: Synthesis of **24**.

Crude compound **20** (800 mg, 0.77 mmol), propargyl bromide (4.6 g, 38 mmol) and NaH (4 g, 167 mmol) was heated to 65 °C under argon atmosphere with dry THF (50 mL) and stirred for 8 hours. Then the mixture was cooled down to room temperature and ethanol (50 mL) was added drop by drop to quench the excess NaH while still stirring. After quenching, water (600 mL) was added to reaction mixture. The resulting deep green precipitate was filtrated and was purified with preparative thin layer chromatography (50 DCM / 1 ethanol).

- Yield: 30 mg
- $C_{68}H_{72}N_8O_8Zn$, MW: 1194.75 g/mol
- MS-MALDI-TOF (*m/z*): 1194.389 $[M]^+$ (Matrix: DIT).
- FT-IR (cm^{-1}): 3289, 2923, 2853, 1727, 1590, 1489, 1463, 1338, 1259, 1088, 1012, 864, 791, 744, 700, 661
- ^1H NMR (DMSO-d_6, δ, ppm): 8.55-7.31 (12H), 4.44 (s, 4H), 4.14-4.04 (m, 12H), 2.17-1.34 (m, 47H)
- ^{13}C NMR (DMSO-d_6, δ, ppm): 169.33, 168.01, 156.31, 156.20, 152.82, 152.55, 141.06, 136.94, 135.14, 130.46, 124.87, 119.65, 117.99, 115.09, 114.50, 112.51, 81.06, 81.03, 77.26, 77.23, 77.20, 69.89, 69.52, 57.84, 57.72, 29.81, 29.29, 28.78, 26.81, 26.64, 25.72, 25.50

6. CONCLUSION

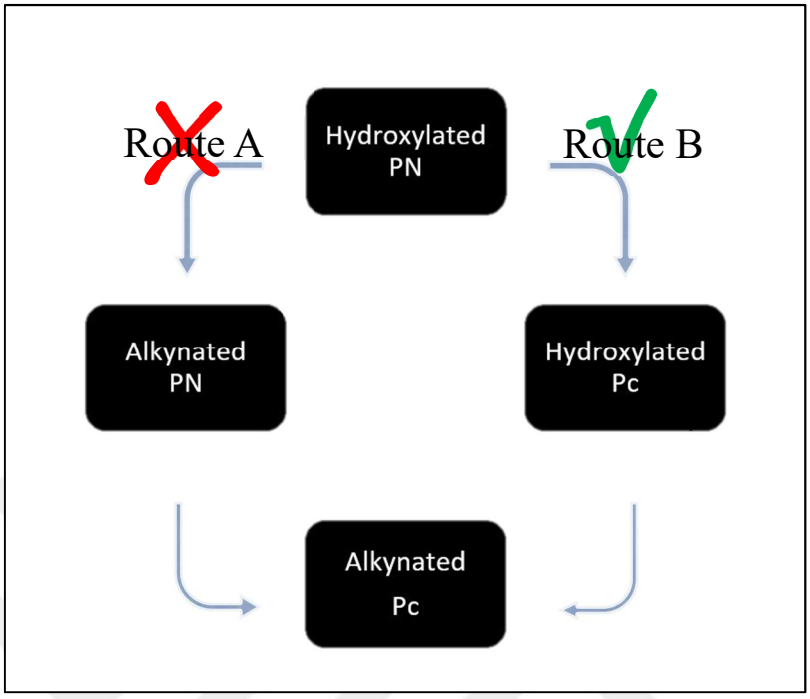

Figure 6.1: Synthesis routes.

During this thesis, hydroxylated phthalonitriles **9**, **10**, **11** and **12** were synthesized and characterized successfully. Alkynated phthalonitriles **13**, **14**, **15** and **16** could not be synthesized in satisfactory yields. Instead, hydroxylated phthalocyanines **17**, **18**, **19** and **20** were synthesized and characterized. Alkynated phthalocyanines **21**, **22**, **23** and **24** from hydroxylated phthalocyanines were synthesized and characterized successfully to be used as building blocks of nanoPMOs.

Non-peripheral hydroxylated or alkynated phthalocyanines Q bands, compared to peripheral ones, are shifted to longer wavelength, as expected. There is no significant effect of spacer length.

All SOG and fluorescence quantum yields of alkynated phthalocyanines **21**, **22**, **23** and **24** have been found approximately the same value. This evidences that neither the position of the substituent, nor the length of the spacer, has a significant effect of this values.

This work has been presented in 28th National Chemistry Congress (Mersin, Turkey, 2016, Mersin University) as a poster presentation.

REFERENCES

[1] Wang S., Gao R., Zhou F., Selke M., (2004), "Nanomaterials and singlet oxygen photosensitizers: potential applications in photodynamic therapy", Journal of Materials Chemistry, 14 (4), 487-493.

[2] Muehlmann L. A., Ma B. C., Longo J. P. F., Santos M. d. F. M. A., Azevedo R. B., (2014), "Aluminum–phthalocyanine chloride associated to poly (methyl vinyl ether-co-maleic anhydride) nanoparticles as a new third-generation photosensitizer for anticancer photodynamic therapy", International Journal of Nanomedicine, 9, 1199.

[3] Tedesco A. C., Rotta J., Lunardi C. N., (2003), "Synthesis, photophysical and photochemical aspects of phthalocyanines for photodynamic therapy", Current Organic Chemistry, 7 (2), 187-196.

[4] Zhang Z., Wang L., Wang J., Jiang X., Li X., Hu Z., Ji Y., Wu X., Chen C., (2012), "Mesoporous silica-coated gold nanorods as a light-mediated multifunctional theranostic platform for cancer treatment", Advanced Materials, 24 (11), 1418-1423.

[5] Iyer A. K., Khaled G., Fang J., Maeda H., (2006), "Exploiting the enhanced permeability and retention effect for tumor targeting", Drug Discovery Today, 11 (17), 812-818.

[6] Croissant J., Salles D., Maynadier M., Mongin O., Hugues V., Blanchard-Desce M., Cattoën X., Wong Chi Man M., Gallud A., Garcia M., (2014), "Mixed Periodic Mesoporous Organosilica Nanoparticles and Core–Shell Systems, Application to in Vitro Two-Photon Imaging, Therapy, and Drug Delivery", Chemistry of Materials, 26 (24), 7214-7220.

[7] Hocine O., Gary-Bobo M., Brevet D., Maynadier M., Fontanel S., Raehm L., Richeter S., Loock B., Couleaud P., Frochot C., (2010), "Silicalites and mesoporous silica nanoparticles for photodynamic therapy", International Journal of Pharmaceutics, 402 (1), 221-230.

[8] Jimenez C. M., Rubio Y. G., Saunier V., Warther D., Stojanovic V., Raehm L., Frochot C., Arnoux P., Garcia M., Morère A., (2016), "20-nm-sized mesoporous silica nanoparticles with porphyrin photosensitizers for in vitro photodynamic therapy", Journal of Sol-Gel Science and Technology, 79 (3), 447-456.

[9] Couleaud P., Morosini V., Frochot C., Richeter S., Raehm L., Durand J.-O., (2010), "Silica-based nanoparticles for photodynamic therapy applications", Nanoscale, 2 (7), 1083-1095.

[10] Mauriello-Jimenez C., Croissant J., Maynadier M., Cattoën X., Man M. W. C., Vergnaud J., Chaleix V., Sol V., Garcia M., Gary-Bobo M., (2015), "Porphyrin-functionalized mesoporous organosilica nanoparticles for two-photon imaging of cancer cells and drug delivery", Journal of Materials Chemistry B, 3 (18), 3681-3684.

[11] Secret E., Maynadier M., Gallud A., Chaix A., Bouffard E., Gary-Bobo M., Marcotte N., Mongin O., El Cheikh K., Hugues V., (2014), "Two-Photon Excitation of Porphyrin-Functionalized Porous Silicon Nanoparticles for Photodynamic Therapy", Advanced Materials, 26 (45), 7643-7648.

[12] Brevet D., Gary-Bobo M., Raehm L., Richeter S., Hocine O., Amro K., Loock B., Couleaud P., Frochot C., Morère A., (2009), "Mannose-targeted mesoporous silica nanoparticles for photodynamic therapy", Chemical Communications (12), 1475-1477.

[13] Furuyama T., Sato T., Kobayashi N., (2015), "A bottom-up synthesis of antiaromatic expanded phthalocyanines: pentabenzotriazasmaragdyrins, ie norcorroles of superphthalocyanines", Journal of the American Chemical Society, 137 (43), 13788-13791.

[14] Web 1, (2017), http://www.phthalocyanines.es/research-lines/selective-synthesis-and-functionalization-of-phthalocyanines (Access Date: 10/01/2017).

[15] Hanack M., Heckmann H., Polley R., (1998), "Phthalocyanines and related compounds", Meth. Org. Chem.(Houben-Weyl), 717-846.

[16] Braun A. v., Tcherniac J., (1907), "Über die Produkte der Einwirkung von Acetanhydrid auf Phthalamid", European Journal of Inorganic Chemistry, 40 (2), 2709-2714.

[17] De Diesbach H., von Der Weid E., (1927), "Quelques sels complexes des o-dinitriles avec le cuivre et la pyridine", Helvetica Chimica Acta, 10 (1), 886-888.

[18] Gregory P., (2000), "Industrial applications of phthalocyanines", Journal of Porphyrins and Phthalocyanines, 4 (4), 432-437.

[19] Linstead R., (1934), "212. Phthalocyanines. Part I. A new type of synthetic colouring matters", Journal of the Chemical Society (Resumed), 1016-1017.

[20] Linstead R., Lowe A., (1934), "216. Phthalocyanines. Part V. The molecular weight of magnesium phthalocyanine", Journal of the Chemical Society (Resumed), 1031-1033.

[21] BEKAROĞLU Ö., (2014), "History, development, and a new concept of phthalocyanines in Turkey", Turkish Journal of Chemistry, 38 (6), 903-922.

[22] Tomoda H., Saito S., Ogawa S., Shiraishi S., (1980), "Synthesis of phthalocyanines from phthalonitrile with organic strong bases", Chemistry Letters, 9 (10), 1277-1280.

[23] Gürek A. G., Hirel C. (2011), "Recent developments of synthetic techniques for porphyrins, phthalocyanines and related systems". "Photosensitizers in Medicine, Environment, and Security", Springer.

[24] Leznoff C.C., Lever A.B.P., (1989), "Phthalocyanines: Properties and Applications" 1st Edition, ISBN: 0-89573-753-1, VHC Publishers.

[25] Tuncel S., (2012), "Mesomorfik Alkoksi ve Alkiltiyo Sübstitüe Kurşun Ftalosiyaninler", Doktoza Tezi, Gebze Yüksek Teknoloji Enstitüsü.

[26] Robertson J. M., (1935), "136. An X-ray study of the structure of the phthalocyanines. Part I. The metal-free, nickel, copper, and platinum compounds", Journal of the Chemical Society (Resumed), 615-621.

[27] Cook M. J., (1993), "Spectroscopy of New Materials", ISBN: 0 471 97423 4, John Wiley&Sons., England.

[28] Balcı M., (2000), "Nükleer Manyetik Rezonans Spektroskopisi", ISBN: 975-7064-23-8, ODTÜ Yayıncılık.

[29] Yüksel F., Gürek A. G., Lebrun C., Ahsen V., (2005), "Synthesis and solvent effects on the spectroscopic properties of octatosylamido phthalocyanines", New Journal of Chemistry, 29 (5), 726-732.

[30] Mack J., Stillman M. J., (2003), "Electronic structures of metal phthalocyanine and porphyrin complexes from analysis of the UV-visible absorption and magnetic circular dichroism spectra and molecular orbital calculations", The Porphyrin Handbook, 16, 43-116.

[31] Nyokong T., Isago H., (2004), "The renaissance in optical spectroscopy of phthalocyanines and other tetraazaporphyrins", Journal of Porphyrins and Phthalocyanines, 8 (09), 1083-1090.

[32] Rio Y., Rodriguez-Morgade M. S., Torres T., (2008), "Modulating the electronic properties of porphyrinoids: a voyage from the violet to the infrared regions of the electromagnetic spectrum", Organic & Biomolecular Chemistry, 6 (11), 1877-1894.

[33] Web 2, (2017), https://en.wikipedia.org/wiki/Fluorescence (Access Date: 20/06/2017).

[34] Berezin M. Y., Achilefu S., (2010), "Fluorescence lifetime measurements and biological imaging", Chemical Reviews, 110 (5), 2641-2684.

[35] Topal S. Z., İşci Ü., Kumru U., Atilla D., Gürek A. G., Hirel C., Durmuş M., Tommasino J.-B., Luneau D., Berber S., (2014), "Modulation of the electronic and spectroscopic properties of Zn (II) phthalocyanines by their substitution pattern", Dalton Transactions, 43 (18), 6897-6908.

[36] Wöhrle D., Schnurpfeil G., Makarov S. G., Kazarin A., Suvorova O. N., (2012), "Practical applications of phthalocyanines–from dyes and pigments to materials for optical, electronic and photo-electronic devices", Macroheterocycles, 5 (3), 191-202.

[37] Giraudeau A., Fan F.-R. F., Bard A. J., (1980), "Semiconductor electrodes. 30. Spectral sensitization of the semiconductors titanium oxide (n-TiO2) and tungsten oxide (n-WO3) with metal phthalocyanines", Journal of the American Chemical Society, 102 (16), 5137-5142.

[38] Li L., Tang Q., Li H., Hu W., Yang X., Shuai Z., Liu Y., Zhu D., (2008), "Organic thin-film transistors of phthalocyanines", Pure and Applied Chemistry, 80 (11), 2231-2240.

[39] İşci Ü., Gürek A. G., Ahsen V., Sorokin A. B., (2009), "Preparation of iron phthalocyanine complex bearing four tetraazamacrocycles as a precursor for oxidation catalyst with two catalytic sites", Journal of Porphyrins and Phthalocyanines, 13 (06), 747-752.

[40] Işci Ü., Dumoulin F., Ahsen V., Sorokin A. B., (2010), "Preparation of N-bridged diiron phthalocyanines bearing bulky or small electron-withdrawing substituents", Journal of Porphyrins and Phthalocyanines, 14 (04), 324-334.

[41] Ümit İ., Dumoulin F., Sorokin A. B., Ahsen V., (2015), "N-bridged dimers of tetrapyrroles complexed by transition metals: syntheses, characterization methods, and uses as oxidation catalysts", Turkish Journal of Chemistry 38, 923-949.

[42] İşci Ü., Caner C., Zorlu Y., Gürek A. G., Dumoulin F., Ahsen V., (2014), "Sulfonamide-substituted iron phthalocyanine: design, solubility range, stability and oxidation of olefins", Dalton Transactions, 43 (48), 17916-17919.

[43] İşci Ü., Faponle A. S., Afanasiev P., Albrieux F., Briois V., Ahsen V., Dumoulin F., Sorokin A. B., de Visser S. P., (2015), "Site-selective formation of an iron (iv)–oxo species at the more electron-rich iron atom of heteroleptic μ-nitrido diiron phthalocyanines", Chemical Science, 6 (8), 5063-5075.

[44] Takano S., Enokida T., Kakuta A., Mori Y., (1984), "A new polymorph of metal-free phthalocyanine", Chemistry Letters, 13 (12), 2037-2040.

[45] Simon J., Bassoul P., Norvez S., (1989), "Molecular materials. III: Towards opto-electronics finalities", New Journal of Chemistry, 13 (1), 13-31.

[46] Casstevens M. K., Samoc M., Pfleger J., Prasad P. N., (1990), "Dynamics of third-order nonlinear optical processes in Langmuir–Blodgett and evaporated films of phthalocyanines", The Journal of Chemical Physics, 92 (3), 2019-2024.

[47] Nalwa H. S., Shirk J. S., Leznoff, C.C., A. B. P Lever, (1996), "Phthalocyanines: Properties and Applications", 4 th Edition Wiley-VCH.

[48] Engel M., Bassoul P., Bosio L., Lehmanns H., Hanacks M., Simon J., (1993), "Mesomorphic molecular materials. Influence of chain length on the structural properties of octa-alkyl substituted phthalocyanines", Liquid Crystals, 15 (5), 709-722.

[49] Simon J., Sirlin C., (1989), "Mesomorphic molecular materials for electronics, opto-electronics, iono-electronics: octaalkyl-phthalocyanine derivatives", Pure and Applied Chemistry, 61 (9), 1625-1629.

[50] Van der Pol J., Neeleman E., Zwikker J., Nolte R., Drenth W., Aerts J., Visser R., Picken S., (1989), "Homologous series of liquid-crystalline metal free and copper octa-n-alkoxyphthalocyanines", Liquid Crystals, 6 (5), 577-592.

[51] Gregory P., (1991), "High Technology Applications of Organic Colorants" 1st Edition, New York, 7, 59, 1991.

[52] Kuder J. E., (1988), "Organic active layer materials for optical recording", Journal of Imaging Science, 32(2), 51-56.

[53] Wöhrle D., Shopova M., Müller S., Milev A., Mantareva V., Krastev K., (1993), "Liposome-delivered Zn (II)-2, 3-naphthalocyanines as potential sensitizers for PDT: synthesis, photochemical, pharmacokinetic and phototherapeutic studies", Journal of Photochemistry and Photobiology B: Biology, 21 (2-3), 155-165.

[54] Schlettwein D., Kaneko M., Yamada A., Wöhrle D., Jaeger N., (1991), "Light-induced dioxygen reduction at thin film electrodes of various porphyrins", The Journal of Physical Chemistry, 95 (4), 1748-1755.

[55] Lever A., Hempstead M., Leznoff C., Liu W., Melnik M., Nevin W., Seymour P., (1986), "Recent studies in phthalocyanine chemistry", Pure and Applied Chemistry, 58 (11), 1467-1476.

[56] Law K. Y., (1993), "Organic photoconductive materials: recent trends and developments", Chemical Reviews, 93 (1), 449-486.

[57] Tuncel S., Dumoulin F., Gailer J., Sooriyaarachchi M., Atilla D., Durmuş M., Bouchu D., Savoie H., Boyle R. W., Ahsen V., (2011), "A set of highly water-soluble tetraethyleneglycol-substituted Zn (II) phthalocyanines: synthesis, photochemical and photophysical properties, interaction with plasma proteins and in vitro phototoxicity", Dalton Transactions, 40 (16), 4067-4079.

[58] Anne C., Bernhard O., Brian W., Tayyaba H., "Photodynamic therapy of Cancer", Radiation Oncology, 9 (40), 605-622.

[59] Web 4, (2017), https://en.wikipedia.org/wiki/Mesoporous_organosilica (Access Date: 20/06/2017).

[60] Croissant J. G., Cattoën X., Man M. W. C., Durand J.-O., Khashab N. M., (2015), "Syntheses and applications of periodic mesoporous organosilica nanoparticles", Nanoscale, 7 (48), 20318-20334.

[61] Web 5, (2017), https://en.wikipedia.org/wiki/Mesoporous_silica (Access Date: 20/06/2017).

[62] Boissiere C., Larbot A., van der Lee A., Kooyman P. J., Prouzet E., (2000), "A new synthesis of mesoporous MSU-X silica controlled by a two-step pathway", Chemistry of Materials, 12 (10), 2902-2913.

[63] Kresge C., Leonowicz M., Roth W., Vartuli J., Beck J., (1992), "Ordered mesoporous molecular sieves synthesized by a liquid-crystal template mechanism", Nature, 359 (6397), 710-712.

[64] Sayari A., Hamoudi S., (2001), "Periodic Mesoporous Silica-Based Organic−Inorganic Nanocomposite Materials", Chemistry of Materials, 13 (10), 3151-3168.

[65] Poyraz A. S., Albayrak C., Dag Ö., (2008), "The effect of cationic surfactant and some organic/inorganic additives on the morphology of mesostructured silica templated by pluronics", Microporous and Mesoporous Materials, 115 (3), 548-555.

[66] Mizutani M., Yamada Y., Yano K., (2007), "Pore-expansion of monodisperse mesoporous silica spheres by a novel surfactant exchange method", Chemical Communications (11), 1172-1174.

[67] Prouzet E., Cot F., Boissière C., Kooyman P. J., Larbot A., (2002), "Nanometric hollow spheres made of MSU-X-type mesoporous silica", Journal of Materials Chemistry, 12 (5), 1553-1556.

[68] Léonard A., Blin J., Robert M., Jacobs P., Cheetham A., Su B., (2003), "Toward a better control of internal structure and external morphology of mesoporous silicas synthesized using a nonionic surfactant", Langmuir, 19 (13), 5484-5490.

[69] Chen Q., Sakamoto Y., Terasaki O., Che S., (2007), "Synthesis of silica mesoporous crystals with controlled structure and morphology using gemini surfactant", Microporous and Mesoporous Materials, 105 (1), 24-33.

[70] Yu C., Tian B., Fan J., Stucky G. D., Zhao D., (2002), "Nonionic block copolymer synthesis of large-pore cubic mesoporous single crystals by use of inorganic salts", Journal of the American Chemical Society, 124 (17), 4556-4557.

[71] Yang H., Coombs N., Ozin G. A., (1997), "Morphogenesis of shapes and surface patterns in mesoporous silica", Nature, 386 (6626), 692.

[72] Wang B., Chi C., Shan W., Zhang Y., Ren N., Yang W., Tang Y., (2006), "Chiral Mesostructured Silica Nanofibers of MCM-41", Angewandte Chemie, 118 (13), 2142-2144.

[73] Chan H. B., Budd P. M., (2001), "Control of mesostructured silica particle morphology", Journal of Materials Chemistry, 11 (3), 951-957.

[74] Trewyn B. G., Giri S., Slowing I. I., Lin V. S.-Y., (2007), "Mesoporous silica nanoparticle based controlled release, drug delivery, and biosensor systems", Chemical Communications (31), 3236-3245.

[75] Stein A., (2001), "Sphere templating methods for periodic porous solids", Microporous and Mesoporous Materials, 44, 227-239.

[76] Yamada Y., Nakamura T., Ishi M., Yano K., (2006), "Reversible control of light reflection of a colloidal crystal film fabricated from monodisperse mesoporous silica spheres", Langmuir, 22 (6), 2444-2446.

[77] Biswas K., Ray J. C., Choi J.-S., Ahn W.-S., (2008), "Morphology control of MSU-1 silica particles", Journal of Non-Crystalline Solids, 354 (1), 1-9.

[78] Yano K., Fukushima Y., (2003), "Particle size control of mono-dispersed super-microporous silica spheres", Journal of Materials Chemistry, 13 (10), 2577-2581.

[79] Inagaki S., Guan S., Fukushima Y., Ohsuna T., Terasaki O., (1999), "Novel mesoporous materials with a uniform distribution of organic groups and inorganic oxide in their frameworks", Journal of the American Chemical Society, 121 (41), 9611-9614.

[80] Asefa T., MacLachlan M. J., Coombs N., Ozin G. A., (1999), "Periodic mesoporous organosilicas with organic groups inside the channel walls", Nature, 402 (6764), 867.

[81] Melde B. J., Holland B. T., Blanford C. F., Stein A., (1999), "Mesoporous sieves with unified hybrid inorganic/organic frameworks", Chemistry of Materials, 11 (11), 3302-3308.

[82] Mizoshita N., Tani T., Inagaki S., (2011), "Syntheses, properties and applications of periodic mesoporous organosilicas prepared from bridged organosilane precursors", Chemical Society Reviews, 40 (2), 789-800.

[83] Van Der Voort P., Esquivel D., De Canck E., Goethals F., Van Driessche I., Romero-Salguero F. J., (2013), "Periodic mesoporous organosilicas: from simple to complex bridges; a comprehensive overview of functions, morphologies and applications", Chemical Society Reviews, 42 (9), 3913-3955.

[84] Shea K. J., Loy D. A., (2001), "Bridged polysilsesquioxanes. Molecular-engineered hybrid organic− inorganic materials", Chemistry of Materials, 13 (10), 3306-3319.

[85] Corriu R. J., (2000), "Ceramics and nanostructures from molecular precursors", Angewandte Chemie International Edition, 39 (8), 1376-1398.

[86] Descalzo A. B., Martínez-Máñez R., Sancenon F., Hoffmann K., Rurack K., (2006), "The supramolecular chemistry of organic–inorganic hybrid materials", Angewandte Chemie International Edition, 45 (36), 5924-5948.

[87] Croissant J. G., Mauriello-Jimenez C., Maynadier M., Cattoën X., Man M. W. C., Raehm L., Mongin O., Blanchard-Desce M., Garcia M., Gary-Bobo M., (2015), "Synthesis of disulfide-based biodegradable bridged silsesquioxane nanoparticles for two-photon imaging and therapy of cancer cells", Chemical Communications, 51 (61), 12324-12327.

[88] Yang Q., Liu J., Zhang L., Li C., (2009), "Functionalized periodic mesoporous organosilicas for catalysis", Journal of Materials Chemistry, 19 (14), 1945-1955.

[89] Inagaki S., Guan S., Ohsuna T., Terasaki O., (2002), "An ordered mesoporous organosilica hybrid material with a crystal-like wall structure", Nature, 416 (6878), 304-307.

[90] Nakajima K., Tomita I., Hara M., Hayashi S., Domen K., Kondo J. N., (2005), "A stable and highly active hybrid mesoporous solid acid catalyst", Advanced Materials, 17 (15), 1839-1842.

[91] Ohashi M., Kapoor M. P., Inagaki S., (2008), "Chemical modification of crystal-like mesoporous phenylene-silica with amino group", Chemical Communications (7), 841-843.

[92] Kamegawa T., Sakai T., Matsuoka M., Anpo M., (2005), "Preparation and Characterization of Unique Inorganic− Organic Hybrid Mesoporous Materials Incorporating Arenetricarbonyl Complexes [− C6H4M (CO) 3−](M= Cr, Mo)", Journal of the American Chemical Society, 127 (48), 16784-16785.

[93] Yoshina-Ishii C., Asefa T., Coombs N., MacLachlan M. J., Ozin G. A., (1999), "Periodic mesoporous organosilicas, PMOs: fusion of organic and inorganic chemistry 'inside'the channel walls of hexagonal mesoporous silica", Chemical Communications (24), 2539-2540.

[94] Olkhovyk O., Pikus S., Jaroniec M., (2005), “Bifunctional periodic mesoporous organosilica with large heterocyclic bridging groups and mercaptopropyl ligands”, Journal of Materials Chemistry, 15 (15), 1517-1519.

[95] Rebbin V., Schmidt R., Fröba M., (2006), “Spherical particles of phenylene-bridged periodic mesoporous organosilica for high-performance liquid chromatography”, Angewandte Chemie International Edition, 45 (31), 5210-5214.

[96] Zhang X., Su F., Song D., An S., Lu B., Guo Y., (2015), “Preparation of efficient and recoverable organosulfonic acid functionalized alkyl-bridged organosilica nanotubes for esterification and transesterification”, Applied Catalysis B: Environmental, 163, 50-62.

[97] Karimi B., Mirzaei H. M., Mobaraki A., (2012), “Periodic mesoporous organosilica functionalized sulfonic acids as highly efficient and recyclable catalysts in biodiesel production”, Catalysis Science & Technology, 2 (4), 828-834.

[98] Karimi B., Esfahani F. K., (2011), “Unexpected golden Ullmann reaction catalyzed by Au nanoparticles supported on periodic mesoporous organosilica (PMO) ”, Chemical Communications, 47 (37), 10452-10454.

[99] De Canck E., Ascoop I., Sayari A., Van Der Voort P., (2013), “Periodic mesoporous organosilicas functionalized with a wide variety of amines for CO 2 adsorption”, Physical Chemistry Chemical Physics, 15 (24), 9792-9799.

[100] Díaz U., Brunel D., Corma A., (2013), “Catalysis using multifunctional organosiliceous hybrid materials”, Chemical Society Reviews, 42 (9), 4083-4097.

[101] Park S. S., Moorthy M. S., Ha C.-S., (2014), “Periodic mesoporous organosilicas for advanced applications”, NPG Asia Materials, 6, e96.

[102] Inagaki S., Ohtani O., Goto Y., Okamoto K., Ikai M., Yamanaka K. i., Tani T., Okada T., (2009), “Light harvesting by a periodic mesoporous organosilica chromophore”, Angewandte Chemie International Edition, 48 (22), 4042-4046.

[103] Takeda H., Goto Y., Maegawa Y., Ohsuna T., Tani T., Matsumoto K., Shimada T., Inagaki S., (2009), “Visible-light-harvesting periodic mesoporous organosilica”, Chemical Communications (40), 6032-6034.

[104] Qian K., Liu F., Yang J., Huang X., Gu W., Jambhrunkar S., Yuan P., Yu C., (2013), “Pore size-optimized periodic mesoporous organosilicas for the enrichment of peptides and polymers”, RSC Advances, 3 (34), 14466-14472.

[105] Chen Y., Meng Q., Wu M., Wang S., Xu P., Chen H., Li Y., Zhang L., Wang L., Shi J., (2014), "Hollow mesoporous organosilica nanoparticles: a generic intelligent framework-hybridization approach for biomedicine", Journal of the American Chemical Society, 136 (46), 16326-16334.

[106] Noureddine A., Trens P., Toquer G., Cattoën X., Wong Chi Man M., (2014), "Tailoring the Hydrophilic/Lipophilic Balance of Clickable Mesoporous Organosilicas by the Copper-Catalyzed Azide–Alkyne Cycloaddition Click-Functionalization", Langmuir, 30 (41), 12297-12305.

[107] Munaweera I., Hong J., D'Souza A., Balkus K. J., (2015), "Novel wrinkled periodic mesoporous organosilica nanoparticles for hydrophobic anticancer drug delivery", Journal of Porous Materials, 22 (1), 1-10.

[108] Comotti A., Bracco S., Valsesia P., Beretta M., Sozzani P., (2010), "Fast molecular rotor dynamics modulated by guest inclusion in a highly organized nanoporous organosilica", Angewandte Chemie International Edition, 49 (10), 1760-1764.

[109] Croissant J., Cattoën X., Man M. W. C., Gallud A., Raehm L., Trens P., Maynadier M., Durand J. O., (2014), "Biodegradable Ethylene-Bis (Propyl) Disulfide-Based Periodic Mesoporous Organosilica Nanorods and Nanospheres for Efficient In-Vitro Drug Delivery", Advanced Materials, 26 (35), 6174-6180.

[110] Corma A., Díaz U., Arrica M., Fernández E., Ortega Í., (2009), "Organic–inorganic nanospheres with responsive molecular gates for drug storage and release", Angewandte Chemie International Edition, 48 (34), 6247-6250.

[111] Djojoputro H., Zhou X., Qiao S., Wang L., Yu C., Lu G., (2006), "Periodic mesoporous organosilica hollow spheres with tunable wall thickness", Journal of the American Chemical Society, 128 (19), 6320-6321.

[112] Cho E.-B., Kim D., Jaroniec M., (2009), "Preparation of mesoporous benzene–silica nanoparticles", Microporous and Mesoporous Materials, 120 (3), 252-256.

[113] Urata C., Yamada H., Wakabayashi R., Aoyama Y., Hirosawa S., Arai S., Takeoka S., Yamauchi Y., Kuroda K., (2011), "Aqueous colloidal mesoporous nanoparticles with ethenylene-bridged silsesquioxane frameworks", Journal of the American Chemical Society, 133 (21), 8102-8105.

[114] Qiao S., Yu C., Xing W., Hu Q., Djojoputro H., Lu G., (2005), "Synthesis and bio-adsorptive properties of large-pore periodic mesoporous organosilica rods", Chemistry of Materials, 17 (24), 6172-6176.

[115] Mohanty P., Landskron K., (2009), "Periodic mesoporous organosilica nanorice", Nanoscale Research Letters, 4 (2), 169.

[116] Mohanty P., Landskron K., (2009), “Simple systematic synthesis of periodic mesoporous organosilica nanoparticles with adjustable aspect ratios”, Nanoscale Research Letters, 4 (12), 1524.

[117] Scott B. J., Wirnsberger G., Stucky G. D., (2001), “Mesoporous and mesostructured materials for optical applications”, Chemistry of Materials, 13 (10), 3140-3150.

[118] Stein A., Melde B. J., Schroden R. C., (2000), “Hybrid inorganic–organic mesoporous silicates—nanoscopic reactors coming of age”, Advanced Materials, 12 (19), 1403-1419.

[119] Knežević N. Ž., Durand J.-O., (2015), “Large pore mesoporous silica nanomaterials for application in delivery of biomolecules”, Nanoscale, 7 (6), 2199-2209.

[120] Liu F., Zhou X., Chen Z., Huang P., Wang X., Zhou Y., (2008), “Preparation of purpurin-18 loaded magnetic nanocarriers in cottonseed oil for photodynamic therapy”, Materials Letters, 62 (17), 2844-2847.

[121] Tada D. B., Vono L. L., Duarte E. L., Itri R., Kiyohara P. K., Baptista M. S., Rossi L. M., (2007), “Methylene blue-containing silica-coated magnetic particles: a potential magnetic carrier for photodynamic therapy”, Langmuir, 23 (15), 8194-8199.

[122] Tang W., Xu H., Kopelman R., Philbert M. A., (2005), “Photodynamic characterization and in vitro application of methylene blue-containing nanoparticle platforms”, Photochemistry and Photobiology, 81 (2), 242-249.

[123] Yan F., Kopelman R., (2003), “The Embedding of Meta-tetra (Hydroxyphenyl)-Chlorin into Silica Nanoparticle Platforms for Photodynamic Therapy and Their Singlet Oxygen Production and pH-dependent Optical Properties”, Photochemistry and Photobiology, 78 (6), 587-591.

[124] Zhou J., Zhou L., Dong C., Feng Y., Wei S., Shen J., Wang X., (2008), “Preparation and photodynamic properties of water-soluble hypocrellin A-silica nanospheres”, Materials Letters, 62 (17), 2910-2913.

[125] Roy I., Ohulchanskyy T. Y., Pudavar H. E., Bergey E. J., Oseroff A. R., Morgan J., Dougherty T. J., Prasad P. N., (2003), “Ceramic-based nanoparticles entrapping water-insoluble photosensitizing anticancer drugs: A novel drug− carrier system for photodynamic therapy”, Journal of the American Chemical Society, 125 (26), 7860-7865.

[126] Kim S., Ohulchanskyy T. Y., Pudavar H. E., Pandey R. K., Prasad P. N., (2007), "Organically modified silica nanoparticles co-encapsulating photosensitizing drug and aggregation-enhanced two-photon absorbing fluorescent dye aggregates for two-photon photodynamic therapy", Journal of the American Chemical Society, 129 (9), 2669-2675.

[127] Ohulchanskyy T. Y., Roy I., Goswami L. N., Chen Y., Bergey E. J., Pandey R. K., Oseroff A. R., Prasad P. N., (2007), "Organically modified silica nanoparticles with covalently incorporated photosensitizer for photodynamic therapy of cancer", Nano Letters, 7 (9), 2835-2842.

[128] Lai C. W., Wang Y. H., Lai C. H., Yang M. J., Chen C. Y., Chou P. T., Chan C. S., Chi Y., Chen Y. C., Hsiao J. K., (2008), "Iridium-Complex-Functionalized Fe3O4/SiO2 Core/Shell Nanoparticles: A Facile Three-in-One System in Magnetic Resonance Imaging, Luminescence Imaging, and Photodynamic Therapy", Small, 4 (2), 218-224.

[129] Rossi L. M., Silva P. R., Vono L. L., Fernandes A. U., Tada D. B., Baptista M. S., (2008), "Protoporphyrin IX nanoparticle carrier: preparation, optical properties, and singlet oxygen generation", Langmuir, 24 (21), 12534-12538.

[130] Tu H. L., Lin Y. S., Lin H. Y., Hung Y., Lo L. W., Chen Y. F., Mou C. Y., (2009), "In vitro studies of functionalized mesoporous silica nanoparticles for photodynamic therapy", Advanced Materials, 21 (2), 172-177.

[131] Low P. S., Henne W. A., Doorneweerd D. D., (2007), "Discovery and development of folic-acid-based receptor targeting for imaging and therapy of cancer and inflammatory diseases", Accounts of Chemical Research, 41 (1), 120-129.

[132] Zhang P., Steelant W., Kumar M., Scholfield M., (2007), "Versatile photosensitizers for photodynamic therapy at infrared excitation", Journal of the American Chemical Society, 129 (15), 4526-4527.

[133] Choi H. S., Liu W., Misra P., Tanaka E., Zimmer J. P., Ipe B. I., Bawendi M. G., Frangioni J. V., (2007), "Renal clearance of nanoparticles", Nature Biotechnology, 25 (10), 1165.

[134] Derfus A. M., Chan W. C., Bhatia S. N., (2004), "Probing the cytotoxicity of semiconductor quantum dots", Nano Letters, 4 (1), 11-18.

[135] Park J.-H., Gu L., Von Maltzahn G., Ruoslahti E., Bhatia S. N., Sailor M. J., (2009), "Biodegradable luminescent porous silicon nanoparticles for in vivo applications", Nature Materials, 8 (4), 331.

[136] Canham L. T., (1995), "Bioactive silicon structure fabrication through nanoetching techniques", Advanced Materials, 7 (12), 1033-1037.

[137] Gaumet M., Gurny R., Delie F., (2010), “Interaction of biodegradable nanoparticles with intestinal cells: the effect of surface hydrophilicity”, International Journal of Pharmaceutics, 390 (1), 45-52.

[138] Zhao F., Shen G., Chen C., Xing R., Zou Q., Ma G., Yan X., (2014), “Nanoengineering of Stimuli-Responsive Protein-Based Biomimetic Protocells as Versatile Drug Delivery Tools”, Chemistry-A European Journal, 20 (23), 6880-6887.

[139] Gao L., Fei J., Zhao J., Cui W., Cui Y., Li J., (2012), “pH-and Redox-Responsive Polysaccharide-Based Microcapsules with Autofluorescence for Biomedical Applications”, Chemistry-A European Journal, 18 (11), 3185-3192.

[140] George R. D., Snow A. W., (1995), “Synthesis of 3-nitrophthalonitrile and tetra-α-substituted phthalocyanines”, Journal of Heterocyclic Chemistry, 32 (2), 495-498.

[141] Young J. G., Onyebuagu W., (1990), “Synthesis and characterization of di-disubstituted phthalocyanines”, The Journal of Organic Chemistry, 55 (7), 2155-2159.

[142] Kumru U., Ermeydan M. A., Dumoulin F., Ahsen V., (2008), “Amphiphilic galactosylated phthalocyanines”, Journal of Porphyrins and Phthalocyanines, 12 (10), 1090-1095.

[143] Machacek M., Cidlina A., Novakova V., Svec J., Rudolf E., Miletin M., Kučera R., Simunek T., Zimcik P., (2015), “Far-red-absorbing cationic phthalocyanine photosensitizers: Synthesis and evaluation of the photodynamic anticancer activity and the mode of cell death induction”, Journal of Medicinal Chemistry, 58 (4), 1736-1749.

[144] Kuznetsova N., Gretsova N., Kalmykova E., Makarova E., Dashkevich S., Negrimovskii V., Kaliya O., Luk'yanets E., (2000), “Relationship between the photochemical properties and structure of pophyrins and related compounds”, Russian Journal of General Chemistry, 70 (1), 133-140.

BIOGRAPHY

Ömer Göler was born in Bursa, Turkey in 1979. He was received Bachelor of Science in Chemistry from Boğaziçi University, Faculty of Arts and Sciences, Department of Chemistry in 2005. He started Master of Science in Chemistry at Gebze Technical University, Graduate School of Natural and Applied Science, Chemistry Department in 2015.

APPENDIX

Appendix A: Copyright Permissions

ROYAL SOCIETY OF CHEMISTRY LICENSE TERMS AND CONDITIONS

Sep 04, 2017

This Agreement between Mr. Omer Goler ("You") and Royal Society of Chemistry ("Royal Society of Chemistry") consists of your license details and the terms and conditions provided by Royal Society of Chemistry and Copyright Clearance Center.

License Number	4181780488787
License date	Sep 04, 2017
Licensed Content Publisher	Royal Society of Chemistry
Licensed Content Publication	Organic & Biomolecular Chemistry
Licensed Content Title	Modulating the electronic properties of porphyrinoids: a voyage from the violet to the infrared regions of the electromagnetic spectrum
Licensed Content Author	Yannick Rio,M. Salomé Rodríguez-Morgade,Tomás Torres
Licensed Content Date	Apr 24, 2008
Licensed Content Volume	6
Licensed Content Issue	11
Type of Use	Thesis/Dissertation
Requestor type	academic/educational
Portion	figures/tables/images
Number of figures/tables/images	3
Format	print and electronic
Distribution quantity	10
Will you be translating?	no
Order reference number	31
Title of the thesis/dissertation	NanoPMOs BUILDING BLOCKS: PROPARGYL FUNCTIONALIZED PHOTOSENSITIZING Zn PHTHALOCYANINES WITH SPACERS OF DIFFERENT LENGTHS AND POSITIONS
Expected completion date	Sep 2017
Estimated size	120
Requestor Location	Mr. Omer Goler Siracevizler Mah. 15.Aydin Sok. No:14 Kat:2 Bursa, 16340 Turkey Attn: Mr. Omer Goler
Billing Type	Invoice
Billing Address	Mr. Omer Goler Siracevizler Mah. 15.Aydin Sok. No:14 Kat:2 Bursa, Turkey 16340 Attn: Mr. Omer Goler
Total	0.00 USD

Figure A1.1: Copyright Permission of Figure 2.6.

ROYAL SOCIETY OF CHEMISTRY LICENSE TERMS AND CONDITIONS

Sep 04, 2017

This Agreement between Mr. Omer Goler ("You") and Royal Society of Chemistry ("Royal Society of Chemistry") consists of your license details and the terms and conditions provided by Royal Society of Chemistry and Copyright Clearance Center.

License Number	4181821360642
License date	Sep 04, 2017
Licensed Content Publisher	Royal Society of Chemistry
Licensed Content Publication	Dalton Transactions
Licensed Content Title	Modulation of the electronic and spectroscopic properties of Zn(ii) phthalocyanines by their substitution pattern
Licensed Content Author	Sevinc Z. Topal,Ümit İşci,Ufuk Kumru,Devrim Atilla,Ayşe G. Gürek,Catherine Hirel,Mahmut Durmuş,Jean-Bernard Tommasino,Dominique Luneau,Savas Berber,Fabienne Dumoulin,Vefa Ahsen
Licensed Content Date	Feb 4, 2014
Licensed Content Volume	43
Licensed Content Issue	18
Type of Use	Thesis/Dissertation
Requestor type	academic/educational
Portion	figures/tables/images
Number of figures/tables/images	3
Format	print and electronic
Distribution quantity	10
Will you be translating?	no
Order reference number	35
Title of the thesis/dissertation	NanoPMOs BUILDING BLOCKS: PROPARGYL FUNCTIONALIZED PHOTOSENSITIZING Zn PHTHALOCYANINES WITH SPACERS OF DIFFERENT LENGTHS AND POSITIONS
Expected completion date	Sep 2017
Estimated size	120
Requestor Location	Mr. Omer Goler Siracevizler Mah. 15.Aydin Sok. No:14 Kat:2 Bursa, 16340 Turkey Attn: Mr. Omer Goler
Billing Type	Invoice
Billing Address	Mr. Omer Goler Siracevizler Mah. 15.Aydin Sok. No:14 Kat:2 Bursa, Turkey 16340 Attn: Mr. Omer Goler
Total	0.00 USD

Figure A1.2: Copyright Permission of Figure 2.8, 2.9 and 2.10.

ROYAL SOCIETY OF CHEMISTRY LICENSE TERMS AND CONDITIONS

Aug 13, 2017

This Agreement between Mr. Omer Goler ("You") and Royal Society of Chemistry ("Royal Society of Chemistry") consists of your license details and the terms and conditions provided by Royal Society of Chemistry and Copyright Clearance Center.

License Number	4167060865331
License date	Aug 13, 2017
Licensed Content Publisher	Royal Society of Chemistry
Licensed Content Publication	Nanoscale
Licensed Content Title	Syntheses and applications of periodic mesoporous organosilica nanoparticles
Licensed Content Author	Jonas G. Croissant,Xavier Cattoën,Michel Wong Chi Man,Jean-Olivier Durand,Niveen M. Khashab
Licensed Content Date	Nov 6, 2015
Licensed Content Volume	7
Licensed Content Issue	48
Type of Use	Thesis/Dissertation
Requestor type	academic/educational
Portion	figures/tables/images
Number of figures/tables/images	3
Format	print and electronic
Distribution quantity	10
Will you be translating?	no
Order reference number	58
Title of the thesis/dissertation	NanoPMOs BUILDING BLOCKS: PROPARGYL FUNCTIONALIZED PHOTOSENSING Zn PHTHALOCYANINES WITH SPACERS OF DIFFERENT LENGTHS AND POSITIONS
Expected completion date	Aug 2017
Estimated size	120
Requestor Location	Mr. Omer Goler Siracevizler Mah. 15.Aydin Sok. No:14 Kat:2 Bursa, 16340 Turkey Attn: Mr. Omer Goler
Billing Type	Invoice
Billing Address	Mr. Omer Goler Siracevizler Mah. 15.Aydin Sok. No:14 Kat:2 Bursa, Turkey 16340 Attn: Mr. Omer Goler
Total	0.00 USD

Figure A1.3: Copyright Permission of Figure 2.12, 2.17 and 2.18.

ROYAL SOCIETY OF CHEMISTRY LICENSE TERMS AND CONDITIONS

Sep 04, 2017

This Agreement between Mr. Omer Goler ("You") and Royal Society of Chemistry ("Royal Society of Chemistry") consists of your license details and the terms and conditions provided by Royal Society of Chemistry and Copyright Clearance Center.

License Number	4181830398803
License date	Sep 04, 2017
Licensed Content Publisher	Royal Society of Chemistry
Licensed Content Publication	Chemical Society Reviews
Licensed Content Title	Syntheses, properties and applications of periodic mesoporous organosilicas prepared from bridged organosilane precursors
Licensed Content Author	Norihiro Mizoshita,Takao Tani,Shinji Inagaki
Licensed Content Date	Dec 7, 2010
Licensed Content Volume	40
Licensed Content Issue	2
Type of Use	Thesis/Dissertation
Requestor type	academic/educational
Portion	figures/tables/images
Number of figures/tables/images	3
Format	print and electronic
Distribution quantity	10
Will you be translating?	no
Order reference number	82
Title of the thesis/dissertation	NanoPMOs BUILDING BLOCKS: PROPARGYL FUNCTIONALIZED PHOTOSENSITIZING Zn PHTHALOCYANINES WITH SPACERS OF DIFFERENT LENGTHS AND POSITIONS
Expected completion date	Sep 2017
Estimated size	120
Requestor Location	Mr. Omer Goler Siracevizler Mah. 15.Aydin Sok. No:14 Kat:2 Bursa, 16340 Turkey Attn: Mr. Omer Goler
Billing Type	Invoice
Billing Address	Mr. Omer Goler Siracevizler Mah. 15.Aydin Sok. No:14 Kat:2 Bursa, Turkey 16340 Attn: Mr. Omer Goler
Total	0.00 USD

Figure A1.4: Copyright Permission of Figure 2.13.

ROYAL SOCIETY OF CHEMISTRY LICENSE TERMS AND CONDITIONS

Sep 04, 2017

This Agreement between Mr. Omer Goler ("You") and Royal Society of Chemistry ("Royal Society of Chemistry") consists of your license details and the terms and conditions provided by Royal Society of Chemistry and Copyright Clearance Center.

License Number	4181830768174
License date	Sep 04, 2017
Licensed Content Publisher	Royal Society of Chemistry
Licensed Content Publication	Chemical Society Reviews
Licensed Content Title	Periodic Mesoporous Organosilicas: from simple to complex bridges; a comprehensive overview of functions, morphologies and applications
Licensed Content Author	Pascal Van Der Voort,Dolores Esquivel,Els De Canck,Frederik Goethals,Isabel Van Driessche,Francisco J. Romero-Salguero
Licensed Content Date	Oct 18, 2012
Licensed Content Volume	42
Licensed Content Issue	9
Type of Use	Thesis/Dissertation
Requestor type	academic/educational
Portion	figures/tables/images
Number of figures/tables/images	3
Format	print and electronic
Distribution quantity	10
Will you be translating?	no
Order reference number	83
Title of the thesis/dissertation	NanoPMOs BUILDING BLOCKS: PROPARGYL FUNCTIONALIZED PHOTOSENSITIZING Zn PHTHALOCYANINES WITH SPACERS OF DIFFERENT LENGTHS AND POSITIONS
Expected completion date	Sep 2017
Estimated size	120
Requestor Location	Mr. Omer Goler Siracevizler Mah. 15.Aydin Sok. No:14 Kat:2 Bursa, 16340 Turkey Attn: Mr. Omer Goler
Billing Type	Invoice
Billing Address	Mr. Omer Goler Siracevizler Mah. 15.Aydin Sok. No:14 Kat:2 Bursa, Turkey 16340 Attn: Mr. Omer Goler
Total	0.00 USD

Figure A1.5: Copyright Permission of Figure 2.14, 2.15 and Table 2.3.

ROYAL SOCIETY OF CHEMISTRY LICENSE TERMS AND CONDITIONS

Sep 04, 2017

This Agreement between Mr. Omer Goler ("You") and Royal Society of Chemistry ("Royal Society of Chemistry") consists of your license details and the terms and conditions provided by Royal Society of Chemistry and Copyright Clearance Center.

License Number	4181831123812
License date	Sep 04, 2017
Licensed Content Publisher	Royal Society of Chemistry
Licensed Content Publication	Journal of Materials Chemistry
Licensed Content Title	Functionalized periodic mesoporous organosilicas for catalysis
Licensed Content Author	Qihua Yang,Jian Liu,Lei Zhang,Can Li
Licensed Content Date	Jan 16, 2009
Licensed Content Volume	19
Licensed Content Issue	14
Type of Use	Thesis/Dissertation
Requestor type	academic/educational
Portion	figures/tables/images
Number of figures/tables/images	3
Format	print and electronic
Distribution quantity	10
Will you be translating?	no
Order reference number	88
Title of the thesis/dissertation	NanoPMOs BUILDING BLOCKS: PROPARGYL FUNCTIONALIZED PHOTOSENSITIZING Zn PHTHALOCYANINES WITH SPACERS OF DIFFERENT LENGTHS AND POSITIONS
Expected completion date	Sep 2017
Estimated size	120
Requestor Location	Mr. Omer Goler Siracevizler Mah. 15.Aydin Sok. No:14 Kat:2 Bursa, 16340 Turkey Attn: Mr. Omer Goler
Billing Type	Invoice
Billing Address	Mr. Omer Goler Siracevizler Mah. 15.Aydin Sok. No:14 Kat:2 Bursa, Turkey 16340 Attn: Mr. Omer Goler
Total	0.00 USD

Figure A1.6: Copyright Permission of Figure 2.16.

ROYAL SOCIETY OF CHEMISTRY LICENSE TERMS AND CONDITIONS

Sep 04, 2017

This Agreement between Mr. Omer Goler ("You") and Royal Society of Chemistry ("Royal Society of Chemistry") consists of your license details and the terms and conditions provided by Royal Society of Chemistry and Copyright Clearance Center.

License Number	4181840379236
License date	Sep 04, 2017
Licensed Content Publisher	Royal Society of Chemistry
Licensed Content Publication	Chemical Communications (Cambridge)
Licensed Content Title	Mannose-targeted mesoporous silica nanoparticles for photodynamic therapy
Licensed Content Author	David Brevet,Magali Gary-Bobo,Laurence Raehm,Sébastien Richeter,Ouahiba Hocine,Kassem Amro,Bernard Loock,Pierre Couleaud,Céline Frochot,Alain Morère,Philippe Maillard,Marcel Garcia,Jean-Olivier Durand
Licensed Content Date	Feb 18, 2009
Licensed Content Volume	0
Licensed Content Issue	12
Type of Use	Thesis/Dissertation
Requestor type	academic/educational
Portion	figures/tables/images
Number of figures/tables/images	3
Format	print and electronic
Distribution quantity	10
Will you be translating?	no
Order reference number	12
Title of the thesis/dissertation	NanoPMOs BUILDING BLOCKS: PROPARGYL FUNCTIONALIZED PHOTOSENSITIZING Zn PHTHALOCYANINES WITH SPACERS OF DIFFERENT LENGTHS AND POSITIONS
Expected completion date	Sep 2017
Estimated size	120
Requestor Location	Mr. Omer Goler Siracevizler Mah. 15.Aydin Sok. No:14 Kat:2 Bursa, 16340 Turkey Attn: Mr. Omer Goler
Billing Type	Invoice
Billing Address	Mr. Omer Goler Siracevizler Mah. 15.Aydin Sok. No:14 Kat:2 Bursa, Turkey 16340 Attn: Mr. Omer Goler
Total	0.00 USD

Figure A1.7: Copyright Permission of Figure 2.19 and 2.20.

JOHN WILEY AND SONS LICENSE TERMS AND CONDITIONS

Sep 04, 2017

This Agreement between Mr. Omer Goler ("You") and John Wiley and Sons ("John Wiley and Sons") consists of your license details and the terms and conditions provided by John Wiley and Sons and Copyright Clearance Center.

License Number	4181840920451
License date	Sep 04, 2017
Licensed Content Publisher	John Wiley and Sons
Licensed Content Publication	Advanced Materials
Licensed Content Title	Two-Photon Excitation of Porphyrin-Functionalized Porous Silicon Nanoparticles for Photodynamic Therapy
Licensed Content Author	Emilie Secret,Marie Maynadier,Audrey Gallud,Arnaud Chaix,Elise Bouffard,Magali Gary-Bobo,Nathalie Marcotte,Olivier Mongin,Khaled El Cheikh,Vincent Hugues,Mélanie Auffan,Céline Frochot,Alain Morère,Philippe Maillard,Mireille Blanchard-Desce,Michael J. Sailor,Marcel Garcia,Jean-Olivier Durand,Frédérique Cunin
Licensed Content Date	Oct 17, 2014
Licensed Content Pages	6
Type of use	Dissertation/Thesis
Requestor type	University/Academic
Format	Print and electronic
Portion	Figure/table
Number of figures/tables	3
Original Wiley figure/table number(s)	Figure 1
Will you be translating?	No
Order reference number	11
Title of your thesis / dissertation	NanoPMOs BUILDING BLOCKS: PROPARGYL FUNCTIONALIZED PHOTOSENSITIZING Zn PHTHALOCYANINES WITH SPACERS OF DIFFERENT LENGTHS AND POSITIONS
Expected completion date	Sep 2017
Expected size (number of pages)	120
Requestor Location	Mr. Omer Goler Siracevizler Mah. 15.Aydin Sok. No:14 Kat:2 Bursa, 16340 Turkey Attn: Mr. Omer Goler
Publisher Tax ID	EU826007151
Billing Type	Invoice
Billing Address	Mr. Omer Goler Siracevizler Mah. 15.Aydin Sok. No:14 Kat:2 Bursa, Turkey 16340 Attn: Mr. Omer Goler
Total	0.00 USD

Figure A1.8: Copyright Permission of Figure 2.21.

ROYAL SOCIETY OF CHEMISTRY LICENSE TERMS AND CONDITIONS

Sep 04, 2017

This Agreement between Mr. Omer Goler ("You") and Royal Society of Chemistry ("Royal Society of Chemistry") consists of your license details and the terms and conditions provided by Royal Society of Chemistry and Copyright Clearance Center.

License Number	4181841144524
License date	Sep 04, 2017
Licensed Content Publisher	Royal Society of Chemistry
Licensed Content Publication	Chemical Communications (Cambridge)
Licensed Content Title	Synthesis of disulfide-based biodegradable bridged silsesquioxane nanoparticles for two-photon imaging and therapy of cancer cells
Licensed Content Author	Jonas G. Croissant,Chiara Mauriello-Jimenez,Marie Maynadier,Xavier Cattoën,Michel Wong Chi Man,Laurence Raehm,Olivier Mongin,Mireille Blanchard-Desce,Marcel Garcia,Magali Gary-Bobo,Philippe Maillard,Jean-Olivier Durand
Licensed Content Date	Jun 18, 2015
Licensed Content Volume	51
Licensed Content Issue	61
Type of Use	Thesis/Dissertation
Requestor type	academic/educational
Portion	figures/tables/images
Number of figures/tables/images	3
Format	print and electronic
Distribution quantity	10
Will you be translating?	no
Order reference number	87
Title of the thesis/dissertation	NanoPMOs BUILDING BLOCKS: PROPARGYL FUNCTIONALIZED PHOTOSENSITIZING Zn PHTHALOCYANINES WITH SPACERS OF DIFFERENT LENGTHS AND POSITIONS
Expected completion date	Sep 2017
Estimated size	120
Requestor Location	Mr. Omer Goler Siracevizler Mah. 15.Aydin Sok. No:14 Kat:2 Bursa, 16340 Turkey Attn: Mr. Omer Goler
Billing Type	Invoice
Billing Address	Mr. Omer Goler Siracevizler Mah. 15.Aydin Sok. No:14 Kat:2 Bursa, Turkey 16340 Attn: Mr. Omer Goler
Total	0.00 USD

Figure A1.9: Copyright Permission of Figure 2.22.

SPRINGER LICENSE
TERMS AND CONDITIONS

Sep 04, 2017

This Agreement between Mr. Omer Goler ("You") and Springer ("Springer") consists of your license details and the terms and conditions provided by Springer and Copyright Clearance Center.

License Number	4181841457118
License date	Sep 04, 2017
Licensed Content Publisher	Springer
Licensed Content Publication	Journal of Sol-Gel Science and Technology
Licensed Content Title	20-nm-sized mesoporous silica nanoparticles with porphyrin photosensitizers for in vitro photodynamic therapy
Licensed Content Author	Chiara Mauriello Jimenez
Licensed Content Date	Jan 1, 2016
Licensed Content Volume	79
Licensed Content Issue	3
Type of Use	Thesis/Dissertation
Portion	Figures/tables/illustrations
Number of figures/tables/illustrations	3
Author of this Springer article	No
Order reference number	8
Original figure numbers	Scheme 1
Title of your thesis / dissertation	NanoPMOs BUILDING BLOCKS: PROPARGYL FUNCTIONALIZED PHOTOSENSITIZING Zn PHTHALOCYANINES WITH SPACERS OF DIFFERENT LENGTHS AND POSITIONS
Expected completion date	Sep 2017
Estimated size(pages)	120
Requestor Location	Mr. Omer Goler Siracevizler Mah. 15.Aydin Sok. No:14 Kat:2 Bursa, 16340 Turkey Attn: Mr. Omer Goler
Billing Type	Invoice
Billing Address	Mr. Omer Goler Siracevizler Mah. 15.Aydin Sok. No:14 Kat:2 Bursa, Turkey 16340 Attn: Mr. Omer Goler
Total	0.00 USD

Figure A1.10: Copyright Permission of Figure 2.23.

ROYAL SOCIETY OF CHEMISTRY LICENSE TERMS AND CONDITIONS

Sep 04, 2017

This Agreement between Mr. Omer Goler ("You") and Royal Society of Chemistry ("Royal Society of Chemistry") consists of your license details and the terms and conditions provided by Royal Society of Chemistry and Copyright Clearance Center.

License Number	4181831465825
License date	Sep 04, 2017
Licensed Content Publisher	Royal Society of Chemistry
Licensed Content Publication	Nanoscale
Licensed Content Title	Large pore mesoporous silica nanomaterials for application in delivery of biomolecules
Licensed Content Author	Nikola Ž. Knežević,Jean-Olivier Durand
Licensed Content Date	Dec 30, 2014
Licensed Content Volume	7
Licensed Content Issue	6
Type of Use	Thesis/Dissertation
Requestor type	academic/educational
Portion	figures/tables/images
Number of figures/tables/images	3
Format	print and electronic
Distribution quantity	10
Will you be translating?	no
Order reference number	119
Title of the thesis/dissertation	NanoPMOs BUILDING BLOCKS: PROPARGYL FUNCTIONALIZED PHOTOSENSITIZING Zn PHTHALOCYANINES WITH SPACERS OF DIFFERENT LENGTHS AND POSITIONS
Expected completion date	Sep 2017
Estimated size	120
Requestor Location	Mr. Omer Goler Siracevizler Mah. 15.Aydin Sok. No:14 Kat:2 Bursa, 16340 Turkey Attn: Mr. Omer Goler
Billing Type	Invoice
Billing Address	Mr. Omer Goler Siracevizler Mah. 15.Aydin Sok. No:14 Kat:2 Bursa, Turkey 16340 Attn: Mr. Omer Goler
Total	0.00 USD

Figure A1.11: Copyright Permission of Table 2.1 and 2.2.